


Summer 2000

# Fluid flow in micro-channels: A stochastic approach

Hilda Marino Black  
*Louisiana Tech University*

Follow this and additional works at: <https://digitalcommons.latech.edu/dissertations>

 Part of the [Fluid Dynamics Commons](#), [Mechanical Engineering Commons](#), and the [Other Statistics and Probability Commons](#)

---

## Recommended Citation

Black, Hilda Marino, "" (2000). *Dissertation*. 157.  
<https://digitalcommons.latech.edu/dissertations/157>

This Dissertation is brought to you for free and open access by the Graduate School at Louisiana Tech Digital Commons. It has been accepted for inclusion in Doctoral Dissertations by an authorized administrator of Louisiana Tech Digital Commons. For more information, please contact [digitalcommons@latech.edu](mailto:digitalcommons@latech.edu).

## **INFORMATION TO USERS**

This manuscript has been reproduced from the microfilm master. UMI films the text directly from the original or copy submitted. Thus, some thesis and dissertation copies are in typewriter face, while others may be from any type of computer printer.

**The quality of this reproduction is dependent upon the quality of the copy submitted.** Broken or indistinct print, colored or poor quality illustrations and photographs, print bleedthrough, substandard margins, and improper alignment can adversely affect reproduction.

In the unlikely event that the author did not send UMI a complete manuscript and there are missing pages, these will be noted. Also, if unauthorized copyright material had to be removed, a note will indicate the deletion.

Oversize materials (e.g., maps, drawings, charts) are reproduced by sectioning the original, beginning at the upper left-hand corner and continuing from left to right in equal sections with small overlaps.

Photographs included in the original manuscript have been reproduced xerographically in this copy. Higher quality 6" x 9" black and white photographic prints are available for any photographs or illustrations appearing in this copy for an additional charge. Contact UMI directly to order.

**Bell & Howell Information and Learning  
300 North Zeeb Road, Ann Arbor, MI 48106-1346 USA  
800-521-0600**

**UMI<sup>®</sup>**



**FLUID FLOW IN MICRO-CHANNELS:**

**A STOCHASTIC APPROACH**

by

**Hilda Marino Black, MS, MST**

**A Dissertation Presented in Partial Fulfillment  
of the Requirements for the Degree  
Doctor of Philosophy**

**COLLEGE OF ENGINEERING AND SCIENCE  
LOUISIANA TECH UNIVERSITY**

**August 2000**

UMI Number: 9975090

UMI<sup>®</sup>

---

UMI Microform 9975090

Copyright 2000 by Bell & Howell Information and Learning Company.

All rights reserved. This microform edition is protected against  
unauthorized copying under Title 17, United States Code.

---

Bell & Howell Information and Learning Company  
300 North Zeeb Road  
P.O. Box 1346  
Ann Arbor, MI 48106-1346

LOUISIANA TECH UNIVERSITY  
THE GRADUATE SCHOOL

July 10, 2000



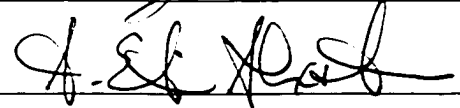
We hereby recommend that the thesis prepared under our supervision by Hilda Marino Black entitled Fluid Flow in Micro-Channels: A Stochastic Approach be accepted in partial fulfillment of the requirements for the Degree of Ph.D. in Applied Computational Analysis and Modeling.

  
\_\_\_\_\_  
Supervisor of Thesis Research

  
\_\_\_\_\_  
Head of Department

\_\_\_\_\_  
Department

Recommendation concurred in:

  
\_\_\_\_\_  
  
\_\_\_\_\_  
  
\_\_\_\_\_


Advisory Committee

Approved:

  
\_\_\_\_\_  
Director of Graduate Studies

  
\_\_\_\_\_  
Dean of the College

Approved:

  
\_\_\_\_\_  
Dean of the Graduate School

GS Form 13  
(1/00)

## APPROVAL FOR SCHOLARLY DISSEMINATION

The author grants to the Prescott Memorial Library of Louisiana Tech University the right to reproduce, by appropriate methods, upon request, any or all portions of this Dissertation. It is understood that "proper request" consists of the agreement, on the part of the requesting party, that said reproduction is for his personal use and that subsequent reproduction will not occur without written approval of the author of this Dissertation. Further, any portions of the Dissertation used in books, papers, and other works must be appropriately referenced to this Dissertation.

Finally, the author of this Dissertation reserves the right to publish freely, in the literature, at any time, any or all portions of this Dissertation.

Author Hilda M. Black

Date July 10, 2000

## **ABSTRACT**

In this study free molecular flow in a micro-channel was modeled using a stochastic approach, namely the Kolmogorov forward equation in three dimensions. Model equations were discretized using Central Difference and Backward Difference methods and solved using the Jacobi method. Parameters were used that reflect the characteristic geometry of experimental work performed at the Louisiana Tech University Institute for Micromanufacturing.

The solution to the model equations provided the probability density function of the distance traveled by a particle in the micro-channel. From this distribution we obtained the distribution of the residence time of a particle in the micro-channel. Knowledge of Residence time will aid both chemical and biomedical engineers in the study of micro-reactors and biological systems, respectively. From the transition probability density obtained in our model and the initial particle density (or number concentration), one can calculate also the distribution of particle or solute concentration in the micro-channel. Model prediction of the distribution of distance traveled by a particle can be applied to experimental data on micro-channel flow being gathered at the Institute for Micromanufacturing at Louisiana Tech University.



## TABLE OF CONTENTS

<b>ABSTRACT</b> .....	<b>ii</b>
<b>LIST OF TABLES</b> .....	<b>v</b>
<b>LIST OF FIGURES</b> .....	<b>vi</b>
<b>NOMENCLATURE</b> .....	<b>ix</b>
<b>ACKNOWLEDGMENTS</b> .....	<b>xi</b>
<b>CHAPTER 1 INTRODUCTION</b>	
1.1 General Overview.....	<b>1</b>
1.2 Objectives.....	<b>8</b>
1.3 Organization of the Dissertation.....	<b>9</b>
<b>CHAPTER 2 RELATED RESEARCH</b> .....	<b>10</b>
<b>CHAPTER 3 MODEL</b>	
3.1 Introduction.....	<b>27</b>
3.2 Equations and Boundary Conditions.....	<b>29</b>
<b>CHAPTER 4 NUMERICAL METHOD</b>	
4.1 Introduction.....	<b>32</b>
4.2 Discretization.....	<b>32</b>
4.3 Treatment of Boundary Conditions.....	<b>33</b>
<b>CHAPTER 5 THREE-DIMENSIONAL MICRO-CHANNEL FLOW</b>	
5.1 Description of Simulation.....	<b>35</b>
5.2 Simulation Results and Discussion of the Stochastic Model.....	<b>37</b>
<b>CHAPTER 6 CONCLUSION AND FUTURE WORK</b> .....	<b>80</b>
<b>APPENDIX A FORTRAN CODE FOR THE STOCHASTIC MODEL</b> .....	<b>82</b>
<b>APPENDIX B C++ PROGRAM FOR PROCESSING X CROSS-SECTIONS</b> .....	<b>95</b>
<b>APPENDIX C C++ PROGRAM FOR PROCESSING DATA ACCORDING TO RHO VALUES</b> .....	<b>97</b>
<b>APPENDIX D C++ PROGRAM FOR ORDERING DATA IN A SINGLE CROSS-SECTION</b> .....	<b>99</b>

<b>APPENDIX E FORTRAN CODE FOR THE IMSL INTEGRATION ROUTINE .....</b>	<b>103</b>
<b>REFERENCES.....</b>	<b>105</b>

## LIST OF TABLES

TABLE	DESCRIPTION	PAGE
5.1	Calculations for the coefficient of variation, $CV$ .....	36
5.2	Times $t$ , used in the numerical simulation based on twice the average time till exit.....	37
5.3	Probability integral ( $\int_{-\infty}^a P(x; t) dx$ ) for the case of the one-dimensional time homogeneous diffusion process with $\sigma = 0.5$ and an absorbing barrier at $a = 10mm$ .....	38

## LIST OF FIGURES

FIGURE	DESCRIPTION	PAGE
1.1	Sizes/characteristics of micro-components comparison to other items.....	4
5.1	Physical domain for micro-channel flow.....	35
5.2	The probability distribution of the distance $x$ traveled by a particle for a homogeneous diffusion process with one absorbing barrier at $a=10mm$ and $t=l$ .....	41
5.3	The probability distribution of the distance $x$ traveled by a particle for a homogeneous diffusion process with one absorbing barrier at $a=10mm$ , $\mu=4$ .....	42
5.4	Probability distribution of $\rho$ between 0.2 and 2 seconds, $\mu=10$ .....	43
5.5	Probability distribution of $\rho$ between 0.04 and 0.4 seconds, $\mu=50$ .....	44
5.6	Probability distribution of $\rho$ between 0.02 and 0.2 seconds, $\mu=100$ .....	45
5.7	Probability distribution of $\rho$ between 0.01 and 0.1 seconds, $\mu=200$ .....	46
5.8	Probability distribution of $\rho$ between 0.004 and 0.04 seconds, $\mu=500$ .....	47
5.9	Probability distribution of time to first passage from the entry to a cross-section, $x$ between 0.5 and 5.0, $\mu=10$ .....	48
5.10	Probability distribution of time to first passage from the entry to a cross-section, $x$ between 5.5 and 9.99, $\mu=10$ .....	49
5.11	Probability distribution of time to first passage from the entry to a cross-section, $x$ between 0.5 and 5.0, $\mu=50$ .....	50
5.12	Probability distribution of time to first passage from the entry to a cross-section, $x$ between 5.5 and 9.99, $\mu=50$ .....	51
5.13	Probability distribution of time to first passage from the entry to a cross-section, $x$ between 0.5 and 5.0, $\mu=100$ .....	52

5.14	Probability distribution of time to first passage from the entry to a cross-section, $x$ between 5.5 and 9.99, $\mu=100$ .....	53
5.15	Probability distribution of time to first passage from the entry to a cross-section, $x$ between 0.5 and 5.0, $\mu=200$ .....	54
5.16	Probability distribution of time to first passage from the entry to a cross-section, $x$ between 5.5 and 9.99, $\mu=200$ .....	55
5.17	Probability distribution of time to first passage from the entry to a cross-section, $x$ between 0.5 and 5.0, $\mu=500$ .....	56
5.18	Probability distribution of time to first passage from the entry to a cross-section, $x$ between 5.5 and 9.99, $\mu=500$ .....	57
5.19	Probability distribution at cross-section $x=5.5$ , $\mu=10$ , $t=1.0s$ .....	58
5.20	Probability distribution at cross-section $x=8.0$ , $\mu=10$ , $t=1.2s$ .....	59
5.21	Probability distribution at cross-section $x=9.99$ , $\mu=10$ , $t=1.6s$ .....	60
5.22	Probability distribution at cross-section $x=9.99$ , $\mu=10$ , $t=1.8s$ .....	61
5.23	Probability distribution at cross-section $x=1.5$ , $\mu=50$ , $t=0.04s$ .....	62
5.24	Probability distribution at cross-section $x=3.0$ , $\mu=50$ , $t=0.08s$ .....	63
5.25	Probability distribution at cross-section $x=5.5$ , $\mu=50$ , $t=0.16s$ .....	64
5.26	Probability distribution at cross-section $x=8.0$ , $\mu=50$ , $t=0.24s$ .....	65
5.27	Probability distribution at cross-section $x=9.99$ , $\mu=50$ , $t=0.32s$ .....	66
5.28	Probability distribution at cross-section $x=7.0$ , $\mu=100$ , $t=0.1s$ .....	67
5.29	Probability distribution at cross-section $x=8.5$ , $\mu=100$ , $t=0.12$ .....	68
5.30	Probability distribution at cross-section $x=9.99$ , $\mu=100$ , $t=0.14s$ .....	69
5.31	Probability distribution at cross-section $x=9.99$ , $\mu=200$ , $t=0.07s$ .....	70
5.32	Probability distribution at cross-section $x=9.99$ , $\mu=200$ , $t=0.08s$ .....	71
5.33	Probability distribution at cross-section $x=9.99$ , $\mu=200$ , $t=0.09s$ .....	72

5.34	Probability distribution at cross-section $x=9.99$ , $\mu=200$ , $t=0.1s$ .....	73
5.35	Probability distribution at cross-section $x=3.0$ , $\mu=500$ , $t=0.004s$ .....	74
5.36	Probability distribution at cross-section $x=9.99$ , $\mu=500$ , $t=0.028s$ .....	75
5.37	Probability distribution at cross-section $x=9.9$ , $\mu=500$ , $t=0.032s$ .....	76
5.38	Probability distribution of $\rho$ between 0.04 and 0.4 seconds 2-D case, $\mu=50$ .....	77
5.39	Probability distribution of $\rho$ between 0.02 and 0.2 seconds 2-D case, $\mu=100$ .....	78
5.40	Probability distribution of $\rho$ between 0.004 and 0.04 seconds 2-D case, $\mu=500$ .....	79

## NOMENCLATURE

$a$	half the length of the $y$ and/or $z$ distance
$f(y,z)$	linearized Navier-Stokes equation
$b_1$	continuously differentiable function on the $(y,z)$ plane
$b_2$	continuously differentiable function on the $(y,z)$ plane
$V$	point volume
$H, h$	channel height
$Kn$	Knudsen number
$L$	flow characteristic length
$p$	pressure
$P$	probability
$t$	time
$Re$	Reynolds number
$Pr$	Prandlt number
$U$	characteristic velocity
$x$	the Cartesian coordinate in the stream-wise direction
$y$	the Cartesian coordinate for width
$z$	the Cartesian coordinate for height
$nx$	grid points in the $x$ direction

$n_y$	grid points in the y direction
$n_z$	grid points in the z direction
$\Delta t$	time interval
$\Delta x$	grid spacing in the x direction
$\Delta y$	grid spacing in the y direction
$\Delta z$	grid spacing in the z direction
$\partial$	Differential operator
$\rho$	Density
$\varphi$	diffusivity of dispersion coefficient of water
$\mu_0$	Flow velocity in the center of the channel
$\mu_y$	$0.0001 * \mu_0$
$\mu_z$	$0.0001 * \mu_0$

### Superscripts

$n+1$	current iteration step
$n$	previous iteration step

### Subscript

$i$	index of grid in the x direction
$j$	index of grid in the y direction
$k$	index of grid in the z direction



## **ACKNOWLEDGMENTS**

This research is supported by the Louisiana Board of Regents fellowship, contract number LEQSF(1997-01)-GF-10. I wish to thank Dr. Richard Greechie for providing me the opportunity to receive this fellowship and study at Louisiana Tech University.

I would also like to express my gratitude and sincere appreciation to Dr. Raja Nassar and Dr. Weizhong Dai for their guidance, numerous office hours, patience, and efforts to make this thesis a reality. Many thanks to Dr. Albert Edwin Alexander for his service on my advisory committee, to Dr. Hisham Hegab for providing information related to his research and to Dr. Les Guice for his encouragement and guidance through my graduate studies.

I would like to thank Danny Schales, Bill Jones, Gene Murphy, and Mary Lee for helping with computer and software problems. I would also like to thank the secretaries in the College of Engineering, particularly Donna Bancks, Sandy Maxey, Frances Welch, Sandy Wilson, and Pam Witt, for their patience, encouragement, and tireless yet often unnoticed efforts.

I would like to thank my family, friends, and fellow teachers who supported me throughout this massive undertaking. Many thanks to Cynthia Vanlandingham for the many “neat” things related to computers and simulations she has shared with me. I would especially like to thank my husband, Eric Black, who encouraged me to pursue this degree while making many sacrifices so that I could complete my studies, as well as

my parents, who worked hard to provide me with a strong educational foundation early in life.

Finally, I dedicate this thesis to the loving memory of my father-in-law, Harry D. Black, my friend, Richard Thomas Aquinas Murphy, O.P, and my aunt, Margrith Arnold Nastasi. I dedicate this especially to my father, Joseph D. Marino, M.D., whose love of mathematics and science sparked my interest in mathematics as a young child. I believe they have put a good word in for me and continue to watch over me now that they have returned to our Heavenly Father.

# **CHAPTER 1**

## **INTRODUCTION**

### **1.1. General Overview**

Although the concept of modeling flow in micro-channels is not new, extensive experimentation has been impossible until recently, as methods for creating micro-environments have become available. Modeling of capillary flow as a field is, therefore, relatively new.

Micro-mechanics technology originated over 20 years ago. Many devices are under development such as flow sensors, valves, pumps, separation capillaries, and chemical detectors. An increasing demand exists for both theoretical and experimental work on fundamental physical and chemical phenomena. Another phenomenon important to liquid flow in small channels is gas bubbles. In principle bubbles can be avoided, but in order to do so, it is important to understand how a gas bubble moves in a micro-channel. Pressure drop across a liquid gas interface of a gas bubble in a capillary tube, as well as the pressure difference needed to move the gas bubble in a straight channel, increases with decreasing channel dimension. Finite Element analyses, finite difference, and boundary element modeling are suitable for micro-fluidic simulation. Only a few applications of finite element analysis for micro-fluids have been reported.

Dosing systems can be part of a transport system in a chemical analysis system or can be used in a drug delivering system. The demands of drug delivery systems correspond to the properties of micro-mechanical systems with small size, chemically

durable materials, robust construction, and the delivery of small precise doses of drugs. Medical applications could imply disposable systems, which sets strong limitations on the cost of the total system. Most of what we need to know about fundamental microfluidics has yet to be learned. Special phenomena--including rarefaction due to the mean free path of gas molecules, velocity in laminar flows, change of liquid viscosity with channel dimension, and surface tension effects encountered with gas bubbles in liquids--need to be considered in establishing fundamental material properties and valid models (Gravesen, Branebjerg, and Jensen, 1993).

Other applications of micro-technology exist. Small accelerometers, with dimensions measured in microns, are now used to deploy air bag systems in automobiles. Tiny pressure sensors for the tip of a catheter are smaller than the head of a pin, and micro-actuators are moving scanning electron microscope tips to image single atoms. New fabrication techniques such as surface silicon micro-machining, bulk silicon micro-machining, LIGA (Lithographie Galvanoformung Abformung), and EDM (Electro Discharge Machining) are making these micro-devices possible. Inherent with these new technologies is the need to develop fundamental science and engineering of small devices. Micro-devices tend to behave differently than the objects we are used to handling in daily life. The inertial forces, for example, tend to be quite small and surface effects tend to dominate their behavior. Friction, electrostatic forces, and viscous effects due to the surrounding air or liquid become increasingly important as the devices become smaller (Beskok, Karniadakis, and Trimmer, 1996).

Advanced micro-components currently in development include micro-channel heat exchangers, gas absorbers, liquid-liquid extractors, chemical reactors, and micro-

actuators for pumps, valves and compressors. These micro-components show the potential for high performance and capacity. These systems will be more compact than conventional, “macro” chemical processing systems, suggesting the potential for distributed and mobile applications. The micro-scale phenomenon should be exploited more effectively to significant advantage in terms of heat and/or mass transport. Cost economies as with the electronics industry, offer economies of mass production. Much of the US investment in micro-system technology is directed toward the development of MEMS for micro-sensor applications. Some micro-sensors are commercially available, and the overall prognosis for the micro-sensor market was recently estimated at \$14B in worldwide sales, enabling \$200B of new product sales. Typical scales for micro-mechanical devices range from microns to millimeters, spanning the range of scales that also includes micro-electronics, ultrasonics, visible and infrared radiation, and biological cells and tissues. Figure 1.1 shows the general comparison between these compact systems with their conventional counterparts (Wegeng *et al.*, 1996).

Epstein, *et al.* (1997) proposed a new class of MEMS devices, “power” MEMS, characterized by thermal, electrical, and mechanical power densities equivalent to those in the best large-sized machines produced today, thus producing powers of 10 to 100 watts in sub-centimeter sized packages. These devices would have significantly different behavior from, but equivalent performance to, their more familiar full-sized embodiments. They could find widespread applications as mobile power sources,

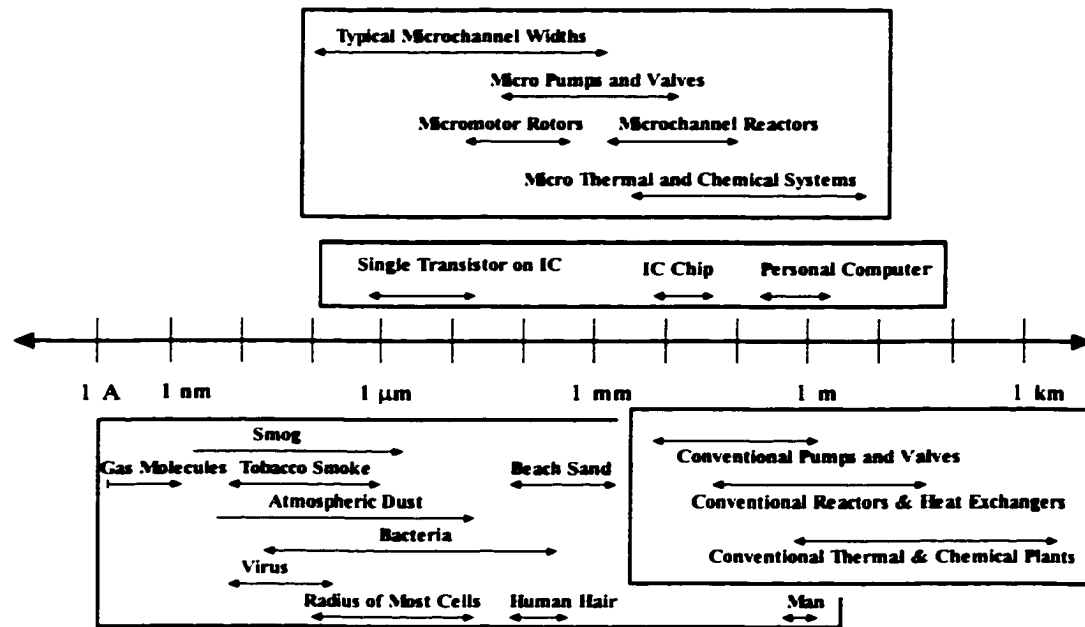


Figure 1.1 Sizes/characteristics of micro-components comparison to other items

propulsion engines, and coolers. The realization of power MEMS presents new challenges both to micro-machining and to the traditional mechanical and electrical engineering disciplines of fluid dynamics, combustion, and electric machinery design.

Ho and Tai (1996) reviewed some of the emerging micro-machining technology, which enables us to fabricate mechanical parts on the order of micron size. Micro-machining technology provides us with micro-sensors and micro-actuators, which facilitate the exploration of all areas of science. Furthermore, these miniature transducers can be integrated with micro-electronics. An integrated system allows the completion of the loop of sensing, information processing, and actuation. This type of system enables real-time control of time varying events, common in fluid dynamics. One opportunity for applying MEMS to flow control is the knowledge that shear flows are sensitive to perturbations.

What has stimulated the development of micro-mechanical components is that manufacturing techniques originally developed for micro-electronics have been extended to micro-mechanical structures and actuators. Researchers thus realize that the same economies of scale enjoyed in the mass production of micro-chips can apply to mechanical systems. However, very little is known about two-phase micro-flow, micro-evaporation, or micro-condensation.

The micro-compressor presents the largest technical challenge in developing a micro-heat pump system. Work is underway on micro-actuators to enable them to power a micro-compressor. Accordingly, the technical question is not whether micro-compressors can be developed, but how powerful and efficient they can be.

Advanced component design for compression and power generation must be developed. In addition, we have to improve our understanding of the physical phenomena that occur in micro-scale processes, including phase-change phenomena, fluid dynamics, and heat transfer. Although first generation micro-mechanical applications generally consist of micro-sensors for the automobile and biotechnology industries, further development activities should yield significant energy applications. The next generation of micro-actuators, designed to provide compressors or other work-to-work conversions, should enable the demonstration of efficient effective micro and sheet heat pumps. In some cases, applications of these products in a distributed mode are expected to reduce or eliminate energy losses associated with central processing. In addition there is the potential to use more efficient methods and improved thermal cycles not available on the macro-scale. Economies of scale, which have already been demonstrated for micro-electronics, will apply, resulting in sheet heat pumps and

engines that have lower capital costs than their macro alternatives (Wegeng and Drost, 1994).

Other practical applications of micro-scale fluid flow include cooling of electronic chips and devices, heat transfer augmentation, aerospace technology, reactors for modification and separation of biological cells and selective membranes. Research on fluid flow in these small channels is consequently necessary to identify the fundamentals and characteristics of fluid forced flow. Analysis and comparison show that the experimental data and results currently available in the literature do not have a high correlation and that some conclusions exist contrary to current theories. As noted in previous investigations, the flow and heat transfer in extremely small or micro-scale flow passages exhibit some unusual behavior and unique performance enhancement (Peng, Peterson, and Wang, 1994b).

Devices having dimensions of the order of microns are being developed for use in cooling of integrated circuits, biochemical applications, and cryogenics (Kavehpour, Faghri, and Asako, 1997). Micro-fabricated channels were also suggested for integrated cooling of electronic circuits, miniature gas chromatographs built on single silicon wafers, and small high-frequency fluidic control systems. In order to design such devices effectively, it is necessary to establish physical laws governing flow in small conduits (Harley, Huang, Bau, and Zemel, 1995).

There is very little fundamental understanding of the behavior of micro-flow. Consequently, there is a need for establishing mathematical models to characterize such flow. One of the biggest questions regarding flow in micro-channels is whether or not the flow can be modeled adequately using the Navier-Stokes equations. Should these



equations be modified and if so, how? When modeling macro-fluid flow, researchers normally neglect several effects. Should the same effects be neglected when modeling flow for micro-channels? Should others be considered?

The fundamental concepts of the continuum field approach to the treatment of matter had their origin well over two centuries ago in the works of Euler and later Cauchy. Classical continuum mechanics is based on the idea that all material bodies possess continuous mass densities, and that the laws of motion and the axioms of constitution are valid for every part of the body regardless of its size. Inherent in the classical viewpoint are drastic limitations on the extent to which continuum descriptions of macroscopic behavior can successfully mirror the fine structure of matter. As limitations become more acute and more refined, more complete descriptions of material behavior are sought.

The inadequacy of the classical continuum approach to describe the mechanics of complex fluids has led to the development of theories of micro-continua. Through these theories continuous media are now regarded as sets of structured particles possessing not only mass and velocity but also a substructure with which is associated a moment-of-inertia density and a micro-deformation tensor. This extension of fluid mechanics required a complete reappraisal of classical concepts in order to account for the local structural aspects and micro-motions. In fact, while many of the principles of classical continuum mechanics remain valid for this new class of fluids, they had to be augmented with additional balance laws and constitutive relations. The presence of microscopic elements in a fluid give rise not only to classical Cauchy stresses but also to couple stresses due to the micro-element interactions.

Although the various theories are quite diverse in their applicability, they all take into account the couple stress so that the continuum under consideration is polar, exhibiting an asymmetric stress tensor. Note that, while a statistical averaging process is employed in the development, the theory itself is based solely on the principles of continuum mechanics and not on molecular or statistical mechanics. By definition, a simple micro-fluid is a fluent medium whose properties and behavior are affected by the local motions of the material particles in each of its volume elements. Such a fluid possesses local inertia. Eringen's simple micro-fluids are isotropic, viscous fluids. In the simplest case of a constitutively linear theory, twenty-two viscosity and material coefficients characterize these fluids. However, a serious difficulty is encountered when the theory is applied to real, nontrivial flow problems.

Even for the linear theory, a problem dealing with simple micro-fluids must be formulated in terms of a system of nineteen partial differential equations in nineteen unknowns and the underlying mathematical problem is not easily amenable to solution. This difficulty has led Eringen and other researchers to consider subclasses of these general micro-fluids, which are more easily amenable to solution and will still allow description of the effects arising from particle micro-motions. Some other theories related to generalized fluid mechanics have been developed in recent literature from a statistical mechanical approach (Arıman, Turk, and Sylvester, 1973).

### **1.2. Objectives**

The emphasis of this research will be to explore free molecular flow. The three-dimensional Stochastic Komolgorov Forward equation (or the Fokker-Planck equation) will be used to investigate micro-flow in rectangular channels. These equations are

perhaps suitable for micro-flow because the model deals with motion at the particle or molecular level. The theory can characterize the flow system through description of distribution of motion or displacement of the micro-particles, which can be verified experimentally at the Louisiana Tech University Institute for Micro-manufacturing.

### **1.3. Organization of the Dissertation**

This dissertation is organized as follows: In chapter 2, a review of related research is presented. In chapter 3, the equations and boundary conditions for a model based on the Kolmogorov three-dimensional forward equations are presented. In chapter 4, the numerical method including numerical schemes and various computation details are discussed. In chapter 5, specific simulation problems and computational results are described. In chapter 6, a conclusion and discussion are provided.

## **CHAPTER 2**

### **RELATED RESEARCH**

Several effects normally neglected when considering macro-scale flow may exist in micro-scale convection. The first of these micro-scale phenomena are two- and three-dimensional transport effects. Another micro-scale effect is that of temperature variations of the transport fluid, which can cause a significant variation in fluid properties throughout a micro-system. In liquids, the influence of molecular polar forces increases. The rarefied dynamics model is based on flow of molecules near a surface, which may be classified as specular or diffuse. Free molecular flow represents the other extreme where interaction between molecules rarely occurs. There is little build-up of molecules near the wall, as in continuum flow. Slip flow occurs between these extremes when there are slight rarefaction effects. The aforementioned effects and conditions are not new, but none of them have been studied extensively in relation to micro-scale flow. Too few experimental data exist to determine if slip flow becomes important as fluid convection systems are reduced in size. Research into micro-systems is just now beginning to shift into areas other than fabrication (Bailey, Ameen, Warrington, and Savoie, 1995).

The laws of hydrodynamic flow developed for a macro-scale continuum fluid (i.e. the Navier-Stokes Theory) may no longer be applicable to micro-scale flow. The currently available experimental data for micro-scale tubes and channels with characteristic dimensions of one to tens of micro-meters are inconclusive. When the

external characteristic length (e.g., film thickness, channel depth) becomes comparable with the internal characteristic length (e.g., molecular dimension, radius of gyration of a polymeric molecule, gas mean free path), the classical Navier-Stokes theory cannot explain the flow behavior. Eringen and Okada introduced a lubrication theory for fluids with micro-structure. This theory produces an excellent fit for data collected by other researchers for film thickness of up to  $300nm$  and is capable of predicting viscosity changes with addition of trace amounts of water to some organic polymers (Papautsky, Brazzle, Ameal, and Frazier, 1998).

Applications of couple stress and micro-polar theories to the problems of Couette and Poiseuille flows between two parallel plates were discussed and compared by Ariman and Cakmak (1967). Comparisons were made with the results given by Stokes. The micro-polar fluid theory presented gave two independent equations to describe the velocity and the micro-rotation velocity fields, thus allowing the specifications of both the velocity and micro-rotation velocity at the boundaries independently.

Ariman, Cakmak, and Hill (1967) analyzed the flow of micro-polar fluids between two concentric cylinders, first for the use of Couette flow and the toroidal pressure gradient being zero, then for the case of Poiseuille flow due to the pressure gradient in the axial direction. Results were presented graphically and compared with classical results and a discussion of the differences was provided.

Eringen (1969) derived equations of motion, constitutive equations, and boundary conditions for a class of micro-polar fluids, which can stretch and contract. Eringen conjectured that the model constructed had applications in liquid crystals, fluids

with polymeric additives, and turbulent motion of Newtonian fluids. The most general of this class is the simple micro-fluids in which the fluid, in addition to its classical translatory degrees of freedom, represented by a velocity field  $v$ , possesses three gyration, vector fields  $v_k$ . These latter degrees of freedom provided the necessary instrument to account for the intrinsic rotary motions and stretch of the local fluid elements. Because of these additional degrees of freedom, the theory of simple micro-fluids was believed to have many important applications in the fields of structural continuum, such as anisotropic fluids, liquid crystals, fluids carrying additives, fluids with surface tensors, etc. The governing equations obtained for such fluids were complicated, and the mathematical treatments of various important fluid notions still remain unstudied.

Ahmad (1976) studied boundary layer flow of micro-polar fluid over a semi-infinite plate and discussed the theory of micro-polar fluid and its application to the dynamics of low concentration suspension flow. Some estimates of the coefficients of viscosity were given in terms of concentrations and length scale of suspension. For variable micro-inertia it was shown that it is possible to find a self-similar solution. The partial differential equations of motion were then reduced to differential equations. Numerical solutions of the equations were then obtained and the distribution of velocity, micro-rotation, shear and couple stress across the boundary layer were plotted. The velocity profile was observed to change slightly in the range of the values studied but the gyration and couple varied appreciatively with small changes in parameters. Different coefficients are used for particles with intense rotational Brownian motion and

for relatively large particles whose orientation is not influenced by the Brownian motion.

Eringen (1980) introduced a continuum theory of anisotropic fluids. Balance laws were based on the micro-polar continuum mechanics. Properly invariant constitutive equations were established and restricted by the second law of thermodynamics. The field equations were solved for the shear flow of rod-like suspensions in viscous fluids. Eringen was interested in the development of a theory which considered the fluid orientable at the outset rather than the classical approach based on building the theory from interactive motions of its constituents. Eringen's work established properly invariant constitution equations for anisotropic micro-polar fluids. Together with the basic laws of micro-polar mechanics, these equations provided the necessary field equations for the treatment of physical problems in this field.

Olmstead and Majumdar (1983) considered the Oseen linearization of the equations governing steady, incompressible flow of a micro-polar fluid in two-dimensions. Attention was focused on the problem of determining the fundamental solution of these equations. The fundamental solution of these equations was reduced to that of finding two scalar functions, each of which satisfies a fourth-order partial differential equation. Since this fundamental solution represents the basic element for all two-dimensional flows, Olmstead and Majumdar foresaw applications such as solving flows past obstacles, investigating various boundary behaviors and examining injection-suction problems. One of the principle applications of the fundamental solution was to obtain an integral for the flow variables.

Kolpashchikov, Migun, and Prokhorenko (1983) deduced formulae for micro-polar fluid viscosity coefficients on the basis of some viscometric and thermal measurements. Results of viscometric measurements allowed the determination of two characteristic parameters of a micro-polar fluid, which were applied for the description of its flow in channels in the majority of cases. The subsequent measurement of fluid heating due to energy dissipation permitted the viscosity coefficients and form of the boundary conditions for the micro-rotation vector to be determined.

A perturbation method to investigate analytically the nonlinear stability behavior of a thin micro-polar liquid film flowing down a vertical plate was used by Hung and Leschziner (1984). The conservation of mass, momentum, and angular momentum were considered and a corresponding nonlinear generalized kinematic equation for the film thickness was derived. Results showed that both supercritical stability and subcritical instability were found in the micro-polar film flow system. This analysis showed that the effect of the micro-polar parameter  $R (=k/\mu)$  was to stabilize the film flow, that is the stability of the flowing film increased with the increasing magnitude of the micro-polar parameter  $R$ . Also, the analysis showed that the micro-polar coefficients,  $\Delta(=h_0^2/j)$  and  $\lambda(=\gamma/\mu j)$ , had very little effect on the stability of the micro-polar film.

The principle of exchange of stabilities was shown to hold for the convection motion in a micro-polar fluid. The convection motion was less stable for micro-polar than for Newtonian viscous fluid. Can, Huy, and Cau (1989) performed this study of convection motion in a micro-polar fluid.



Das and Sanyal (1990) discussed unsteady flow of a micro-polar fluid with periodic pressure gradient. They obtained and depicted through figures the expressions for velocity and the micro-rotation components.

Micro-polar fluids are models for rheologically complex liquids such as blood and dilute suspensions introduced by Eringen. Easwaran and Majumdar (1990) explicitly constructed fundamental singular solutions for the non-steady (causal) Stokes-linearized two-dimensional equations of micro-polar flow. The resulting solutions required the factorization of a fourth-order partial differential operator into two quadratic operators. This factorization was achieved under a certain condition on the parameters of the problem. The use of the fundamental solutions in unsteady flow problems was discussed.

Ciarletta (1995) was concerned with the linear theory of heat-conducting micro-polar fluids. His study presented the fundamental system of fluid equations and derived a linear theory appropriate to small departures from an equilibrium state. Ciarletta established a representation of the Galerkin type and derived the fundamental solutions in the case of steady vibrations. A uniqueness result and a variational theory were presented.

Rees and Bassom (1996) considered the Blasius boundary-layer flow of a micro-polar fluid over a flat plate. A full derivation of the boundary-layer equations was given. The resulting non-similar equations were solved using the Keller-box method and solutions for a range of parameters were presented. Rees and Bassom found that a two-layer structure developed as the distance downstream increased. An asymptotic analysis of the structure was presented, and the agreement between the

analysis and the numerical solution was excellent. A wide selection of numerical results were presented giving the evolution of the velocity and gyration component profiles, and the shear stress and rate of change of gyration components at the solid surface.

Guohua Liu (1999) modeled fluid flow in micro-channels using the Navier-Stokes equations. A micro-fluid model was developed to investigate the influence of micro-effects, such as gyration, in micro-scale flows. This model was based on Eringen's simple micro-fluid, and was simplified for an incompressible, two-dimensional, isothermal, and micro-isotropic case.

Beskok and Karniadakis (1992) developed a spectral element methodology to simulate unsteady two- and three-dimensional flows in complex micro-domains. Simulation tests were performed for a variety of prototype internal and external flows that demonstrate the validity and flexibility of the developed methodology in modeling fluid dynamics and transport in complex micro-geometries. The effort of slip-flow on skin friction reduction and associated increases in mass flow rate as well as the variation of the normal stresses is investigated as a function of the Knudsen number. Results demonstrate that a "stand-alone" simulation approach free of numerical artifacts can be employed to efficiently predict momentum and energy transport in micro-devices.

Gas flow in micro-channels is typically classified into one of four flow regimes: continuum flow, slip flow, transition flow, and free molecular flow. Chen, Lee, and Sheu (1998) presented a numerical study of gas flow in micro-channels in terms of slip flow. The model they proposed assumed the fluid is a continuum with a slip boundary condition on the channel wall. Results revealed interesting features of micro-channel

flows. The pressure gradient was smaller at the inlet and increased gradually toward the outlet. Chen *et al.* reasoned that as the fluid proceeds along the channel, fluid pressure drops due to friction against the walls. This pressure drop reduces the density but increases the velocity since the continuity equation has to be satisfied. Two channels with dimensions of  $3000\mu\text{m}$  by  $40\mu\text{m}$  by  $1.2\mu\text{m}$  and  $7500\mu\text{m}$  by  $52.25\mu\text{m}$  by  $1.33\mu\text{m}$  were used. Because of the extraordinarily small dimensions, a large pressure gradient was required to drive the flow. Although the pressure gradient is large, the velocity remains very small in the cases studied owing to the high shear stress at the wall. (Nitrogen maximum velocity =  $1.16\text{ m/s}$  mass flow rate =  $4.60 \times 10^{-9}$  for a pressure ratio of 2.701) Since the Reynolds numbers were small ( $10^{-3}$  to  $10^{-2}$ ) for the flows simulated, they were safely assumed to be laminar.

Beskok and Karniadakis (1995) presented models and a computational methodology for simulating gas micro-flows in the slip-flow regime for which the Knudsen number is less than 0.3. The formulation was based on the classical Maxwell/Smoluchowski boundary conditions that allow partial slip at the wall. A high-order slip boundary condition developed in previous work was modified so that it could be easily implemented to provide enhanced numerical stability. This modification also extends a previous formulation for incompressible flows to include compressibility effects primarily responsible for the nonlinear pressure distribution in micro-channel flow. Beskok and Karniadakis focused on the competing effects of compressibility and rarefaction in internal flows in long channels. Several simulation results were presented and comparisons were provided with available experimental data. A specific set of benchmark experiments was proposed to systematically study compressibility,

rarefaction, and viscous heating at the micro-scale level in order to provide validation to numerical models and the slip flow theory in general as well as to establish absolute standards in the relatively young field of fluid mechanics.

Kavehpour, Faghri, and Asako (1997) used a two-dimensional flow and heat transfer model to study gas compressibility and rarefaction in micro-channels assuming a slip flow regime. The numerical methodology was based on the control volume finite difference scheme. To verify the model, the mass flow rate was compared with the experimental results of helium through a micro-channel. It was seen that the effect of rarefaction and compressibility is a function of Reynolds number. The mass flow and friction coefficient results were compared with the available experimental results. The friction coefficients and Nusselt number (for both constant wall temperature and constant wall heat flux) were reduced in comparison with the continuum results. Also, it was found that rarefaction and compressibility were related and had a pronounced effect on fluid flow characteristics. For higher Reynolds numbers, the effect of Mach number was more important than the effect of Knudsen number, and for lower Reynolds numbers, the effect of Knudsen number was dominant.

Arkilic, Breuer, and Schmidt (1994) measured helium mass flows through micro-channels (52.25 micro-meters wide 1.22 micro-meters deep and 7500 micro-meters long) for inlet pressures ranging from 1.2 to 2.5 atmospheres with outlet pressures at atmospheric level. The effect of the slip velocity on the mass flow prediction of the Navier-Stokes equations was investigated and compared with the measured flow results. It was found that the no-slip solutions of the Navier-Stokes equations failed to adequately model the momentum transferred from the fluid to the

channel walls and therefore underestimated the mass flow for given inlet and outlet pressures. However, by including a slip-flow boundary condition at the wall, which was derived from a momentum balance, one can accurately model the mass flow-pressure relationship. Even at atmospheric conditions the ratio of the mean free path to the characteristic dimension was found to be appreciable. This ratio, known as the Knudsen number, increased and the exchange of energy and momentum between the systems and the environment exhibited behavior that was attributed to the discrete molecular composition of the environment: the gas exhibited non-continuum dynamics. Arkilic, Breuer, and Schmidt (1994) developed a simple model that predicted an increase in the mass flow (decrease in friction factor) for micro-channels. They also demonstrated a model that predicted an increase in the mass flow for given inlet and outlet pressures for micro-channel flows that was based on the no-slip solution to the Navier-Stokes Equations. Arkilic, Breuer, and Schmidt designed and fabricated a micro-machined device that allowed verification of this model. It was shown that, for a large Knudsen number, flows that flow in micro-channels may not be modeled with the no-slip boundary condition.

Choi, Barron, and Warrington (1991) measured the friction factors, inner-wall surface roughness, and convective heat transfer coefficients for flow of nitrogen gas in micro-tubes for both the laminar and turbulent flow regimes. The experimental results indicated significant departures from the thermofluid correlation used for conventional-sized tubes. In turbulent flow, the experimental results indicated that the Colburn analogy,  $j_H=f/8$ , was not valid for micro-tubes having inside diameters less than 90 micro-meters. The measured Nusselt numbers for convective heat transfer in micro-

tubes in turbulent flow were as much as 7 times the values by the Colburn analogy. The  $L/D$  ratio for the tubes was between 640 (81-micro-meter tube) and 8100 (3-micro-meter tube), so the flow was fully established both hydraulically and thermally. The measured friction factors in laminar flow were less than those predicted from the macro-tube correlation, and the friction factors in the turbulent flow were also smaller than those predicted by conventional correlations. No roughness dependence was observed from the micro-tube data obtained in this study. The measured heat transfer coefficients in laminar flow exhibited a Reynolds number dependence in contrast to the conventional prediction for fully established laminar flow, in which the Nusselt number is constant. Neither the Colburn analogy nor the Petukhov analogy between momentum and energy transport was supported by the present data for micro-tubes. One suggested reason for this result is the suppression of the turbulent eddy motion in the radial direction (but not in the axial direction) due to the small diameter of the channels.

Beskok and Karniadikis (1997) studied backwards-facing step channel as complex prototype geometry for separated micro-flows. This test case was important in quantifying the behavior of rarefied flows under severe adverse pressure gradients and separation in the slip flow regimen (Knudsen number  $Kn \leq 0.1$ ), with the objective of investigating the validity of continuum-based slip models under separation. Solutions of compressible Navier-Stokes equations subject to various velocity slip and temperature jump boundary conditions are compared against predictions of direct simulation Monte Carlo (DSMC) method, employing a variable hard sphere (VHS) model.

Pong, Ho, Liu, and Tai (1994) measured the pressure distribution along a micron-sized channel by using a surface micro-machined micro-flow system. Both nitrogen and helium were used as a working medium in order to examine the effects of the Knudsen number. Two generations of micro-flow systems were manufactured and examined. The pressure distribution was found to be a nonlinear function inside a micro-channel having a uniform cross-sectional area. The distribution was affected by the viscous dissipation. As the Knudsen number changed the nonlinear pressure distribution also changed, possibly a Knudsen number effect. An integrated micro-channel/pressure sensor system was fabricated using combined surface micro-machining and bulk micro-machining.

Stokes (1966) considered the effects of couple stresses in fluids. Linearized constitutive equations were posed for force and couple stress. A series of boundary-value problems were solved to indicate the effects of couple stresses as well as for experiments measuring the various material constants. Stokes found that a size effect comes in which is not present in the non-polar case (couple stresses absent). A size-dependent effect, not existing in the non-polar case, was predicted. The effects of couple stresses were quite large for small values of the non-dimensional number  $a = h/l$ , where  $h$  = typical dimension of the flow geometry, and  $l$  = the material constant  $l = (\eta/\mu)^{1/2}$ . If  $l$  was a function of the molecular dimensions of the liquid, then it varied greatly for different liquids. Stokes expected couple stresses to appear in noticeable magnitudes in liquids with very large molecules. He recommended experimentation on fluids having very different molecular sizes in order to search for the existence of couple stresses experimentally.

Pfahler (1992) experimentally measured flow resistance of the channels. A viscosity model that included wall effect to explain the data was developed but had limited success. Non-Newtonian fluids such as serum, plasma, washed blood cells, and whole blood were used. Experimental methodology was developed to examine the behavior of Newtonian and non-Newtonian fluids in extremely small channels.

Experiments were conducted by Peng, Peterson, and Wang (1994b) to investigate the flow characteristics of water flowing through rectangular micro-channels having hydraulic diameters of 0.133-0.367 *mm* and *H/W* ratios of 0.333-1. As the size of channels and/or tubes diminished to the order of several hundred to 0.1 micro-meters, the fluid flow behavior in these micro-channels or tubes was strongly influenced by the wall effect, and deviated from the normal situation described by the Navier-Stokes equations. The experiments indicated several aspects significantly different from the flow in conventional-sized channels. First, the flow mode conversion from laminar to transition regime occurred at much smaller Reynolds numbers, and the transition region was limited in a smaller Reynolds number zone than for normal channels. Accordingly, the fully developed turbulent flow took place at lower Reynolds number. The conversion Reynolds numbers were heavily dependent on the hydraulic diameter of the micro-channel. Second, the friction behavior for both laminar and turbulent flow deviated from the classical theories. Finally, experiments and analyses indicated that the geometric parameters of micro-channels, especially the hydraulic diameter and *H/W* ratio, had a critical effect on liquid flow through micro-channels, and determined the flow friction performance.



Harley, Huang, Bau, and Zemel (1995) presented compressible gas flow in channels as an experimental and theoretical investigation of low Reynolds number and high subsonic Mach number. Nitrogen, helium, and argon gases were used. The measured friction factor was in good agreement with theoretical predictions assuming isothermal, locally fully developed, first-order, and slip-flow. Numerical simulations were performed assuming pressure to be uniform in the conduit cross-sections perpendicular to the direction of the flow and neglecting the transverse velocity. Consequently, the 'locally fully developed' approximation led to predictions, which are in reasonable agreement with the Navier-Stokes equations, and with experimental observations.

Stanley (1997) investigated the fluid mechanic and heat transfer characteristics of two-phase, two-compartment flow in rectangular micro-channels. Both single-phase and two-phase experiments were performed. Dimensional analysis was used to determine the important pressure drop and heat transfer parameters. These parameters were curve-fit against experimental data, using multiple linear regression techniques. Two flow models were considered. One was for homogenous flow, which considered the fluid properties to be averages, based on the quality of the two components. The other was separated flow, which considered each component of the flow separately. Flow experiments were conducted on an apparatus built by Stanley and Darin Bailey (1996). Yu, Warrington, Barron, and Ameel (1994) investigated fluid flow and heat transfer characteristics of dry nitrogen gas and water in micro-tubes, with diameters of 19, 52, and 102 micro-meters, for  $Re$  ranging from 250 to over 20,000 and  $Pr$  ranging from 0.7 to 5.0. The friction factor results confirmed the findings of earlier

investigators who reported a lower value for the product,  $f^*Re$ , for laminar flow in micro-tubes than for larger tubes (e.g., 53 instead of 64). In the turbulent regime, the heat transfer was enhanced, and the Nusselt number was considerably higher than would be predicted for larger tubes. A theoretical scaling analysis indicated that turbulent momentum and energy transport in the radial direction was significant in the near wall zone in a micro-tube. By considering the turbulent eddy interacting with the walls as a frequent event, an analogy was developed that could account for the lower friction factors and increased heat transfer in the turbulent flow regime for micro-tubes. However, these research efforts did not adequately explain the heat and momentum transfer processes in micro-tubes or micro-channels in terms of the governing parameters. There appeared to be a lack of systematic research on this subject. Measurements of the flow rate and inlet pressure were sufficient to determine the friction factor both for compressible (nitrogen gas) and incompressible (water) flow. From the previous scaling analysis, it was reasoned qualitatively that the friction factor should be lower in micro-tubes than in larger tubes. In the laminar zone, flow friction was lower than that predicted by the Navier-Stokes equations, but the relation between  $f$  and  $Re$  remains linear both in compressible and incompressible flow. In the turbulent flow regime, flow friction was also found to be reduced compared with large tubes. In the turbulent regime, heat transfer was enhanced, and the Nusselt number was much higher than that predicted by conventional relations for a large tube.

The experimental measurements by Peng, Peterson, and Wang (1994a) indicated that the upper bound of the laminar heat transfer regime occurred at a Reynolds number of 200-700, and fully turbulent convective heat transfer was reached at Reynolds

numbers of 400-1500. The transition Reynolds number diminished with a reduction of the micro-channel dimensions, and the transition range was observed to become smaller in magnitude. The geometric parameters were found to be important variables that could significantly affect the flow characteristics and heat transfer. Practical applications involving the thermal control of high-density electronics, bioengineering devices, and mini heat exchangers have all used micro-structures capable of unusually high levels of heat removal. New empirical correlations for the predictions of heat transfer were suggested based on this additional experimental data. The experiments demonstrated that the laminar convective heat transfer had maximum value when the aspect ratio  $H/W$  was approximately equal to 0.75. Decreasing the hydraulic diameter caused the turbulent heat transfer transition to diminish to nearly zero as the aspect ratio approached unity.

A micro-flow sensor for fluids, which operates over the  $5\mu\text{m}/\text{min}$  to  $500\mu\text{m}/\text{min}$  range, allowing the detection of minute volumes, down to nanoliter resolution was reported by Gass, Van der Schoot, and De Rooij (1993). To meet the ever-increasing demand in high-precision flow control, Gass proposed a new approach based on drag force measurement that will allow easy integration with other micro-fluid elements such as silicon micro-fabricated pumps. The flow sensor was also presented, explaining the operating principle, the manufacturing process and the experimental result obtained.

When a soluble substance is introduced into a fluid flowing slowly through a small, bore tube it spreads out under the combined action of molecular diffusion and the variation of velocity over the cross-section. Taylor (1953) showed analytically that the distribution of concentration produced in this way is centered at a point, which moves

with the mean speed of flow and is symmetrical about it in spite of the asymmetry of the flow. The dispersion along the tube was governed by a coefficient of diffusivity, calculated from the observed distributions of concentration. Since the analysis related the longitudinal diffusivity to the coefficient of molecular diffusion, observations of concentration along a tube provided a new method for measuring diffusion coefficients. The coefficient obtained was found, with potassium permanganate, to agree with that measured in other ways. The results were believed to be useful to physiologists who may wish to know how a soluble salt is dispersed in blood streams.

Aris (1955) presented a new basis for Taylor's analysis, which removed the restrictions of solute in terms of its moments in the direction of flow. Aris showed that the rate of growth of the variance was proportional to the sum of the molecular diffusion coefficient,  $D$ , and the Taylor diffusion coefficient  $ka^2U^2/D$ , where  $U$  is the mean velocity and  $a$  is the dimension characteristic of the cross-section of the tube. An expression for  $k$  was given in the most general case, and it was shown that the distribution of the solute is normal.

Bhattacharya and Gupta (1984) presented a new derivation of Taylor's theory of solute transport in a straight capillary. The results involved Brownian motion and the integral of an ergodic Markov process that was asymptotically a Brownian motion.

## CHAPTER 3

### MODEL

#### 3.1. Introduction

Typically, a flow is considered to be in one of four regimes according to its Knudsen number. Different authors defined these regimes using slightly different Knudsen number ranges. For gas flow, Beskok & Karniadakis (1992) proposed the following classification:

$Kn \leq 0.001$	Continuum Flow
$0.001 < Kn \leq 0.1$	Slip Flow
$0.1 < Kn \leq 10$	Transition Flow
$Kn > 10$	Free Molecular Flow

We follow this classification as have other researchers (Bailey *et al.*, 1995; Kavehpour *et al.*, 1997; Chen *et al.*, 1998).

In most applications of fluid mechanics, the physical dimensions of the bodies about which a flow may be taking place are very large compared to the size of the molecules themselves and to the distance between molecular interactions. In such a case, the density and other fluid properties will vary smoothly from one point to another. The term *continuum* describes this idea, and such fluids are considered *continuous* in this sense (Sabersky, 1999).

Slip flow and transition flows are additional classifications for rarefied gas,

which cannot be considered an absolutely continuous medium nor a free-molecule flow in the Knudsen number range between  $10^{-3}$  and 10 (Beskok, Karniadakis, and Trimmer, 1996). At normal pressures, a gas may be considered a continuum, but when the pressure is sufficiently low, the average distance between molecules may become large compared to the size of an object over which the flow takes place. Such a tenuous, or *rarefied*, gas is still a fluid, but it does not fulfill the requirements of a continuum fluid (Sabersky, 1999).

For continuum flow, the Navier-Stokes equations govern the flow. In the slip-flow regime, deviations from the state of continuum are relatively small, and the flow is still governed by the Navier-Stokes equations. The rarefaction effect of the flow is modeled through the partial slip at the wall using Maxwell's velocity slip and von Smoluchowski's temperature jump boundary condition. The validity of this kind of model was assessed by various authors (Beskok, 1996; Chen *et al.*, 1998). For flows in the high transition or free molecular regimes, the Navier-Stokes equations break down and have to be substituted either by the Boltzmann equation, which is valid at the microscopic level, by continuum approximations (Liu, 1999), or by stochastic models.

The aspect ratio, defined as channel length to channel height or width, of a micro-channel often is large. If we neglect flow change in the direction of width, usually achieved when the aspect ratio is greater than 7, then the flow can be reasonably assumed to be two-dimensional in the streamwise direction. It can be shown that for flows with a large aspect ratio, the three-dimensional flow rate is calculated by  $Q_{3D} = Q_{2D}(1 - h^2/w^2)$ , where  $h$  and  $w$  are channel height and width, respectively (Chen *et al.*, 1998).

### **3.2. Equations and Boundary Conditions**

In the classic work of Taylor (1953) continued by Aris (1956), it was shown that when a solute in low concentration is injected into a liquid flowing through an infinite straight capillary of uniform cross-section with a steady convective velocity, the concentration along the capillary (averaged over the cross-section) is asymptotically Gaussian. Let the  $x$ -axis be taken to be a line inside the capillary parallel to its length and thus the direction of flow; the cross-section  $E$  is the  $(y, z)$ -plane bounded by a smooth curve  $\Gamma$ . Let  $C(x, t)$  denote the solute concentration at the point  $x=(x, y, z)$  at time  $t$ . Taylor's starting equation is

$$\frac{\partial C}{\partial t} = D_0 \left( \frac{\partial^2 C}{\partial x^2} + \frac{\partial^2 C}{\partial y^2} + \frac{\partial^2 C}{\partial z^2} \right) - U_0 f(y, z) \frac{\partial C}{\partial x} \quad \text{for } \bar{x} \in R^1 \times E^0, t > 0 \quad (3.1)$$

$$\frac{\partial C}{\partial \nu} = 0 \quad \text{for } \bar{x} \in R^1 \times \Gamma, t > 0. \quad (3.2)$$

Here (i)  $D_0$  is the Einstein molecular diffusion coefficient, (ii)  $(U_0 f(y, z), 0, 0)$  is the velocity field of the liquid,  $U_0$  being the maximum velocity in the direction of flow at the center of the channel, (iii)  $\partial / \partial \nu$  denotes differentiation along the outward normal to the capillary boundary.  $E^0$  is the interior of the cross-section  $E$ . The case explicitly dealt with by Taylor (1953) was that of a circular cross-section  $E = \{y^2 + z^2 \leq a^2\}$ ,

where the velocity at a distance  $r = \sqrt{y^2 + z^2}$  from the centerline of the channel is

$$U_0 f(y, z) = U_0 \left( 1 - \frac{y^2 + z^2}{a^2} \right). \quad (3.3)$$

This equation is modified for an assumed velocity field of

$(U_0 f(y, z), b_1(y, z), b_2(y, z))$ , where  $b_1$  and  $b_2$  are continuously differentiable functions on

the cross-section  $E$ .  $D_0$  is replaced by  $\varphi$ , the diffusivity or dispersion coefficient of water. The modified Taylor equation expressed in terms of particle motion instead of concentration gives rise to the Fokker-Planck or Kolmogorov forward equation:

$$\frac{\partial P}{\partial t} = \varphi \left( \frac{\partial^2 P}{\partial x^2} + \frac{\partial^2 P}{\partial y^2} + \frac{\partial^2 P}{\partial z^2} \right) - \mu_0 f(y, z) \frac{\partial P}{\partial x} - \frac{\partial(b_1 P)}{\partial y} - \frac{\partial(b_2 P)}{\partial z}$$

$$\text{for } \bar{x} \in R^1 \times E^0, t > 0 \quad (3.4)$$

and

$$\varphi \frac{\partial P}{\partial \nu} - P(b \cdot \nu) = 0 \text{ for } \bar{x} \in R^1 \times \Gamma, t > 0. \quad (3.5)$$

where  $P = P(x, y, z; t)$  is the transition probability density that a particle starting at the point

$x_0, y_0, z_0$  at time  $t_0$  is in position  $x, y, z$  at time  $t$ .  $\varphi \left( \frac{\partial^2 P}{\partial x^2} + \frac{\partial^2 P}{\partial y^2} + \frac{\partial^2 P}{\partial z^2} \right)$  represents the

diffusion part of the equation,  $\mu_0 f(y, z) \frac{\partial P}{\partial x} - \frac{\partial(b_1 P)}{\partial y} - \frac{\partial(b_2 P)}{\partial z}$  represents the convection

part of the equation, and  $b \cdot \nu = b_1 \nu_1 + b_2 \nu_2$  is the velocity at the boundary in the

direction of the unit normal (Bhattacharya and Majumdar, 1980, eq. [4.21]).

For the rectangular channel the linearized Navier-Stokes equation is modified to:

$$f(y, z) = \left( 1 - \frac{y^2}{a^2} \right) \left( 1 - \frac{z^2}{a^2} \right) \quad (3.6)$$

The drift or convective part of the equation resulting from this modification is

$$b_1 = \mu_y \left( 1 - \frac{y^2}{a^2} \right) \quad (3.7)$$

$$b_2 = \mu_z \left( 1 - \frac{z^2}{a^2} \right) \quad (3.8)$$



$\mu_y = \mu_z$  and indicate the velocities in the  $y$  and  $z$  directions respectively.  $\mu_y$  and  $\mu_z$  are one or two orders of magnitude smaller than  $\mu_0$ .

The modeled channel has geometric dimensions  $x = 10$  mm and  $y = z = 0.1$ mm.

The initial conditions for  $x=0$  are

$$P(x, y, z, t_0) = \frac{1}{V} \quad (3.9)$$

where  $V = \Delta x \Delta y (ny - 1) \Delta z (nz - 1)$ ;  $ny$  and  $nz$  represent the number of grid points in the  $y$  and  $z$  directions. The boundary conditions for the  $x$  direction are

when  $x = 0$  (entrance)

when  $x = 10$ mm (exit)

$$\varphi \frac{\partial}{\partial x} P - \mu_0 f P = 0$$

$$P = 0$$

The boundary conditions for the  $y$  and  $z$  directions are symmetrical.

The boundary conditions for the  $y$  direction are

when  $y = -0.05$ mm

when  $y = 0.05$ mm

$$-\varphi \frac{\partial}{\partial y} P + P b_1 = 0$$

$$\varphi \frac{\partial}{\partial y} P - P b_1 = 0$$

The boundary conditions for the  $z$  direction are

when  $z = -0.05$ mm

when  $z = 0.05$ mm

$$-\varphi \frac{\partial}{\partial z} P + P b_2 = 0$$

$$\varphi \frac{\partial}{\partial z} P - P b_2 = 0$$

## CHAPTER 4

### NUMERICAL METHOD

#### 4.1. Introduction

As stated in chapter 3, the modified Fokker-Planck or Kolmogorov forward equation in 3-D is

$$\frac{\partial P}{\partial t} = \varphi \left( \frac{\partial^2 P}{\partial x^2} + \frac{\partial^2 P}{\partial y^2} + \frac{\partial^2 P}{\partial z^2} \right) - \mu_0 f(y, z) \frac{\partial P}{\partial x} - \frac{\partial(b_1 P)}{\partial y} - \frac{\partial(b_2 P)}{\partial z}$$

for  $\bar{x} \in R^1 \times E^0$ ,  $t > 0$ , where  $\bar{x} = (x, y, z; t)$  (4.1)

and

$$\varphi \frac{\partial P}{\partial v} - P(b \cdot v) = 0 \text{ for } \bar{x} \in R^1 \times \Gamma, t > 0. \quad (4.2)$$

Equation (4.1) was discretized using the Central Difference and Backward Difference methods described by Strickwerda (1989). The Jacobi method was used to solve the equation.

#### 4.2. Discretization

Using the Central Difference and Backward Difference methods Equation (4.1) becomes:

$$\begin{aligned}
\frac{\partial P}{\partial t} &= \frac{P_{ijk}^{n+1} - P_{ijk}^n}{\Delta t} = \\
&\frac{1}{2} \varphi \left( \frac{P_{i+1,jk}^{n+1} - 2P_{ijk}^{n+1} + P_{i-1,jk}^{n+1}}{\Delta x^2} \right) + \frac{1}{2} \varphi \left( \frac{P_{i+1,jk}^n - 2P_{ijk}^n + P_{i-1,jk}^n}{\Delta x^2} \right) \\
&+ \frac{1}{2} \varphi \left( \frac{P_{ij,k+1}^{n+1} - 2P_{ijk}^{n+1} + P_{ij,k-1}^{n+1}}{\Delta y^2} \right) + \frac{1}{2} \varphi \left( \frac{P_{ij,k+1}^n - 2P_{ijk}^n + P_{ij,k-1}^n}{\Delta y^2} \right) \\
&+ \frac{1}{2} \varphi \left( \frac{P_{ijk+1}^{n+1} - 2P_{ijk}^{n+1} + P_{ijk-1}^{n+1}}{\Delta z^2} \right) + \frac{1}{2} \varphi \left( \frac{P_{ijk+1}^n - 2P_{ijk}^n + P_{ijk-1}^n}{\Delta z^2} \right) \\
&- \mu_0 f_{jk} \frac{P_{ijk}^{n+1} - P_{i-1,jk}^{n+1}}{\Delta x} - \left( \frac{b_{1_{jk}} P_{ijk}^{n+1} - b_{1_{j-1k}} P_{ij-1k}^{n+1}}{\Delta y} \right) - \left( \frac{b_{2_{jk}} P_{ijk}^{n+1} - b_{2_{jk-1}} P_{ijk-1}^{n+1}}{\Delta z} \right)
\end{aligned} \tag{4.3}$$

where  $P_{ijk}^n = P(i\Delta x, j\Delta y, k\Delta z; n\Delta t) \cong P(x, y, z; t)$ ;  $\Delta x$ ,  $\Delta y$ , and  $\Delta z$  are the grid sizes in the  $x$ ,  $y$ , and  $z$  directions. Here  $i = 1, 2, \dots, nx$ ;  $j = 1, 2, \dots, ny$ ;  $k = 1, 2, \dots, nz$ .

### **4.3. Treatment of Boundary Conditions**

The discretized boundary conditions for the  $x$  direction are:

**Entrance:** when  $x = 0$  ( $i = 0$ ), the first-order discretized boundary condition is

$$\varphi \left( \frac{P_{1,jk} - P_{0,jk}}{\Delta x} \right) - \mu_0 f_{0jk} P_{0,jk} = 0 \tag{4.4}$$

**Exit:** when  $x = 10mm$  ( $i = nx$ )

$$P_{n,jk} = 0 \tag{4.5}$$

We consider the center line in the  $x$ -direction of the channel to have  $(x, 0, 0)$  coordinates.

As such  $y = -a + j * \Delta y$  and  $z = -a + k * \Delta z$ . Here,  $ny\Delta y = nz\Delta z = 2a = 0.1 \text{ mm}$ .

Hence, the discretized boundary conditions for the  $y$  direction are

$$\text{when } y = -a \text{ (} j = 0 \text{)}$$

$$-\frac{\varphi P_{i1k} - \varphi P_{i0k}}{\Delta y} + P_{i0k} b_{1,0k} = 0 \quad (4.6)$$

$$\text{at } j = a, b_1(0) = 0 \text{ and } P_{i0k} = P_{i1k}$$

when  $y = a$  ( $j = ny$ )

$$\frac{\varphi P_{inyk} - \varphi P_{iny-1k}}{\Delta y} - P_{inyk} b_{1,nyk} = 0 \quad (4.7)$$

$$\text{at } j = ny, b_1(ny) = 0 \text{ and } P_{inyk} = P_{iny-1k}$$

The discretized boundary conditions for the  $z$  direction are

when  $z = -a$  ( $k = 0$ )

$$-\frac{\varphi P_{ji1} - \varphi P_{ji0}}{\Delta z} + P_{ji0} b_{1,jo} = 0 \quad (4.8)$$

$$\text{at } k = 0, b_2(0) = 0 \text{ and } P_{ji0} = P_{ji1}$$

when  $z = a$  ( $k = nz$ )

$$\frac{\varphi P_{ijnz} - \varphi P_{ijnz-1}}{\Delta z} - P_{ijnz} b_{2,ynz} = 0 \quad (4.9)$$

$$\text{at } k = nz, b_2(nz) = 0 \text{ and } P_{ijnz} = P_{ijnz-1}$$

# CHAPTER 5

## THREE-DIMENSIONAL MICRO-CHANNEL FLOW

### 5.1. Description of Simulation

To illustrate the use of the present methods, we apply them to a developing flow in a three-dimensional micro-channel, as shown in Figure 5.1.

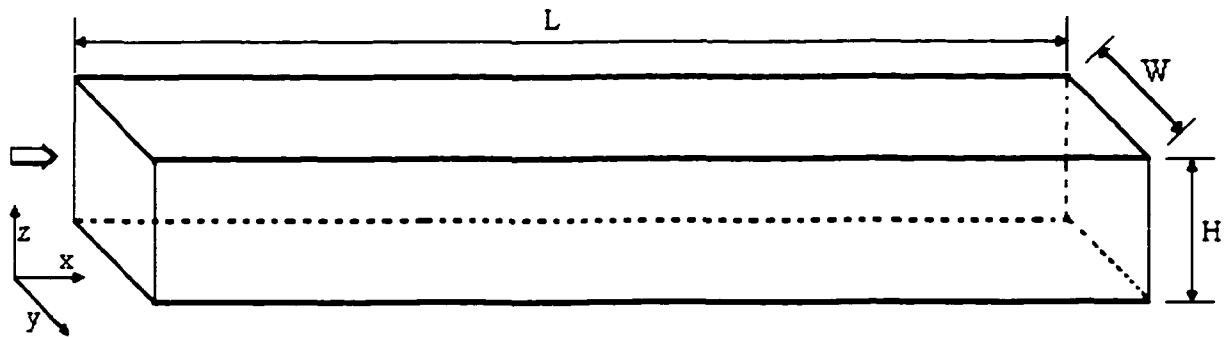


Figure 5.1 Physical domain for micro-channel flow

The channel length was considered to be 100 times its height and width with a length of 10mm in the  $x$  direction and 0.1 mm in both the  $y$  and  $z$  directions. In the  $x$  direction 1001 grid points were used. In the  $y$  and  $z$  directions 11 grid points were used. The grid size for the  $x$ ,  $y$  and  $z$  directions,  $\Delta x$ ,  $\Delta y$ , and  $\Delta z$  respectively, was 0.01.

The diffusivity coefficient of water,  $\phi$ , was set at 0.125 based on velocity measurements of flow in a bubble column (Nassar, Schmidt, and Luebbert, 1992). When  $\phi$  was held constant at 0.125 the coefficient of variation for each velocity was less than or equal to 5% (see Table 5.1).

Table 5.1 Calculations for the coefficient of variation,  $CV$ 

$\phi=\sigma^2/2$	$\sigma^2$	$\sigma$	$\mu$	$CV$
0.125	0.25	0.5	10	0.0500
0.125	0.25	0.5	50	0.0100
0.125	0.25	0.5	100	0.0050
0.125	0.25	0.5	200	0.0025
0.125	0.25	0.5	500	0.0010

The velocity,  $U_0$ , in the x direction at the middle of the channel was given values on the interval  $(0, \text{bound}]$  where bound is the length of the channel in the x direction. The velocities for the y and z directions,  $\mu_y$  and  $\mu_z$ , were multiples of  $\mu_0$ . Since the velocities in the y and z direction are usually much smaller than the velocity in the x direction,  $\mu_y$  and  $\mu_z$  were set equal to  $0.001 * \mu_0$ .

The value of  $a$  in Equation (2.6), represents half the length in the y and z directions given that the channel is symmetrical in the y and z direction. The value of  $\Delta t$  was 0.001. Calculations were performed for various lengths of time  $t$  to model the flow based on the average time of passage for a particle to exit the channel (see Table 5.2). A tolerance level of  $10^{-2}$  was used.

Numerical computations were performed for the stochastic model using the SGI Origin2000 parallel computer with 16 CPU at the Louisiana Tech University Center for Numerical Simulation and Modeling. C++ and Fortran were used in programming and Excel in data post-processing. A grid of  $1001 \times 11 \times 11$  nodes was used for all computations ( $\Delta x=0.01$ ,  $\Delta y=0.01$ ,  $\Delta z=0.01$ ,  $n_x=1000$ ,  $n_y=10$ ,  $n_z=10$ ). The time step was  $\Delta t=0.001$ .

Table 5.2 Times  $t$ , used in the numerical simulation based on twice the average time,  $\bar{t}$ , till exit.

length=10mm			time in seconds for each 10th of $2\bar{t}$									
$\bar{t} = \text{length/velocity}$												
Velocity (mm/s)	$\bar{t}$ (s)	$2\bar{t}$ (s)	1/10	2/10	3/10	4/10	5/10	6/10	7/10	8/10	9/10	10/10
10	1.00	2.00	0.200	0.400	0.600	0.800	1.000	1.200	1.400	1.600	1.800	2.000
50	0.20	0.40	0.040	0.080	0.120	0.160	0.200	0.240	0.280	0.320	0.360	0.400
100	0.10	0.20	0.020	0.040	0.060	0.080	0.100	0.120	0.140	0.160	0.180	0.200
200	0.05	0.10	0.010	0.020	0.030	0.040	0.050	0.060	0.070	0.080	0.090	0.100
500	0.02	0.04	0.004	0.008	0.012	0.016	0.020	0.024	0.028	0.032	0.036	0.040
			time steps for dt=0.001 for each 10th of $2\bar{t}$									
10	1.00	2.00	200	400	600	800	1000	1200	1400	1600	1800	2000
50	0.20	0.40	40	80	120	160	200	240	280	320	360	400
100	0.10	0.20	20	40	60	80	100	120	140	160	180	200
200	0.05	0.10	10	20	30	40	50	60	70	80	90	100
500	0.02	0.04	4	8	12	16	20	24	28	32	36	40

## 5.2. Simulation Results and Discussion of the Stochastic Model

Table 5.3 presents the probability integral  $\int_{-\infty}^d P(x;t)dx$  for the distance  $x$  traveled in the 1-D case at time  $t$  (Cox and Miller, 1965, p221, Eq[71]) for different particle velocities,  $\mu$ . An IMSL integration routine was used to integrate  $P(x;t)$ . As seen in Table 5.3, the total probability is equal to or less than one. The probability sum can be less than one because the distribution is truncated at the exit "d" as a result of the boundary condition  $P(d;t)=0$ .

Figures 5.2 shows the probability distribution for a homogenous diffusion process with  $t=1$ , one absorbing barrier at  $d=10\text{mm}$ , and velocity  $\mu=2,4,6,8$ , and 10. It can be seen in the figure that the variance  $\sigma^2 t$  is constant, but as expected, the distribution shifts with an increase in the mean,  $\mu$ . Figure 5.3 shows the probability

Table 5.3 Probability integral  $\int_{-\infty}^d P(x;t)dx$  of the one-dimensional time homogeneous diffusion process,  $P(x;t)$ , with  $\sigma = 0.5$  and an absorbing barrier at  $d=10mm$ .

	$\int_{-\infty}^d P(x;t)dx$				
t (sec)	u=2	u=4	u=6	u=8	u=10
0.25	1.00E+00	1.00E+00	1.00E+00	1.00E+00	1.00E+00
0.50	1.00E+00	1.00E+00	1.00E+00	1.00E+00	1.00E+00
0.75	1.00E+00	1.00E+00	1.00E+00	1.00E+00	1.00E+00
1.00	1.00E+00	1.00E+00	1.00E+00	1.00E+00	1.00E+00
1.25	1.00E+00	1.00E+00	1.00E+00	4.89E-01	3.42E-06
1.50	1.00E+00	1.00E+00	9.45E-01	4.92E-04	1.28E-16
1.75	1.00E+00	1.00E+00	2.15E-01	6.10E-10	3.05E-30
2.00	1.00E+00	9.97E-01	2.10E-03	8.24E-18	6.95E-46

distribution for a homogeneous diffusion process with  $t$  between 0.25 and 2.0,  $\mu=4$ , and one absorbing barrier at  $d=10mm$ . As indicated in the figure, variance  $\sigma^2 t$  increases with time as expected. As predicted by Taylor (1953) and Aris (1956) the distance traveled seems to be Gaussian for low  $\mu$  when the barrier is not reached. As expected, the probability density varies with the velocity,  $\mu$ . For  $\mu=10$ , the density is not normal, but is truncated at the absorbing barrier (or exit to the channel) where  $P(x;t)=0$ .

The distance  $\rho$  each particle traveled from the center of the channel entrance, (0,0,0), was calculated using the distance formula  $\rho = \sqrt{x^2 + y^2 + z^2}$ . Considering the three dimensional nature of the channel, there are many possible non-unique  $\rho$  values. The values of  $P(x,y,z;t)$  for equal  $\rho$  values were summed to calculate the probability a particle would travel a particular  $\rho$  regardless of the direction of this distance. Figures 5.4 - 5.8 show the probability distributions of  $\rho$  for different times,  $t$ . Because of the boundary condition at the exit, it is important to note that these distributions may not



add to one as was shown for the 1-D case. The numerical solution is known to be stable, but due to numerical errors, it is possible that for a given  $\Delta t$ ,  $\Delta x$ ,  $\Delta y$ , and  $\Delta z$  the sum of probabilities could exceed one. In such a situation, one needs to modify  $\Delta t$ ,  $\Delta x$ ,  $\Delta y$ , and  $\Delta z$  in order to obtain more accurate results. It is seen from these figures that according to expectation, the distribution shifts towards larger  $\rho$  values with an increase in time,  $t$ . As for the 1-D analytical solution (Figure 5.3), for a small  $\mu$  value of 4 the distribution appears to be symmetric. For larger velocities, the distributions are skewed to the right and the variance of a distribution increases with an increase in velocity,  $\mu$  (see Figure 5.8). Distributions are truncated at the absorbing boundary (or exit to the channel) where  $P(x,y,z;t)=0$ .

The probability distributions of time until first passage from entry to a cross-section  $x$  are presented in Figures 5.9-5.18. It is seen, as expected, that the time to first passage increases as  $x$  increases. Also for a given  $x$ , the time to first passage decreases with an increase in the velocity  $\mu$ .

Figures 5.19-5.37 present probability distributions of the  $(y, z)$  positions of a particle within a given cross-section  $x$  for different velocities and times,  $t$ . It is seen from these figures, that the distributions are symmetric due to the symmetry in parameters and boundary conditions at the wall. However, due to the imposition of boundary conditions, the distributions are not bivariate normals as would be the case in a boundary-free situation.

For most of these figures the leading edge (or farthest  $x$  cross-section reached by the particles for a given time) was selected except in the case where a slight amount of probability was present in that cross-section.

The  $x$  cross-section graphs are typically rounded except for the  $\mu=10$  case, Figures 5.19-5.22, where the velocity is at its lowest. This outcome would indicate that the probability distribution moves faster at the center of the channel for larger velocities than smaller velocities, which would be expected.

In general the probability distributions of the  $(y, z)$  positions of a particle within a given  $x$  cross-section appear higher in the middle of the cross-section. This characteristic is not the case in Figure 5.34. Here the cross-section is the very last possible cross-section,  $x=9.99$ , and time corresponds to twice the average time for exit. In this figure most of the probability distribution has exited the channel. The concave nature of the graph indicates that the probability distribution is higher in the corners and at the walls of the channel, due to the reflective boundaries at the walls. The difference has been exaggerated for graphing purposes but is not very dramatic in reality.

For comparison purposes, the code was modified for the 2-dimensional case for  $\phi = 0.125$ . Figures 5.38-40 show plots of the distribution of the distance  $\rho$  traveled at different times,  $t$ , for  $\mu=50$ ,  $100$ , and  $500$ , respectively. These plots give results similar to the 3-D cases shown in Figures 5.5, 5.6, and 5.8, respectively.

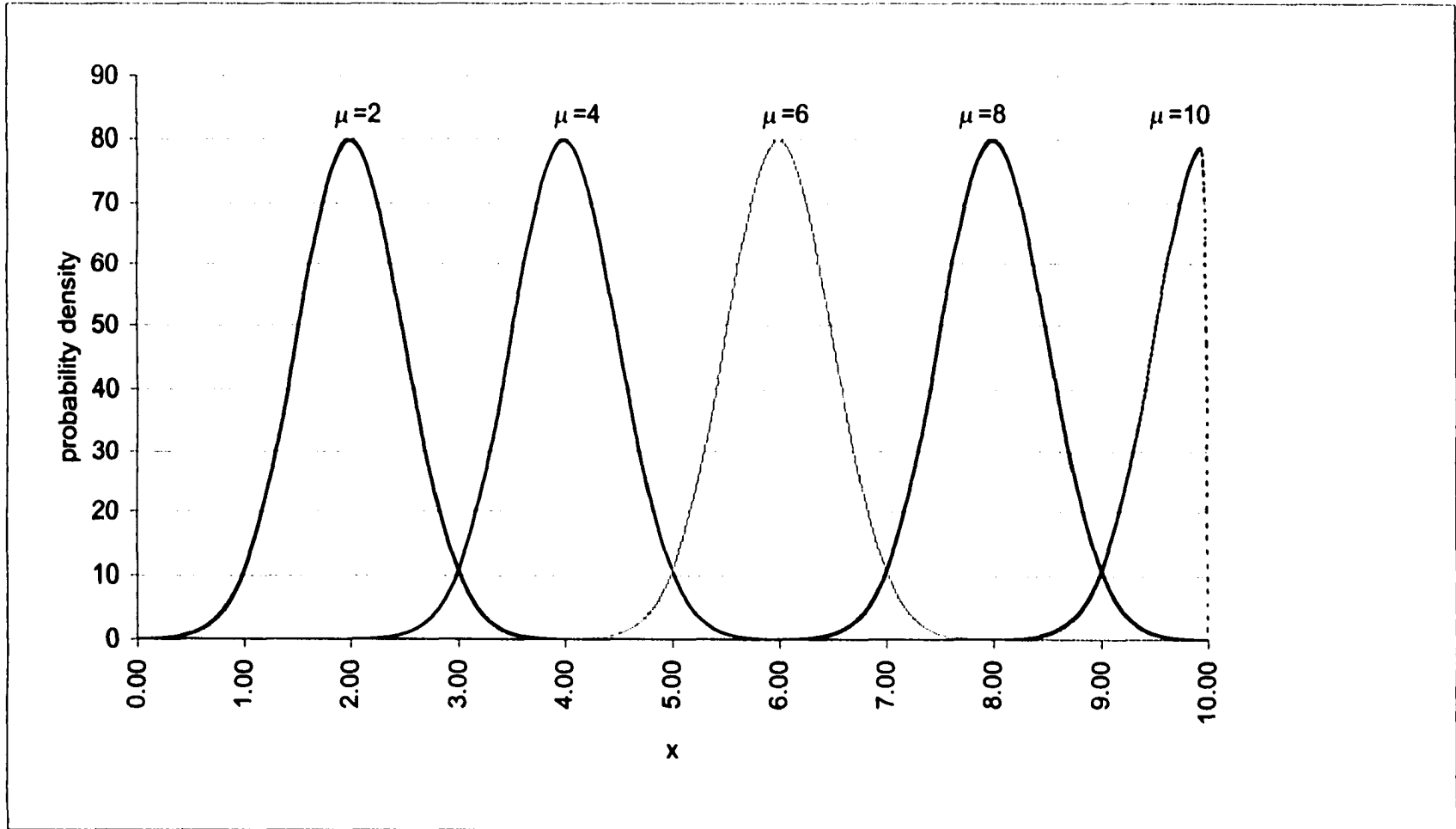


Figure 5.2. The probability distribution of the distance  $x$  traveled by a particle for a homogeneous diffusion process with one absorbing barrier at  $d=10\text{mm}$  and  $t=1$

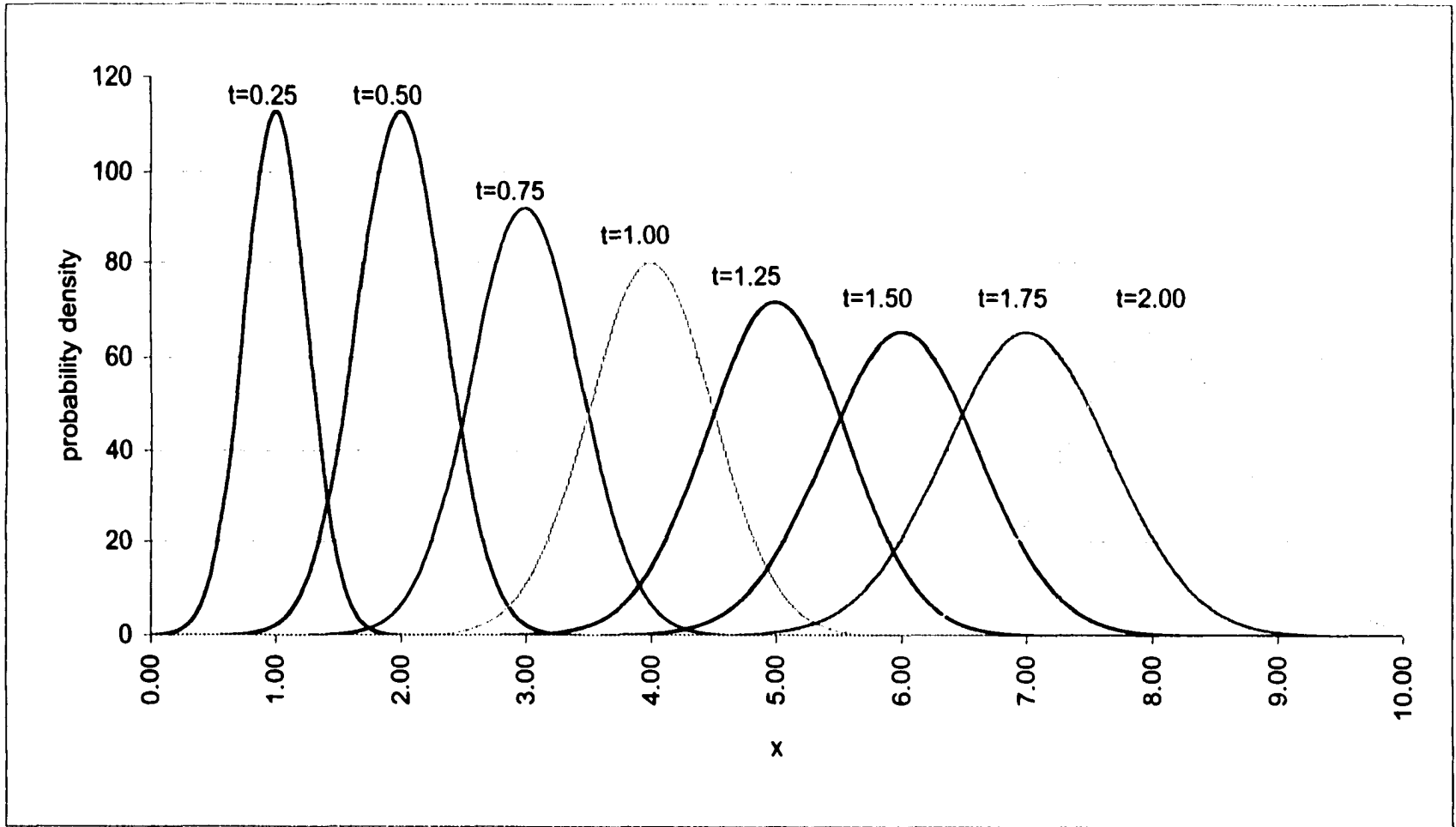


Figure 5.3. The probability distribution of the distance  $x$  traveled by a particle for a homogeneous diffusion process with one absorbing barrier at  $d=10mm$ ,  $\mu=4$

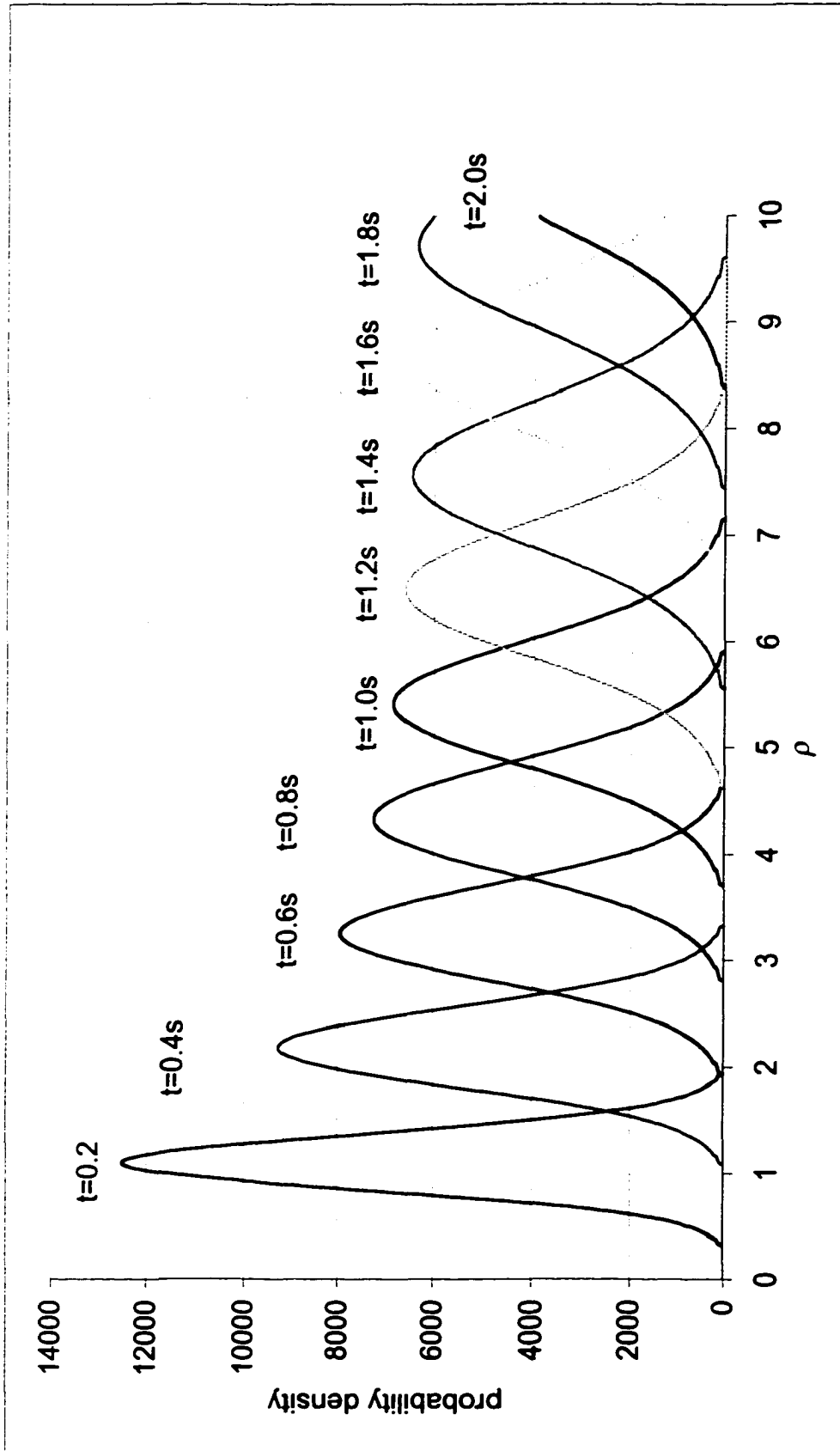


Figure 5.4. Probability distribution of  $\rho$  between 0.2 and 2 seconds,  $\mu = 10$

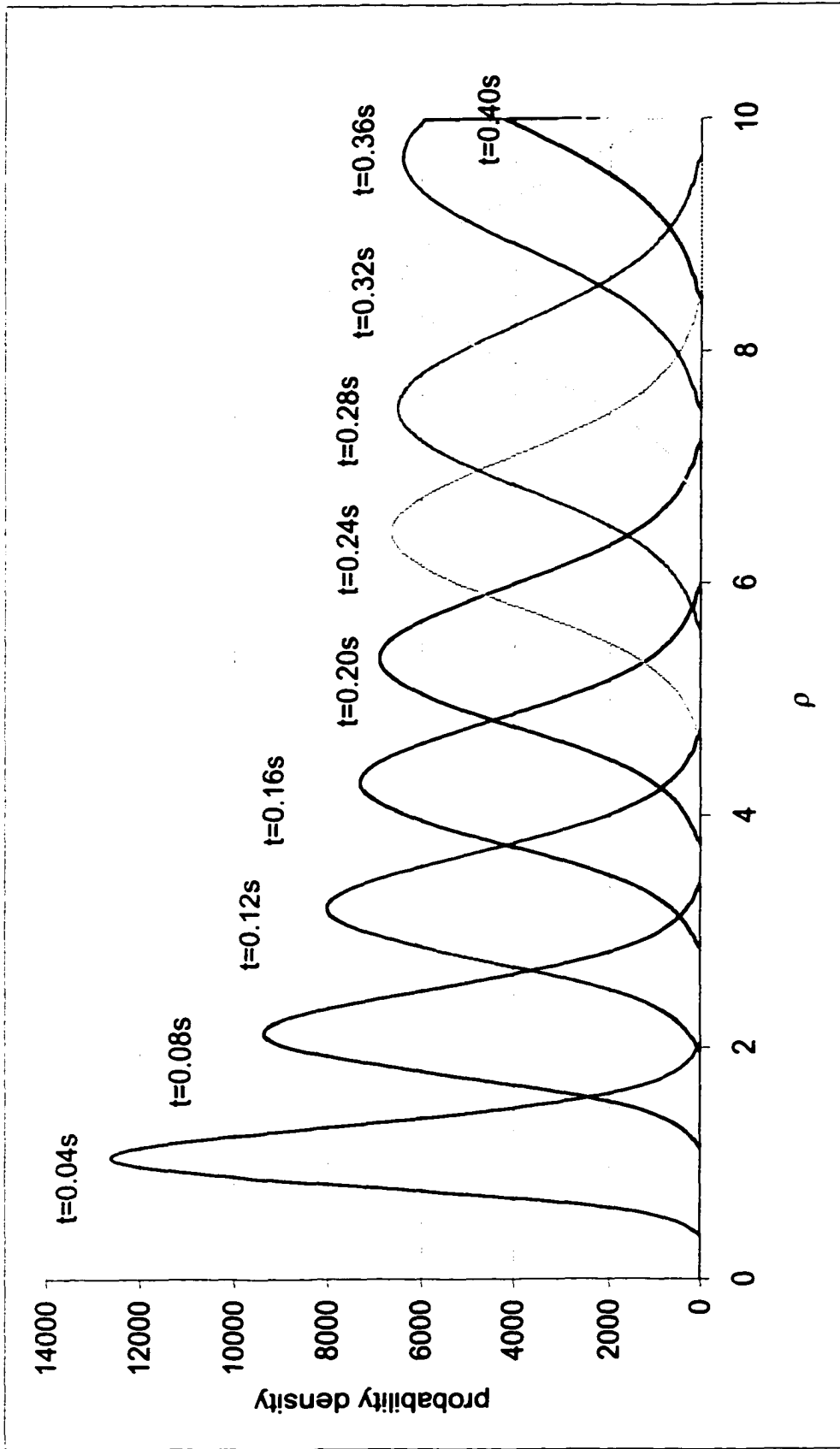


Figure 5.5. Probability distribution of  $\rho$  between 0.04 and 0.4 seconds,  $\mu = 50$

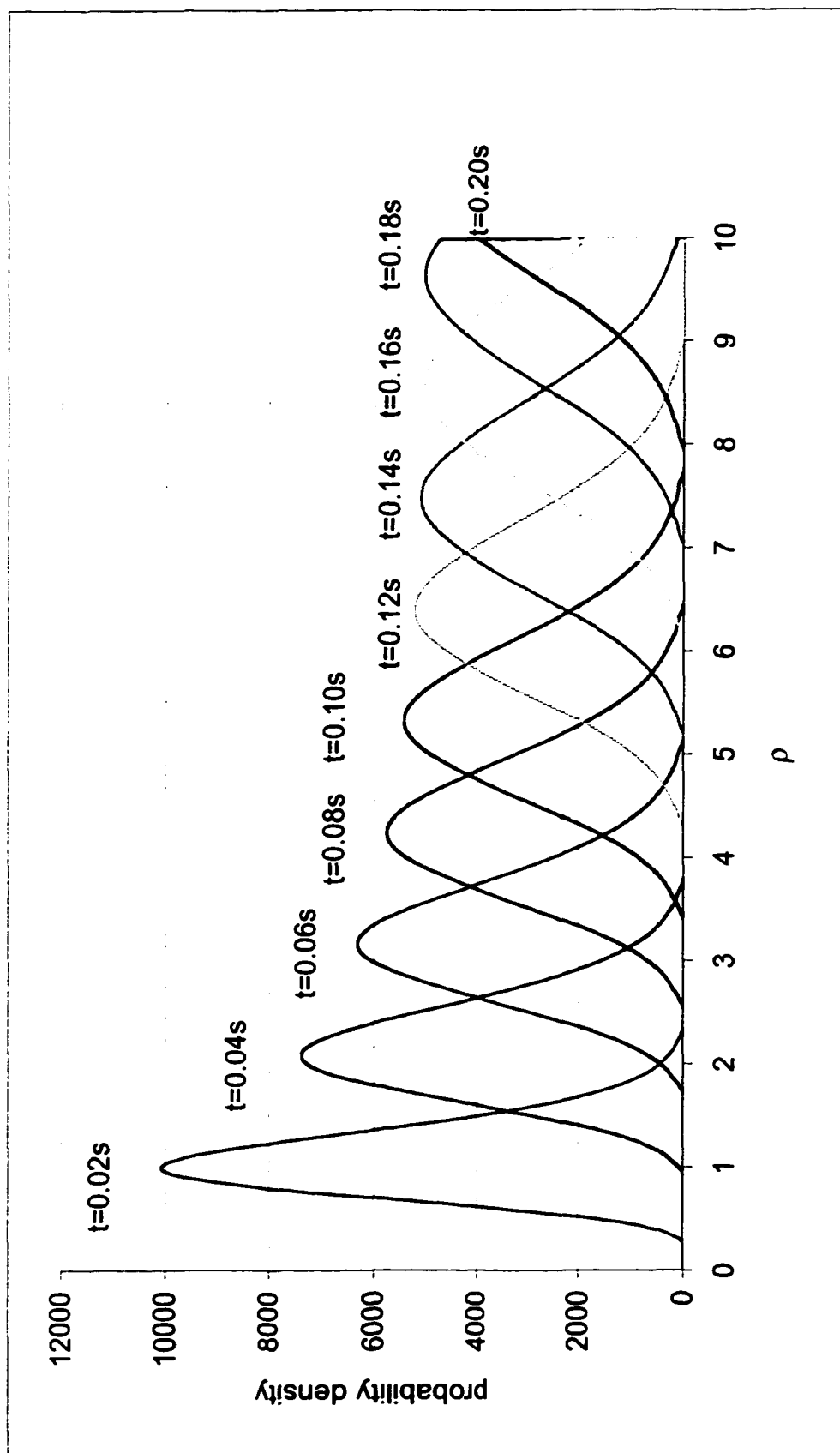


Figure 5.6. Probability distribution of  $\rho$  between 0.02 and 0.2 seconds,  $\mu = 100$

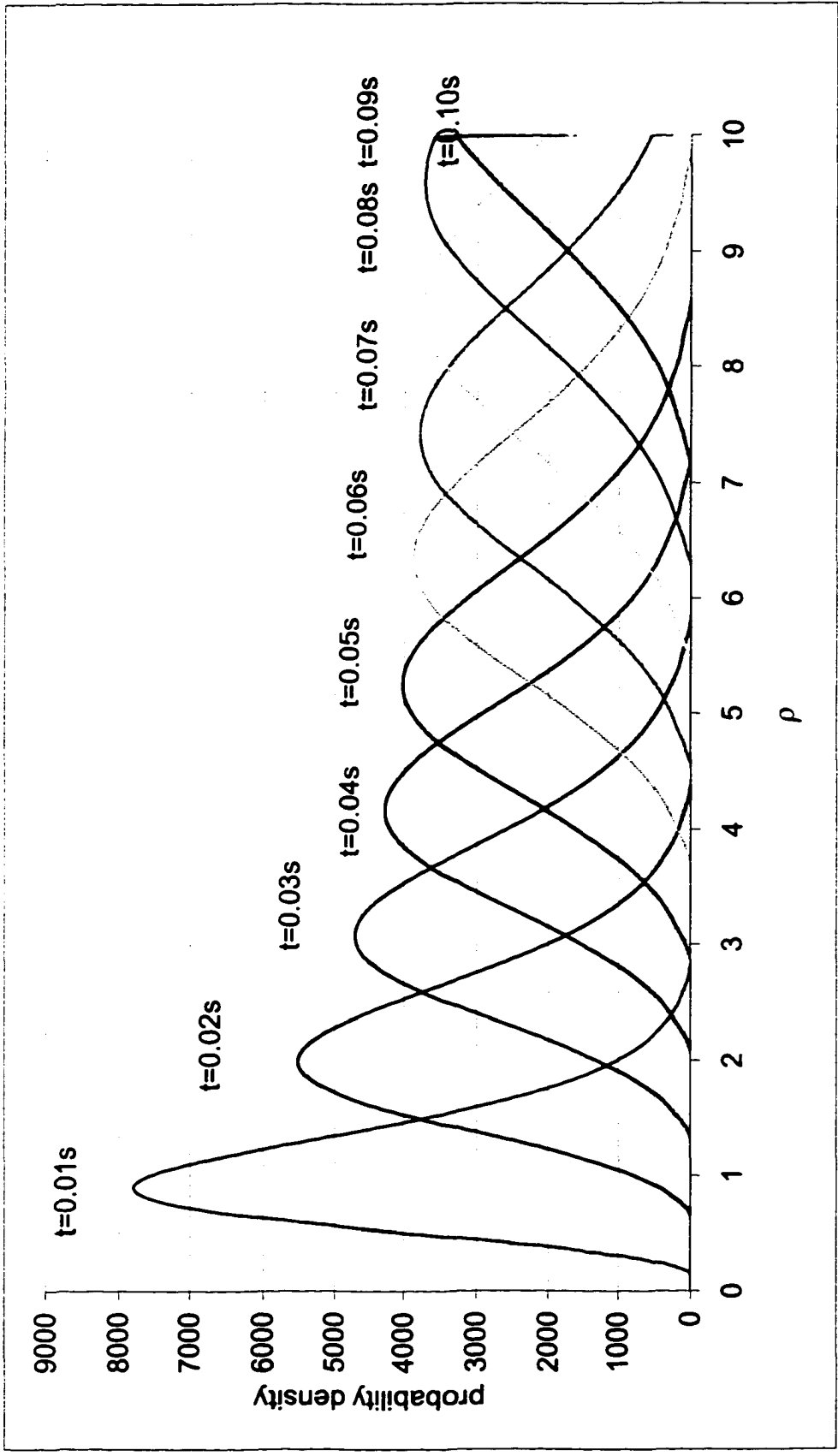


Figure 5.7. Probability distribution of  $\rho$  between 0.01 and 0.1 seconds,  $\mu = 200$



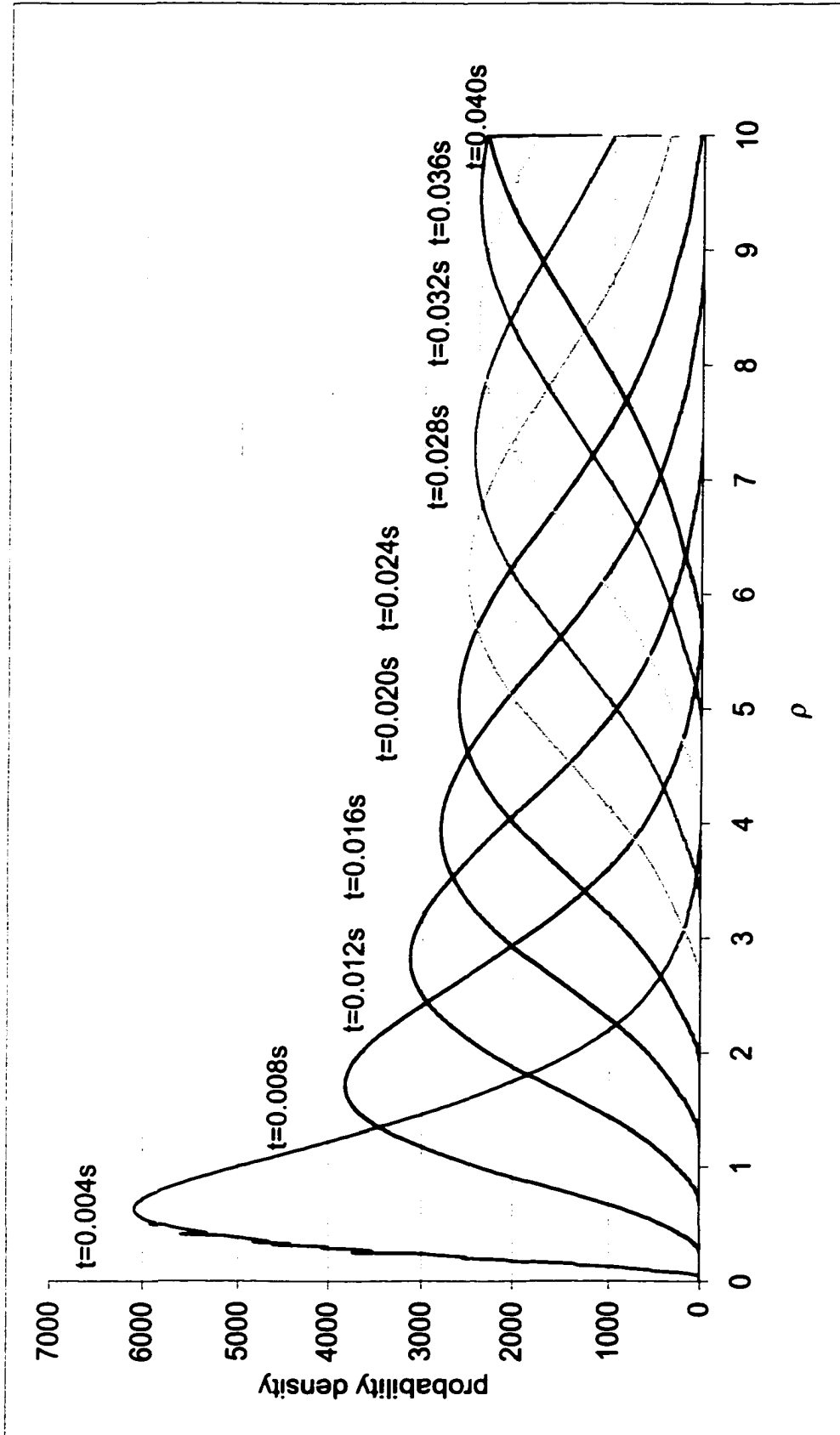


Figure 5.8. Probability distribution of  $\rho$  between 0.004 and 0.04 seconds,  $\mu = 500$

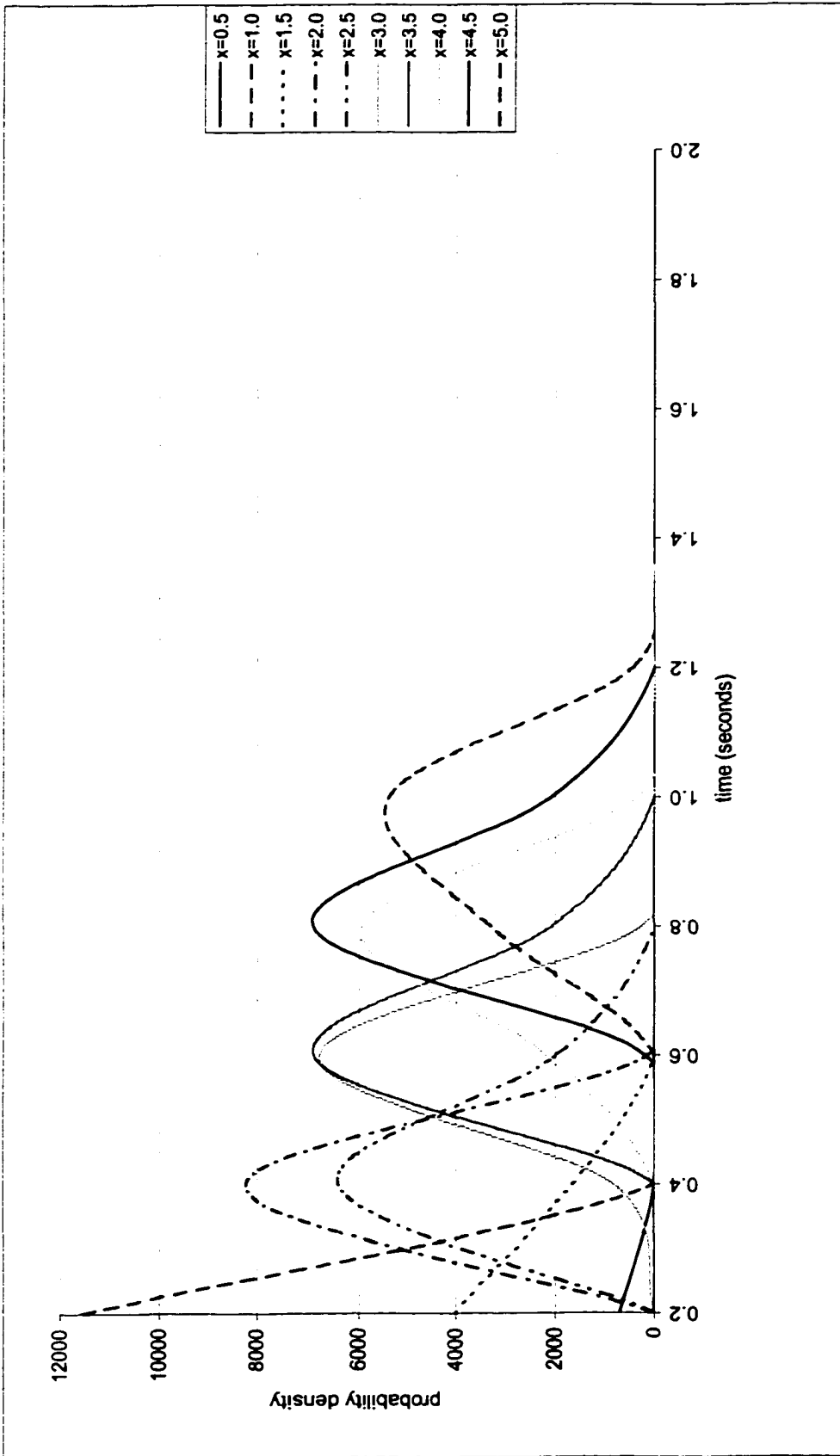


Figure 5.9. Probability distribution of time to first passage from the entry to a cross-section,  $x$  between 0.5 and 5.0,  $\mu = 10$

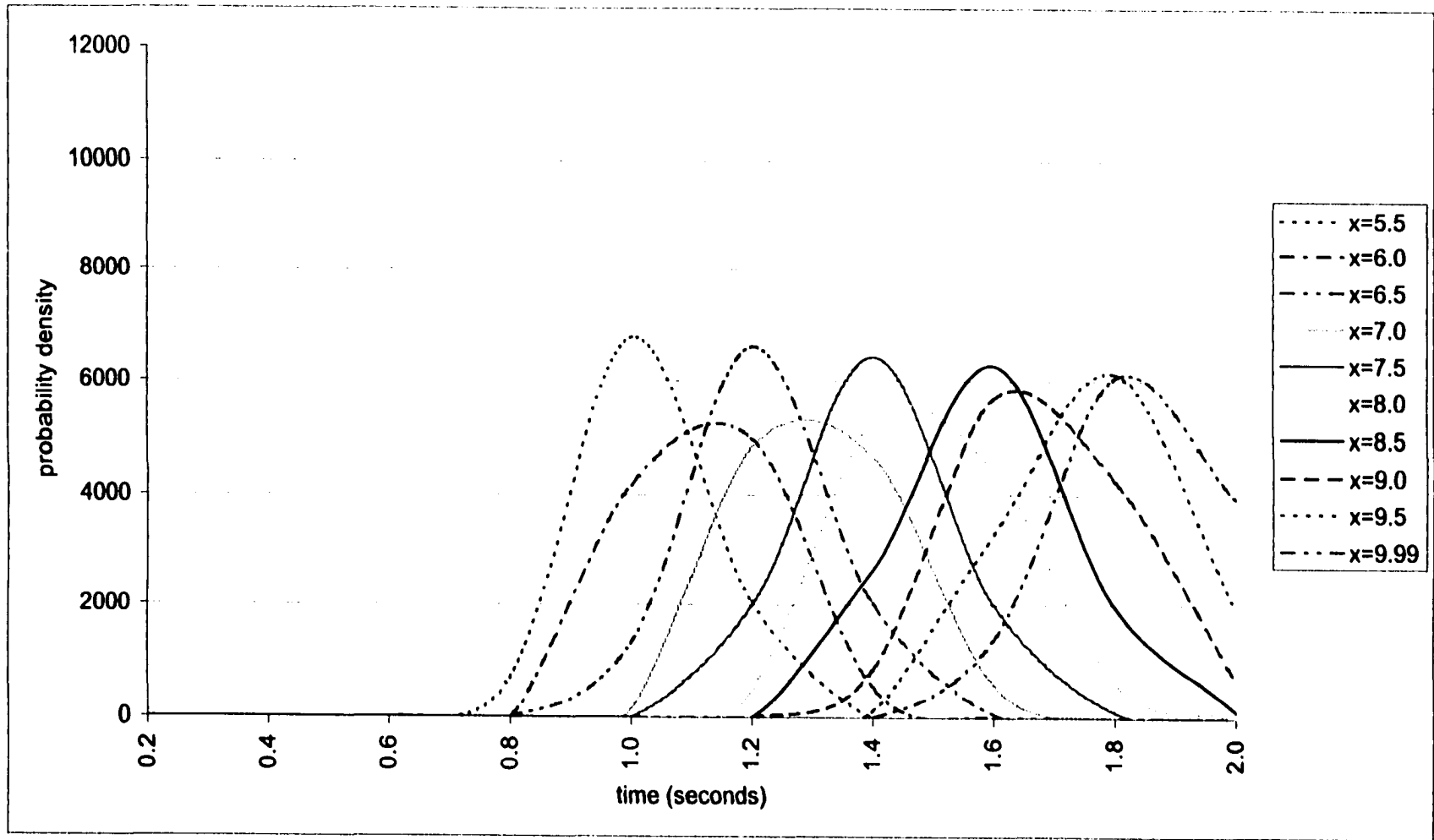


Figure 5.10. Probability distribution of time to first passage from the entry to a cross-section,  $x$  between 5.5 and 9.99,  $\mu = 10$

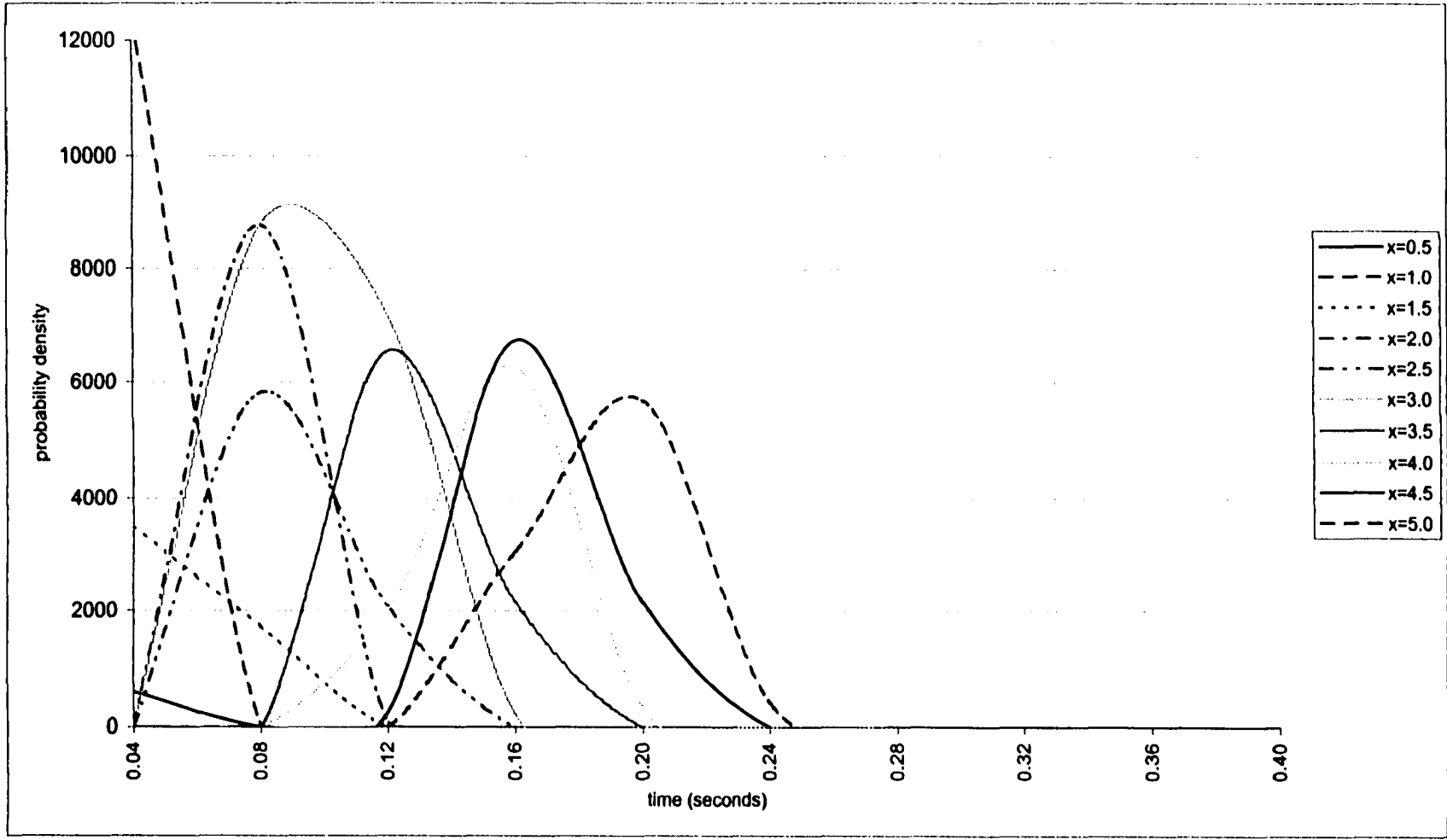


Figure 5.11. Probability distribution of time to first passage from the entry to a cross-section,  $x$  between 0.5 and 5.0,  $\mu = 50$

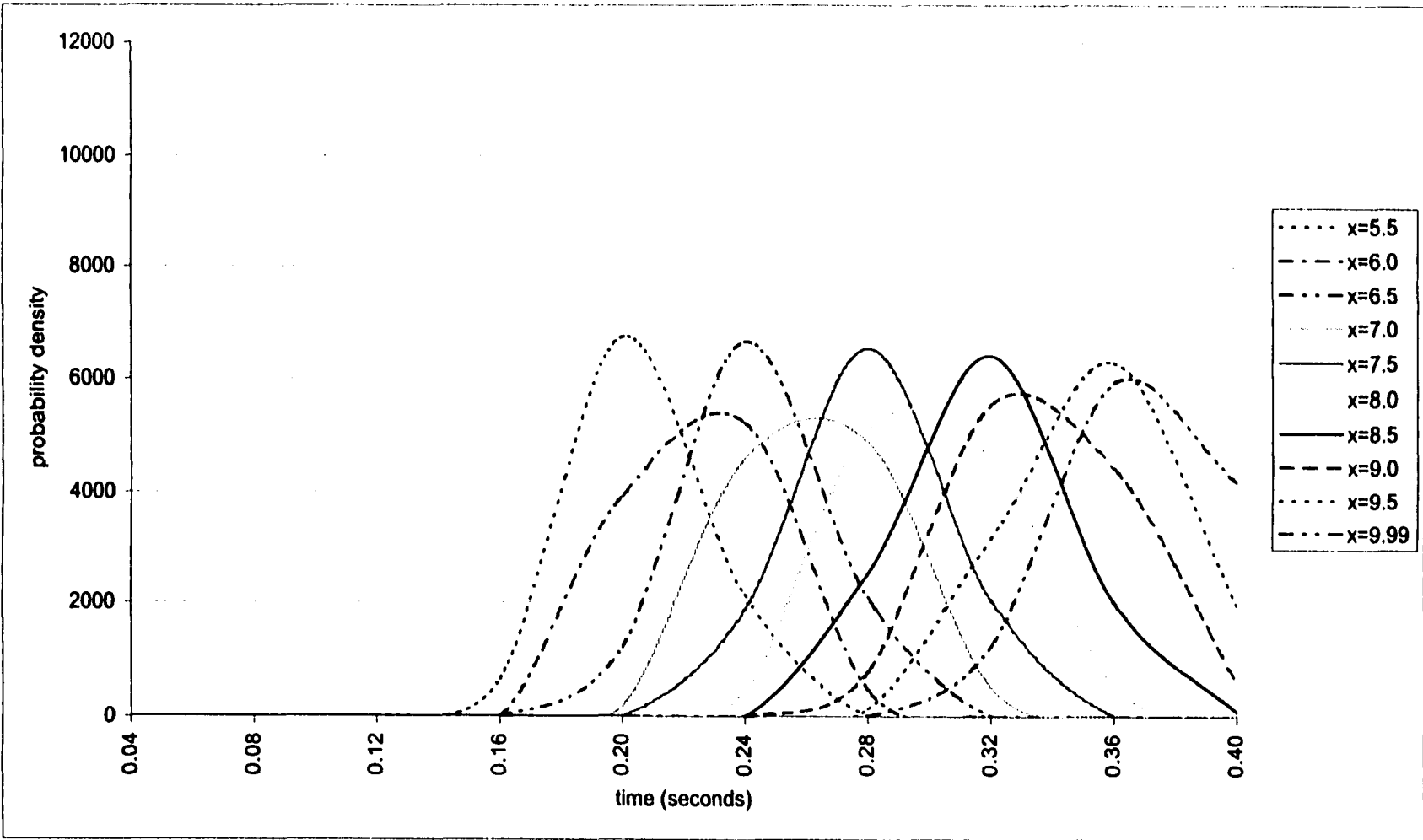


Figure 5.12. Probability distribution of time to first passage from the entry to a cross-section,  $x$  between 5.5 and 9.99,  $\mu = 50$

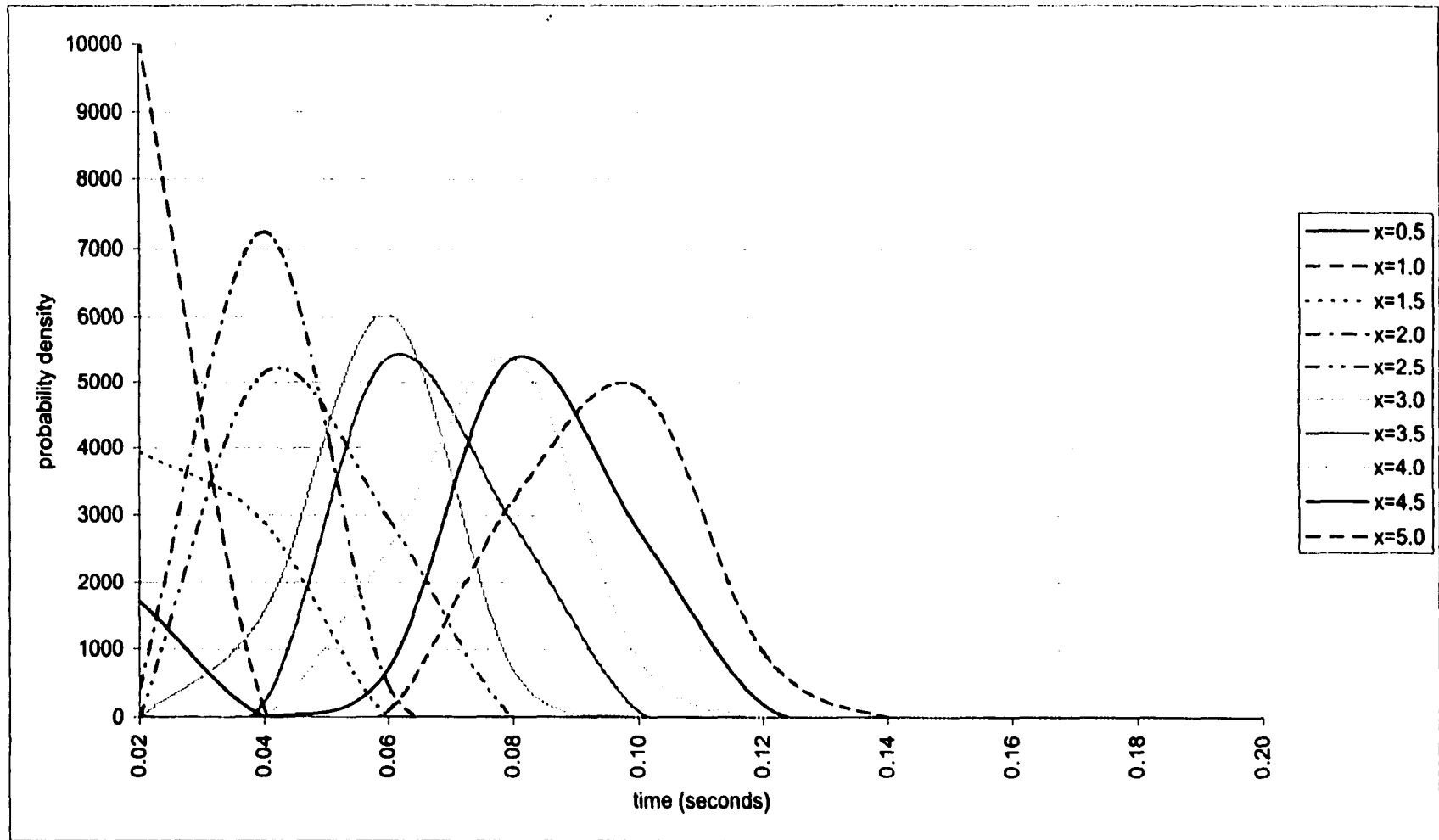


Figure 5.13. Probability distribution of time to first passage from the entry to a cross-section,  $x$  between 0.5 and 5.0,  $\mu=100$

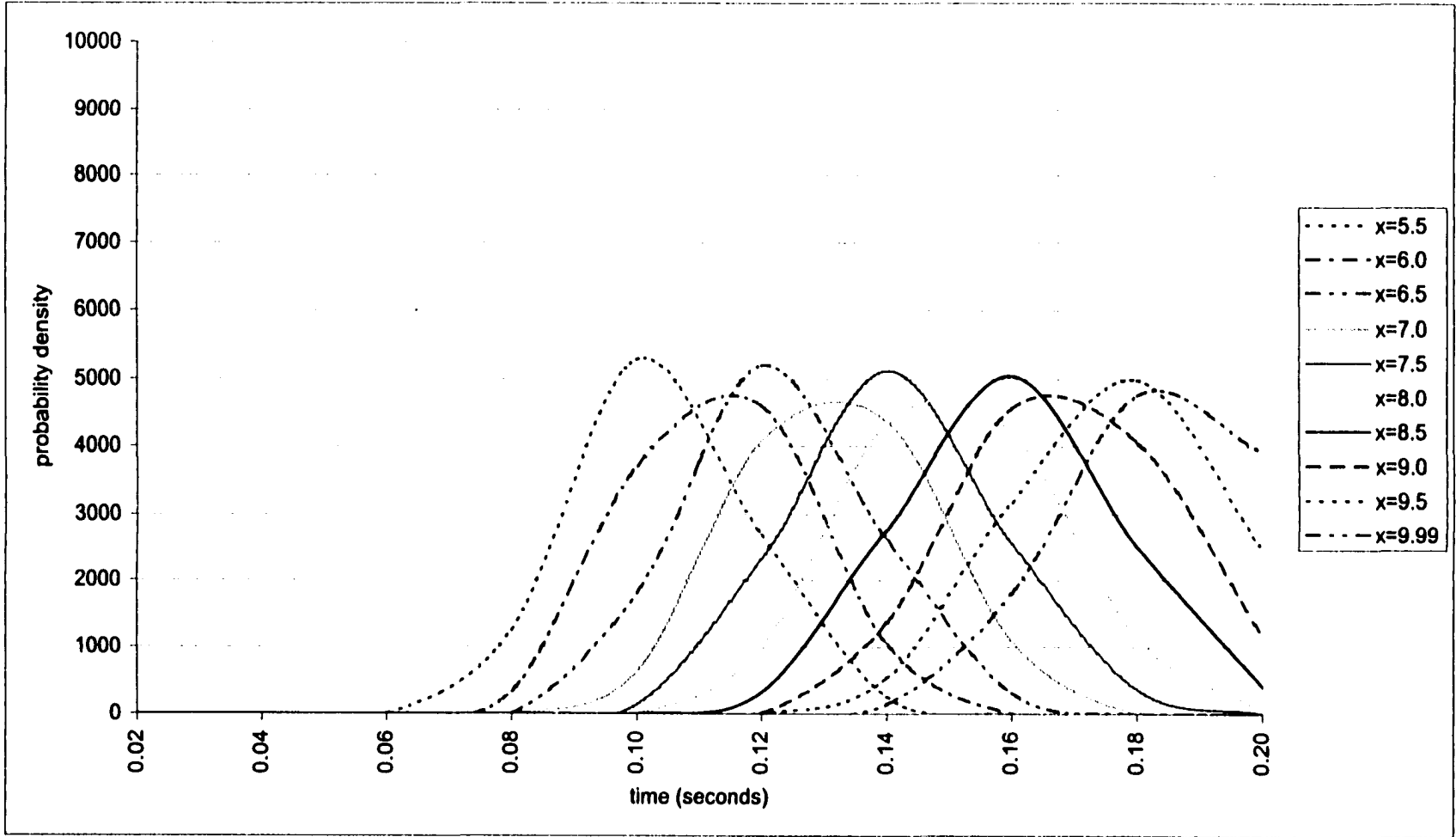


Figure 5.14. Probability distribution of time to first passage from the entry to a cross-section,  $x$  between 5.5 and 9.99,  $\mu = 100$

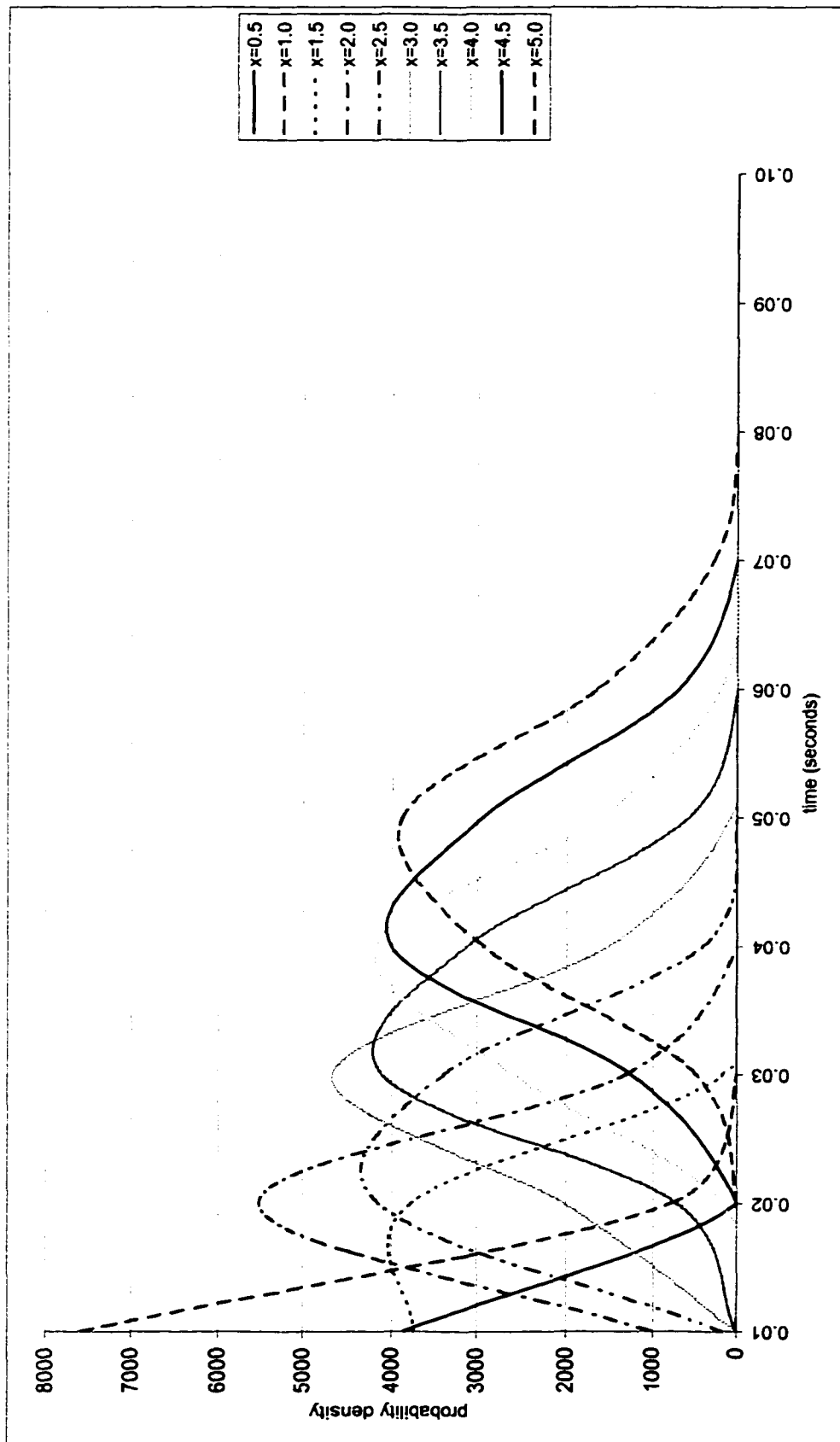


Figure 5.15. Probability distribution of time to first passage from the entry to a cross-section,  $x$  between 0.5 to 5.0,  $\mu = 200$



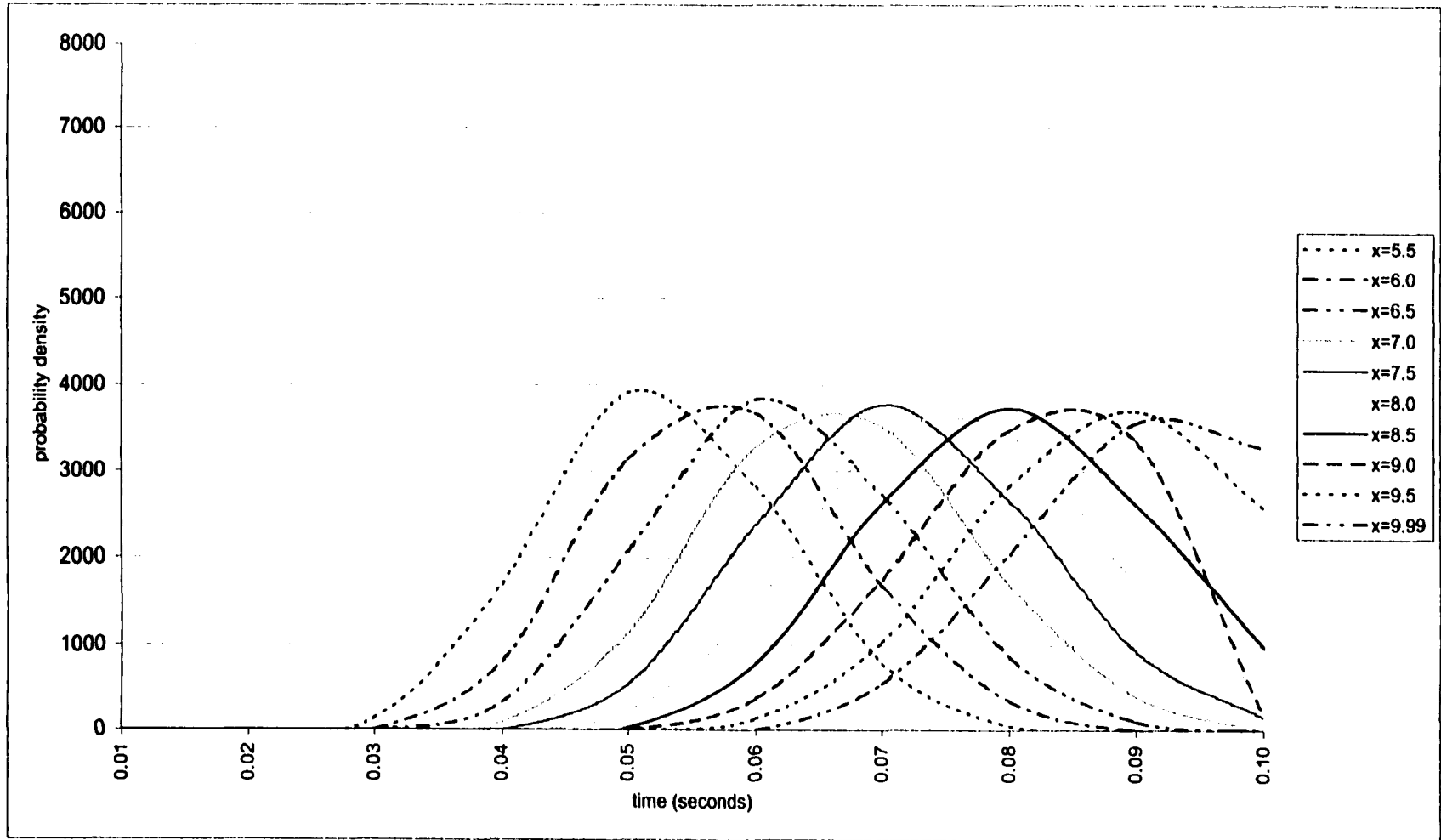


Figure 5.16. Probability distribution of time to first passage from the entry to a cross-section,  $x$  between 5.5 and 9.99,  $\mu = 200$

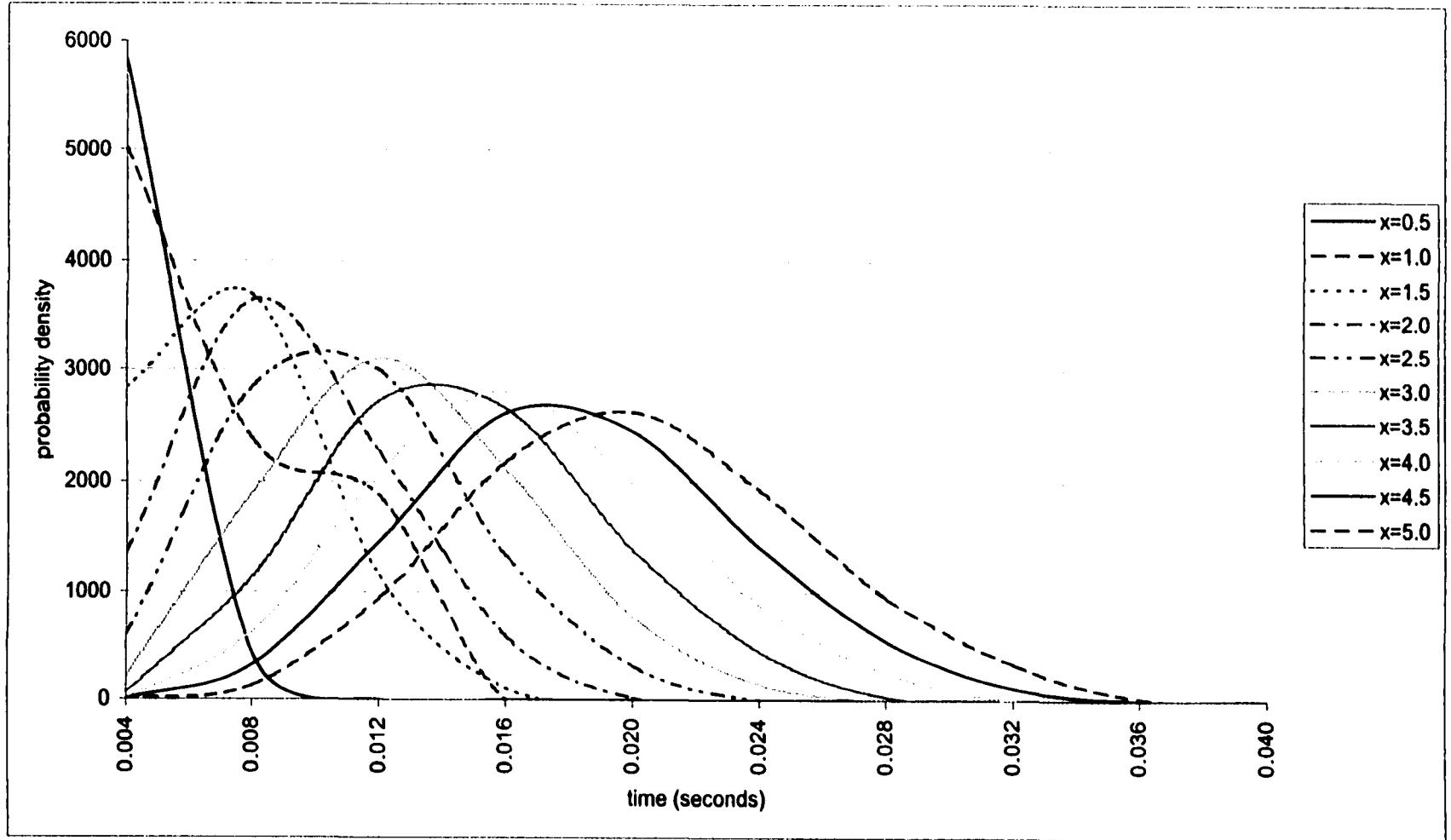


Figure 5.17. Probability distribution of time to first passage from the entry to a cross-section,  $x$  between 0.5 to 5.0,  $\mu = 500$

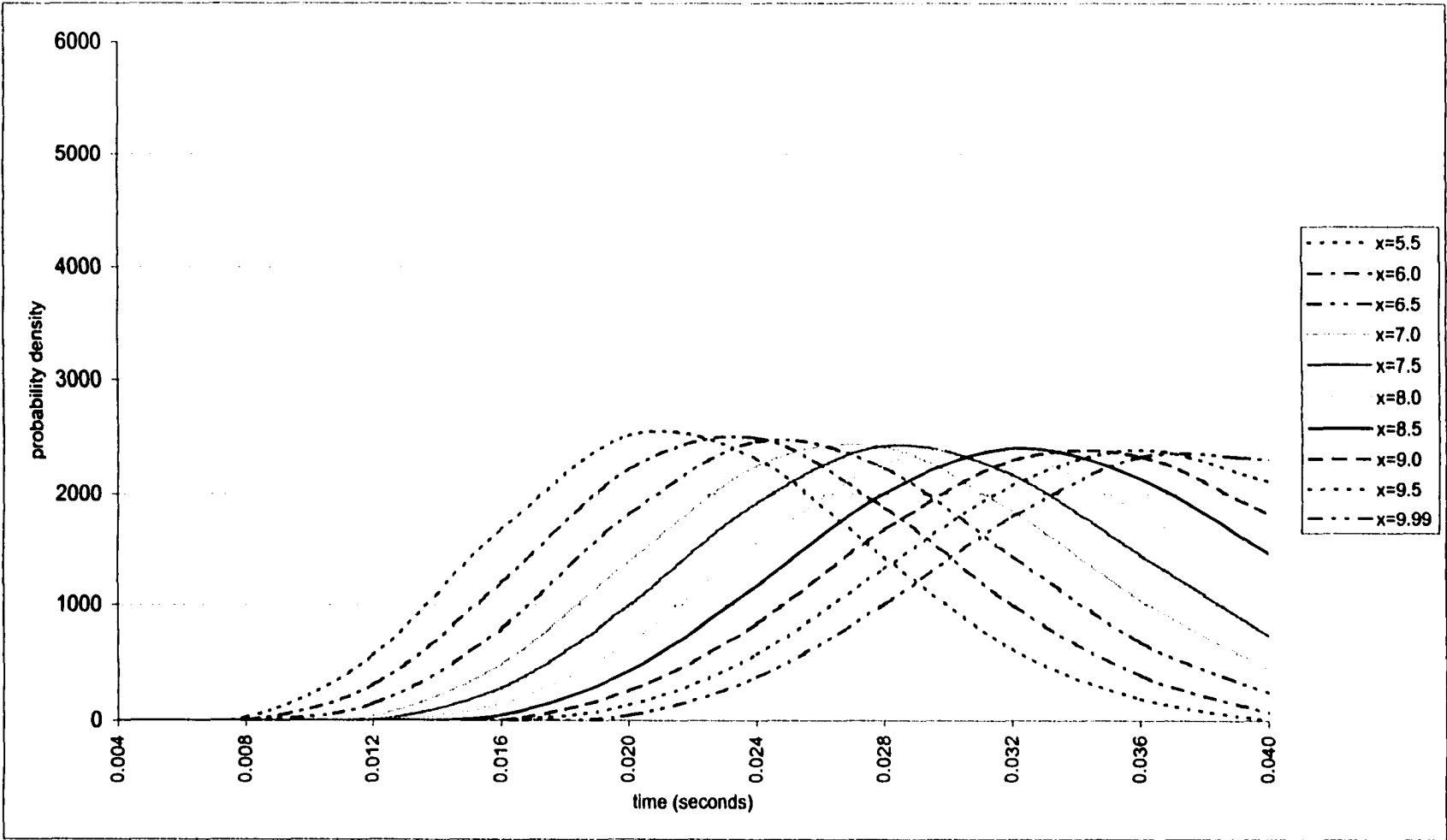


Figure 5.18. Probability distribution of time to first passage from the entry to a cross-section,  $x$  between 5.5 to 9.99,  $\mu = 500$

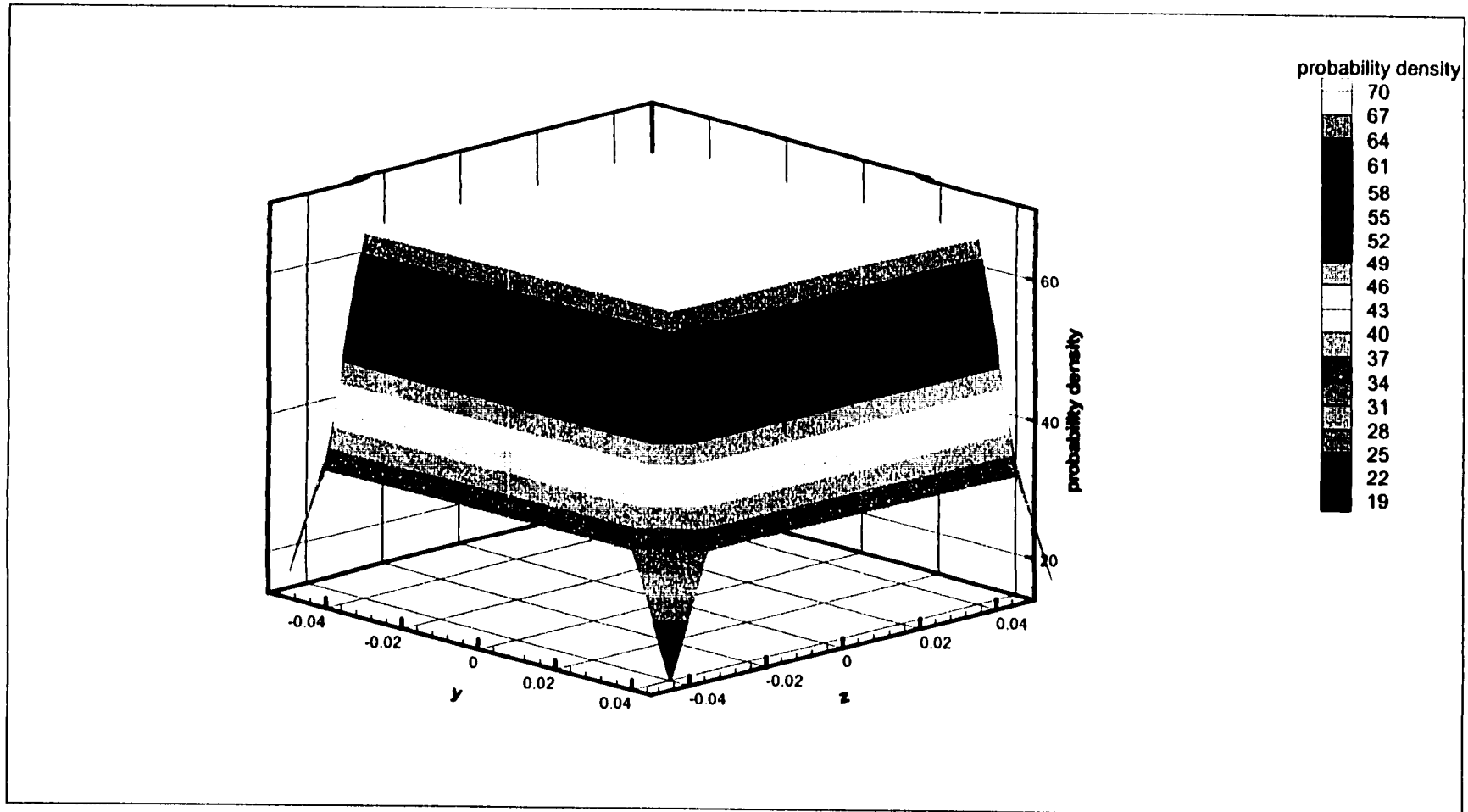


Figure 5.19. Probability distribution at cross-section  $x=5.5$ ,  $\mu=10$ ,  $t=1s$

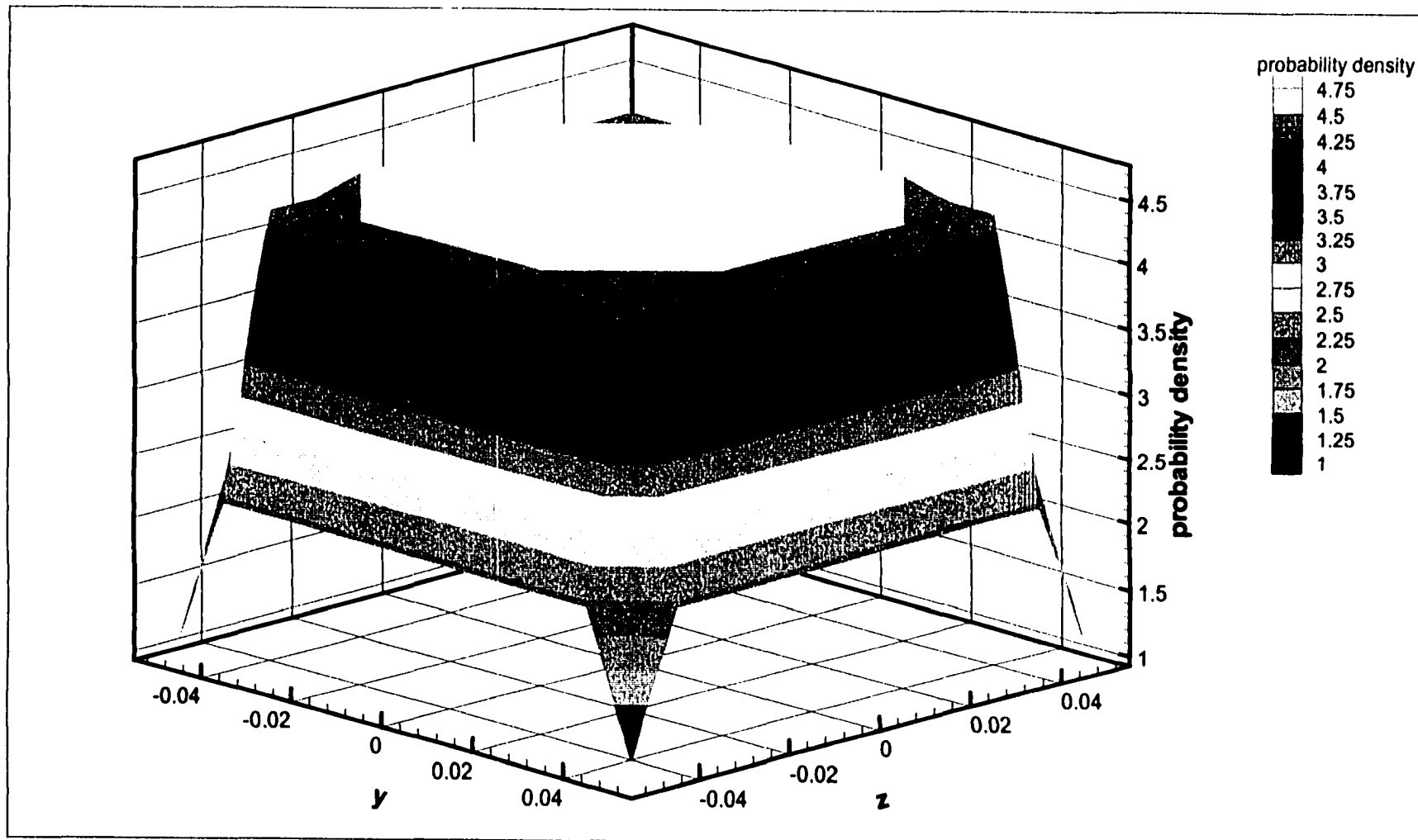


Figure 5.20. Probability distribution at cross-section  $x=8.0$ ,  $\mu=10$ ,  $t=1.2s$

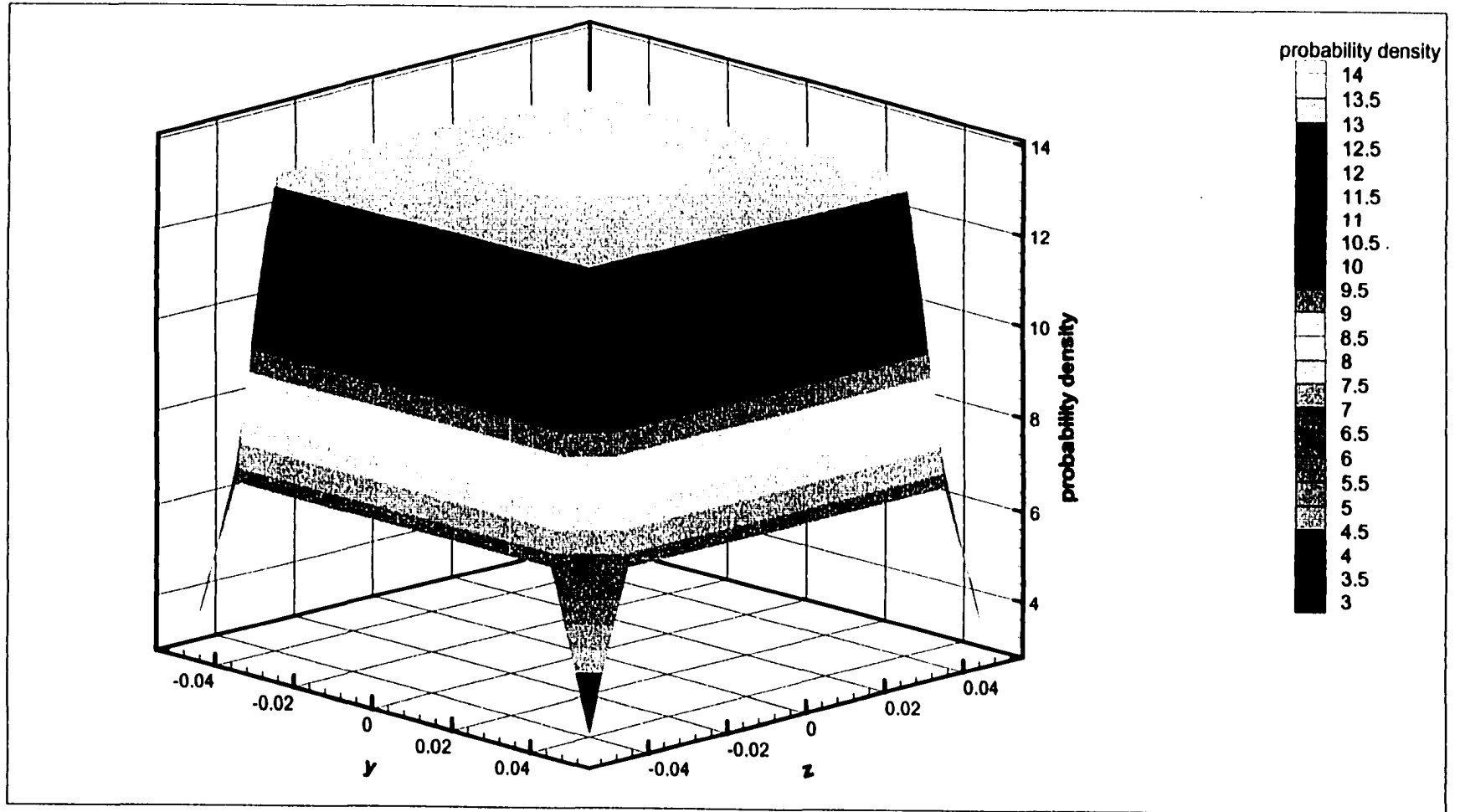


Figure 5.21. Probability distribution at cross-section  $x=9.99$ ,  $\mu=10$ ,  $t=1.6s$

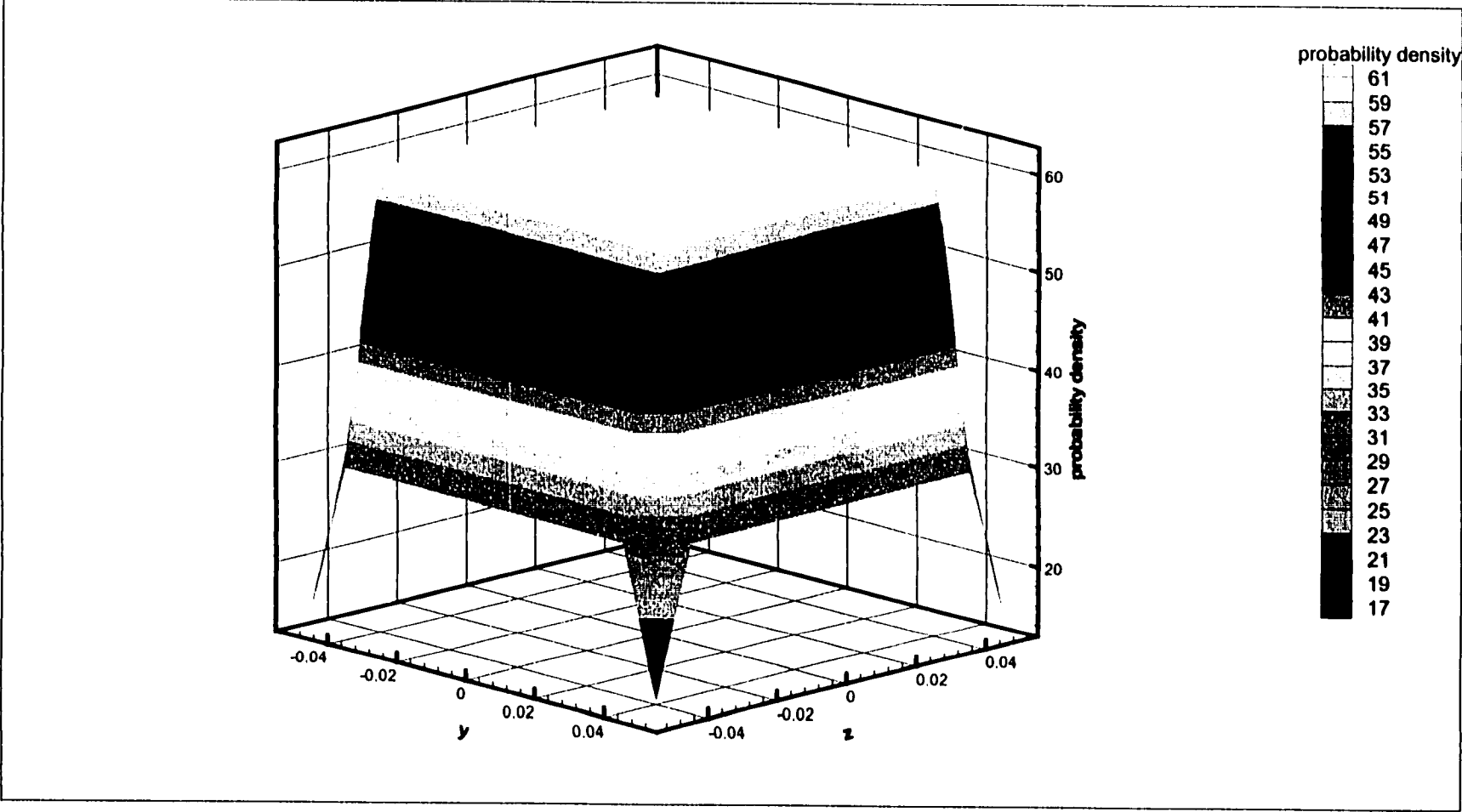


Figure 5.22. Probability distribution at cross-section  $x=9.99$ ,  $\mu=10$ ,  $t=1.8s$

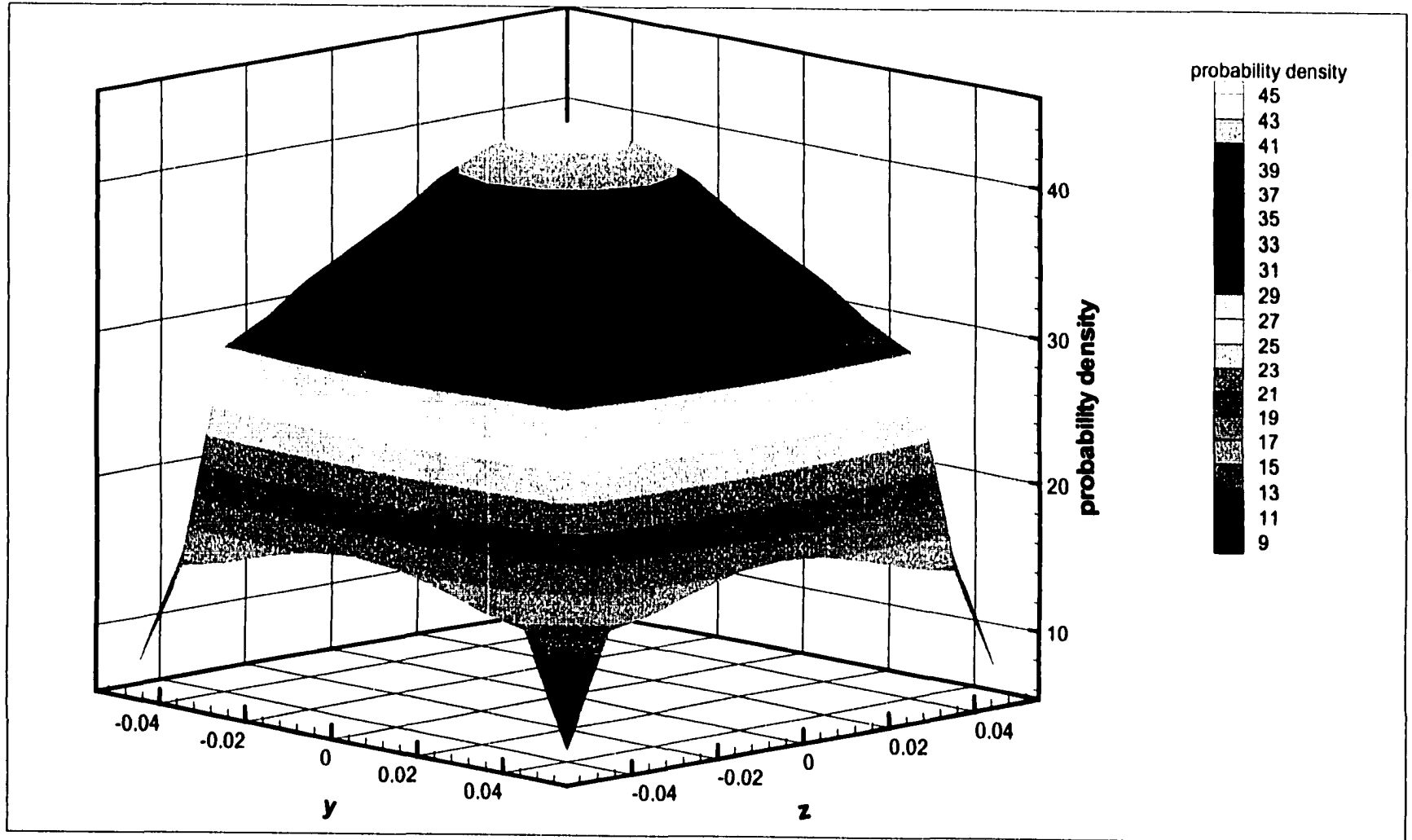


Figure 5.23. Probability distribution at cross-section  $x=1.5$ ,  $\mu=50$ ,  $t=0.04s$



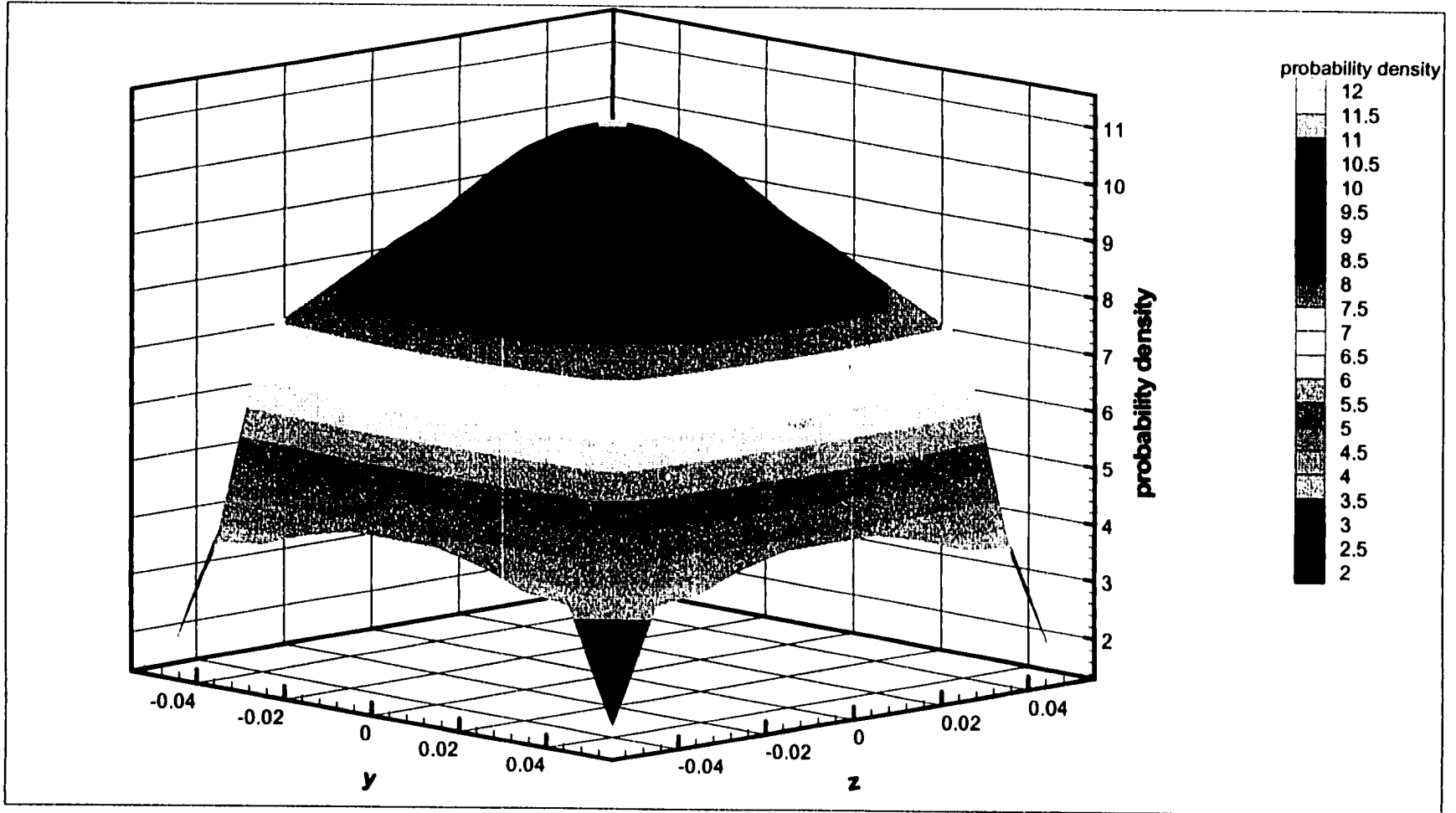


Figure 5.24. Probability distribution at cross-section  $x=3.0$ ,  $\mu=50$ ,  $t=0.08s$

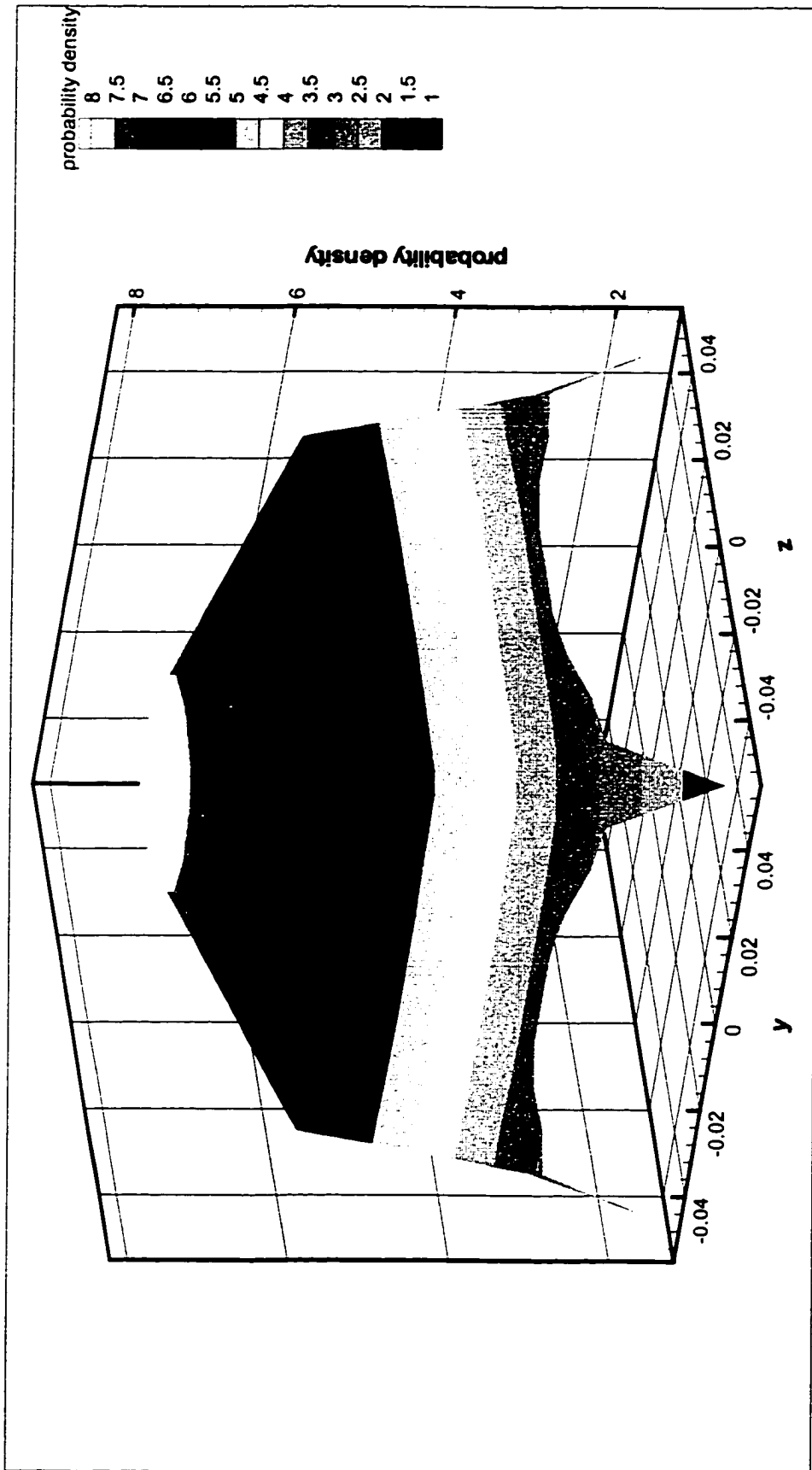


Figure 5.25. Probability distribution at cross-section  $x=5.5$ ,  $\mu=50$ ,  $t=0.16s$

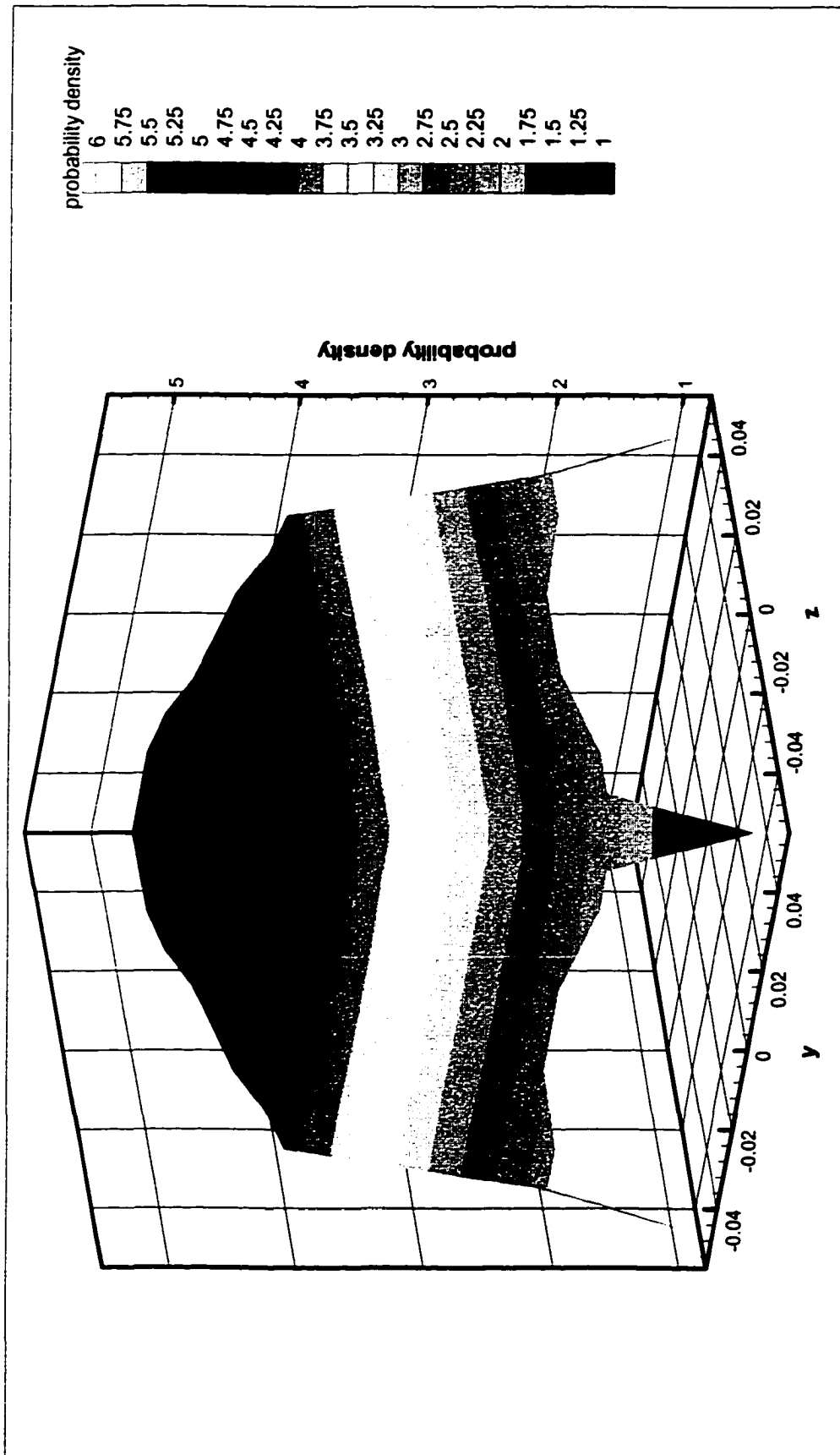


Figure 5.26. Probability distribution at cross-section  $x=8.0$ ,  $\mu=50$ ,  $\tau=0.24s$

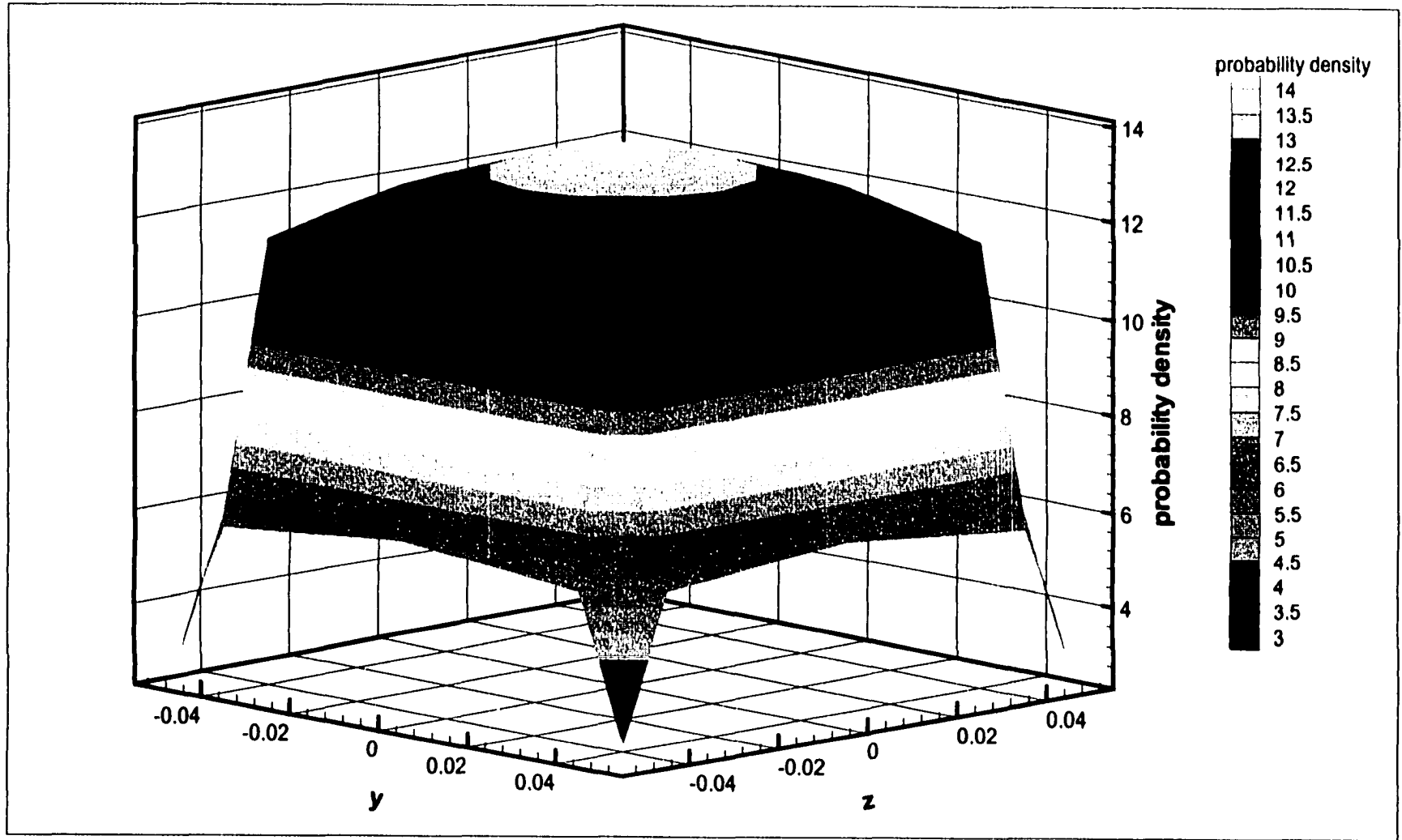


Figure 5.27. Probability distribution at cross-section  $x=9.99$ ,  $\mu=50$ ,  $t=0.32s$

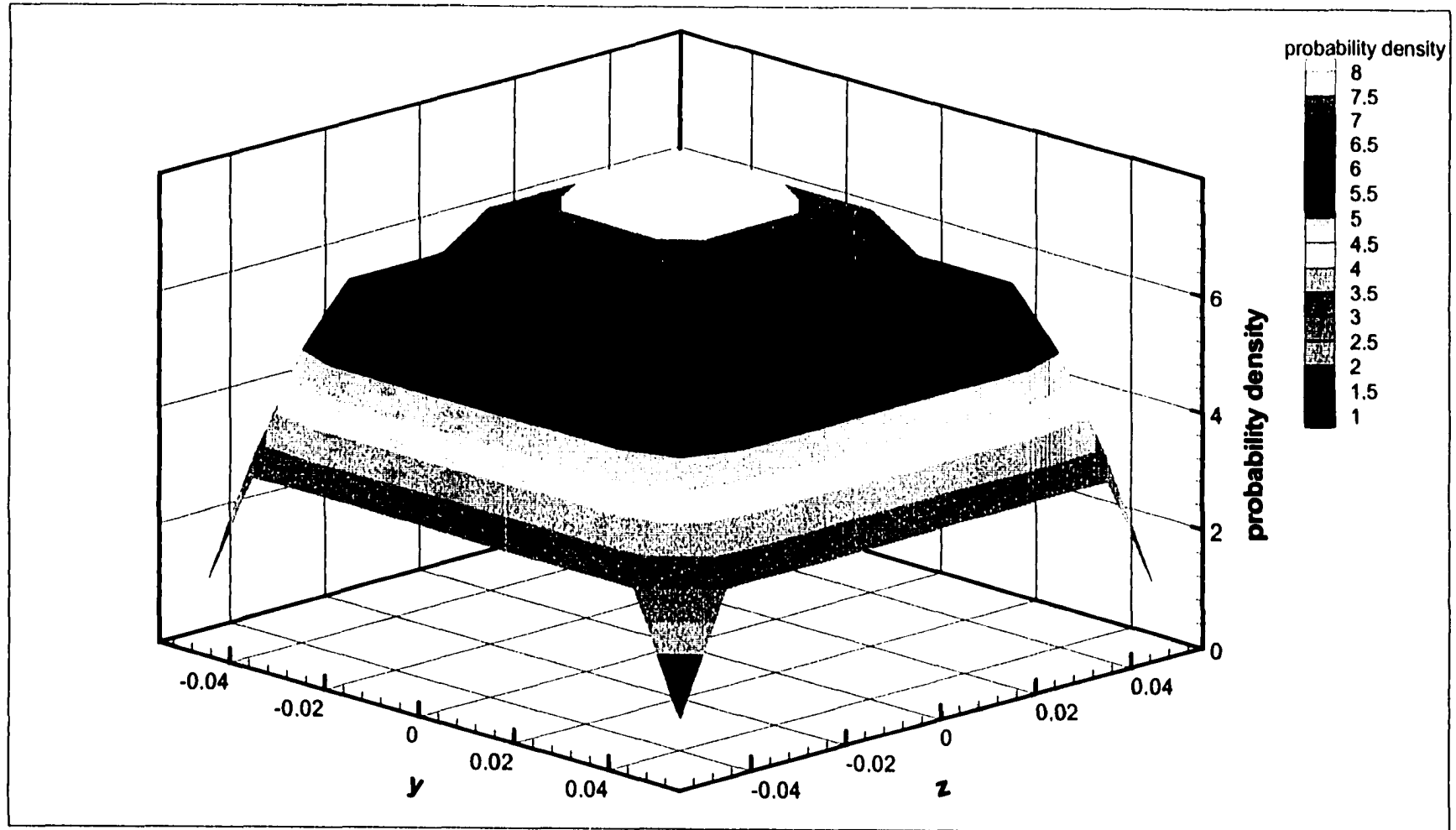


Figure 5.28. Probability distribution at cross-section  $x=7.0$ ,  $\mu=100$ ,  $t=0.1s$

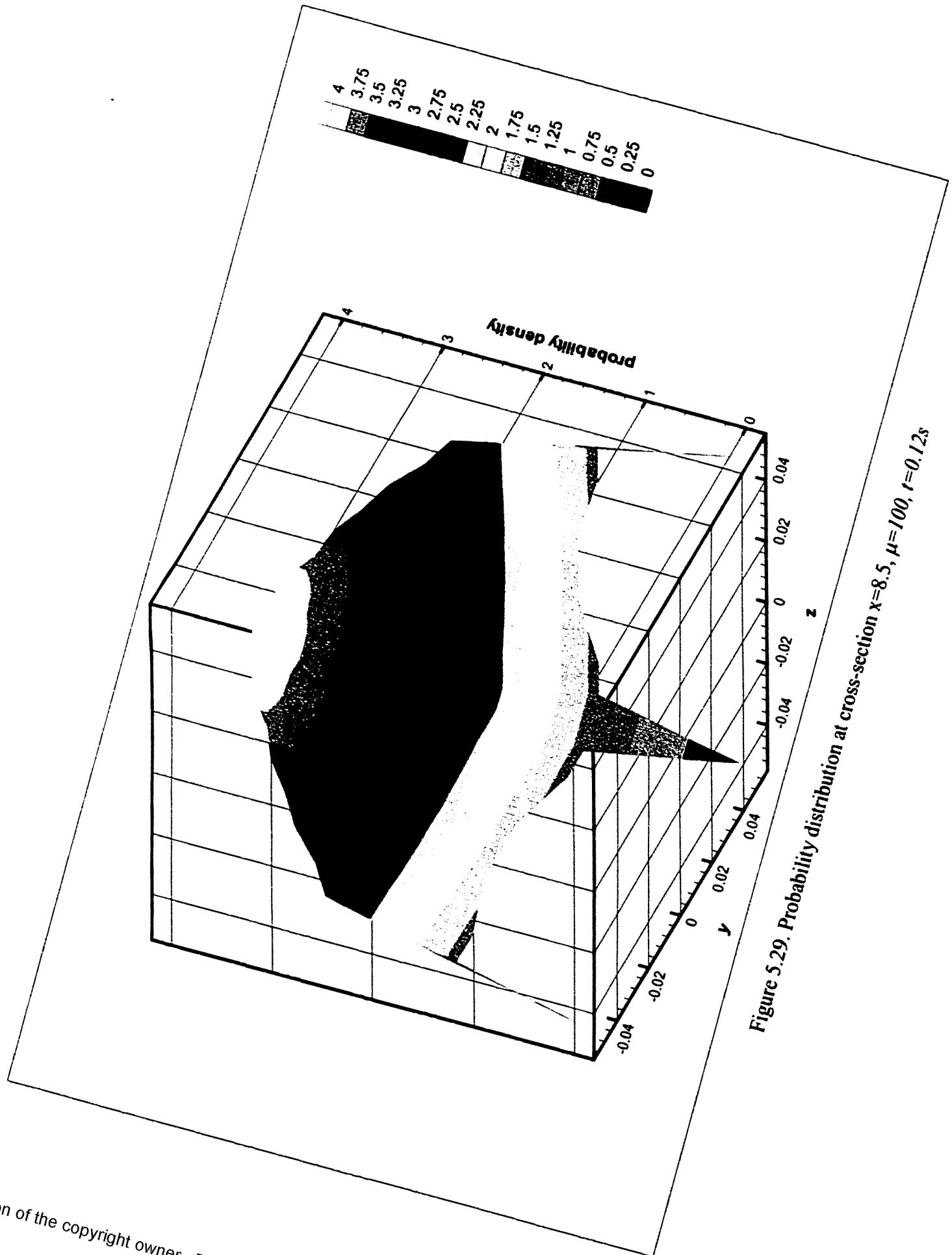


Figure 5.29. Probability distribution at cross-section  $x=8.5$ ,  $\mu=100$ ,  $r=0.12s$

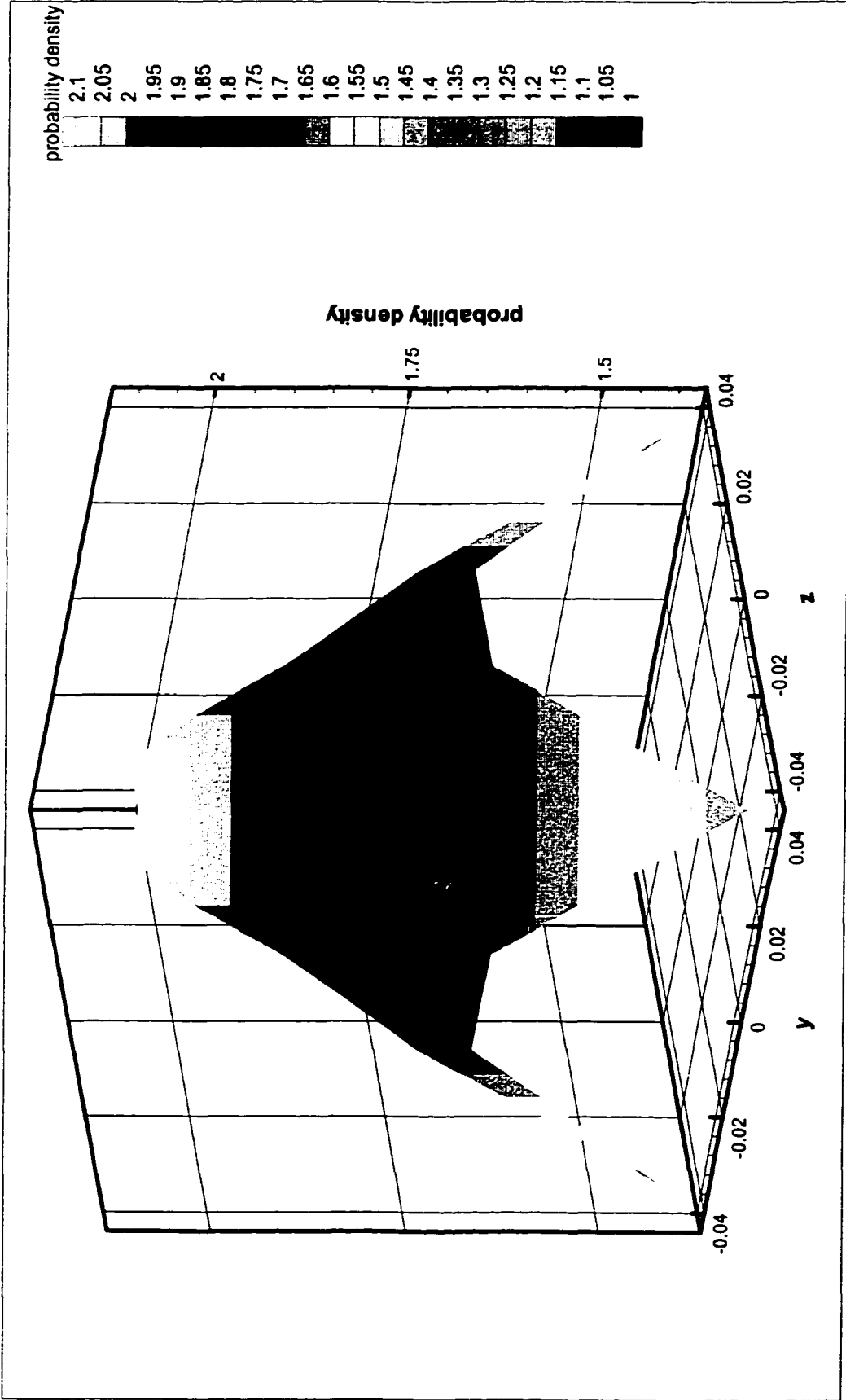


Figure 5.30. Probability distribution at cross-section  $x=9.99$ ,  $\mu=100$ ,  $t=0.14s$

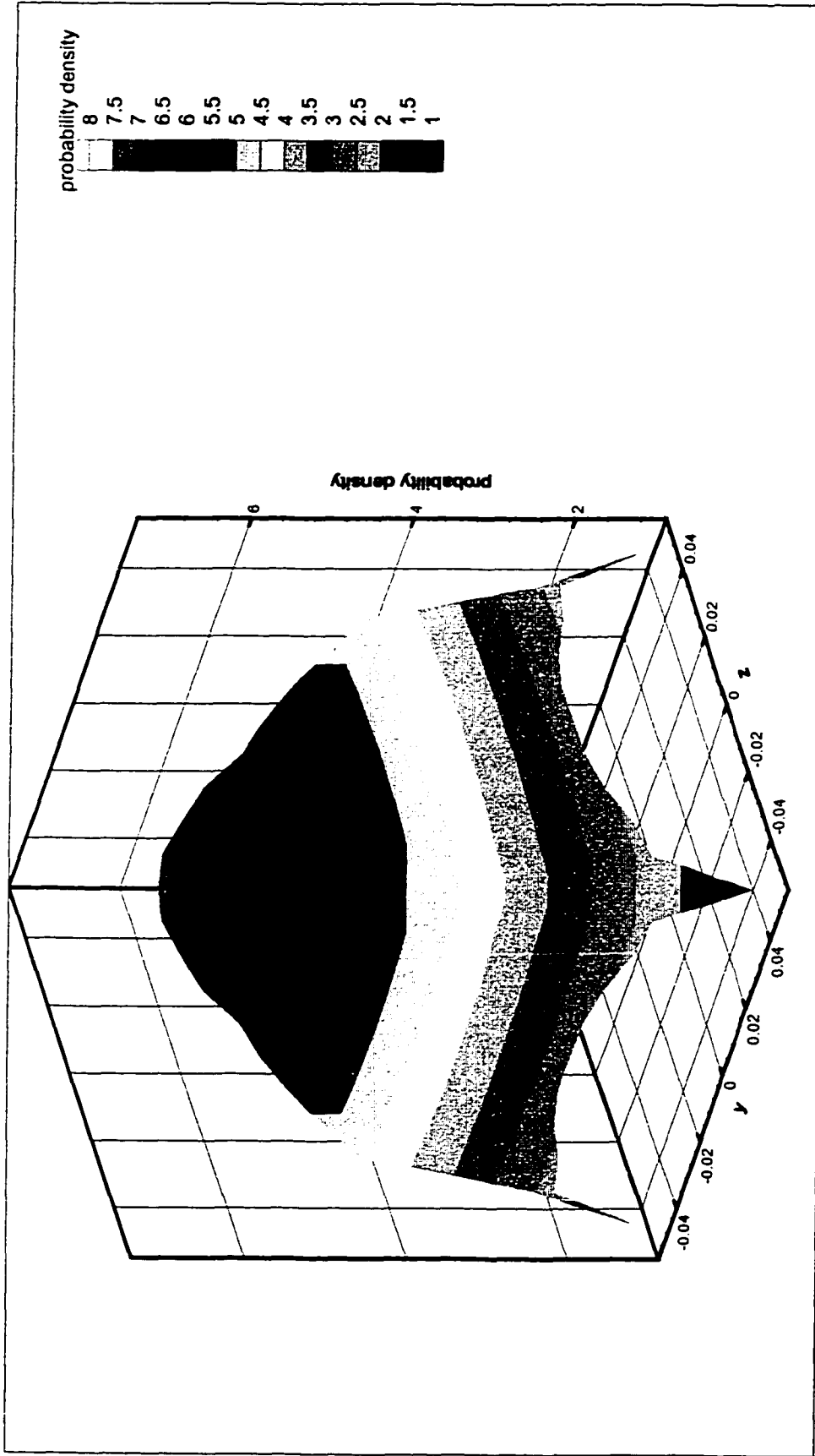


Figure 5.31. Probability distribution at cross-section  $x=9.99$ ,  $\mu=200$ ,  $t=0.07s$



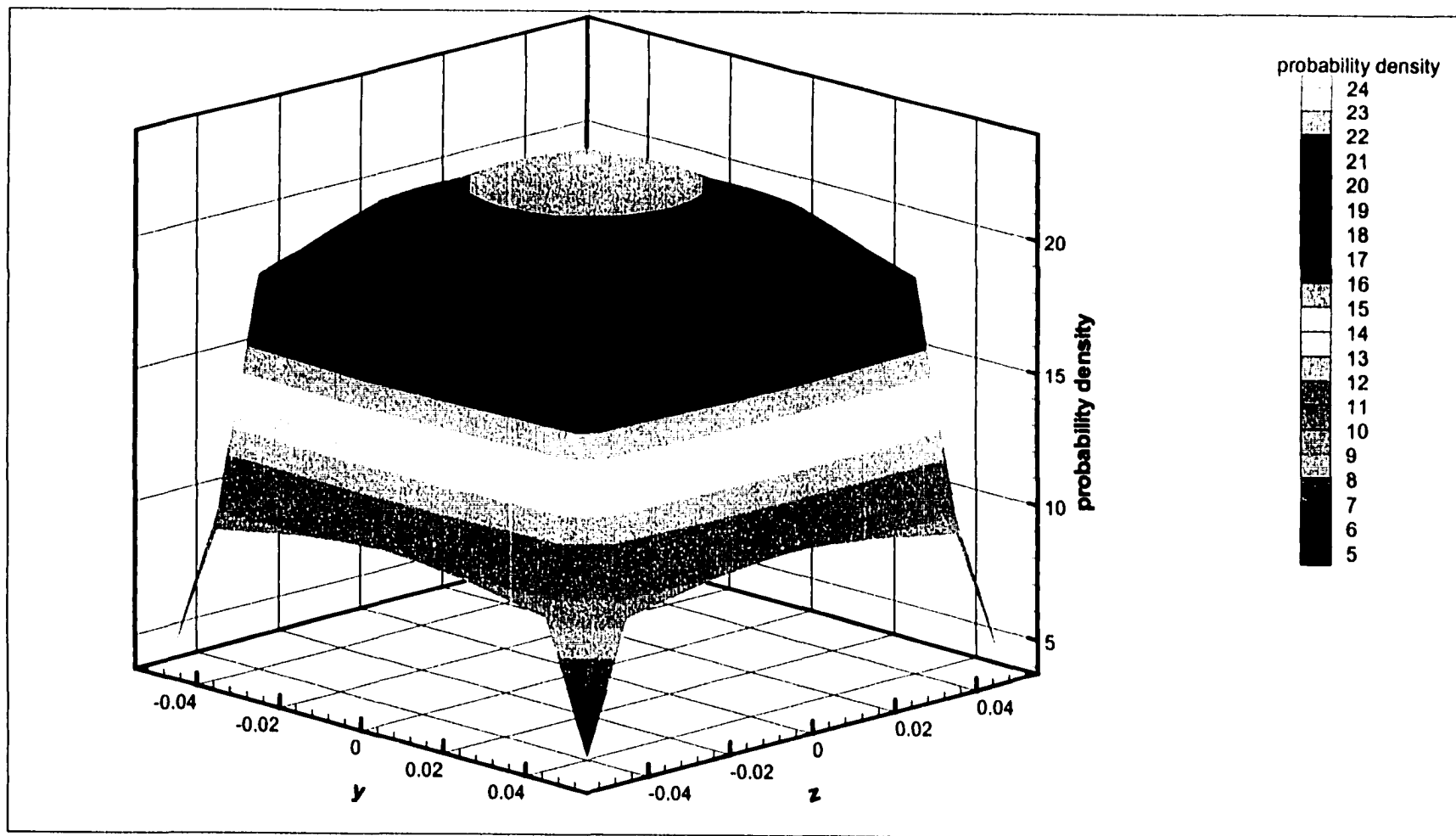


Figure 5.32. Probability distribution at cross-section  $x=9.99$ ,  $\mu=200$ ,  $t=0.08s$

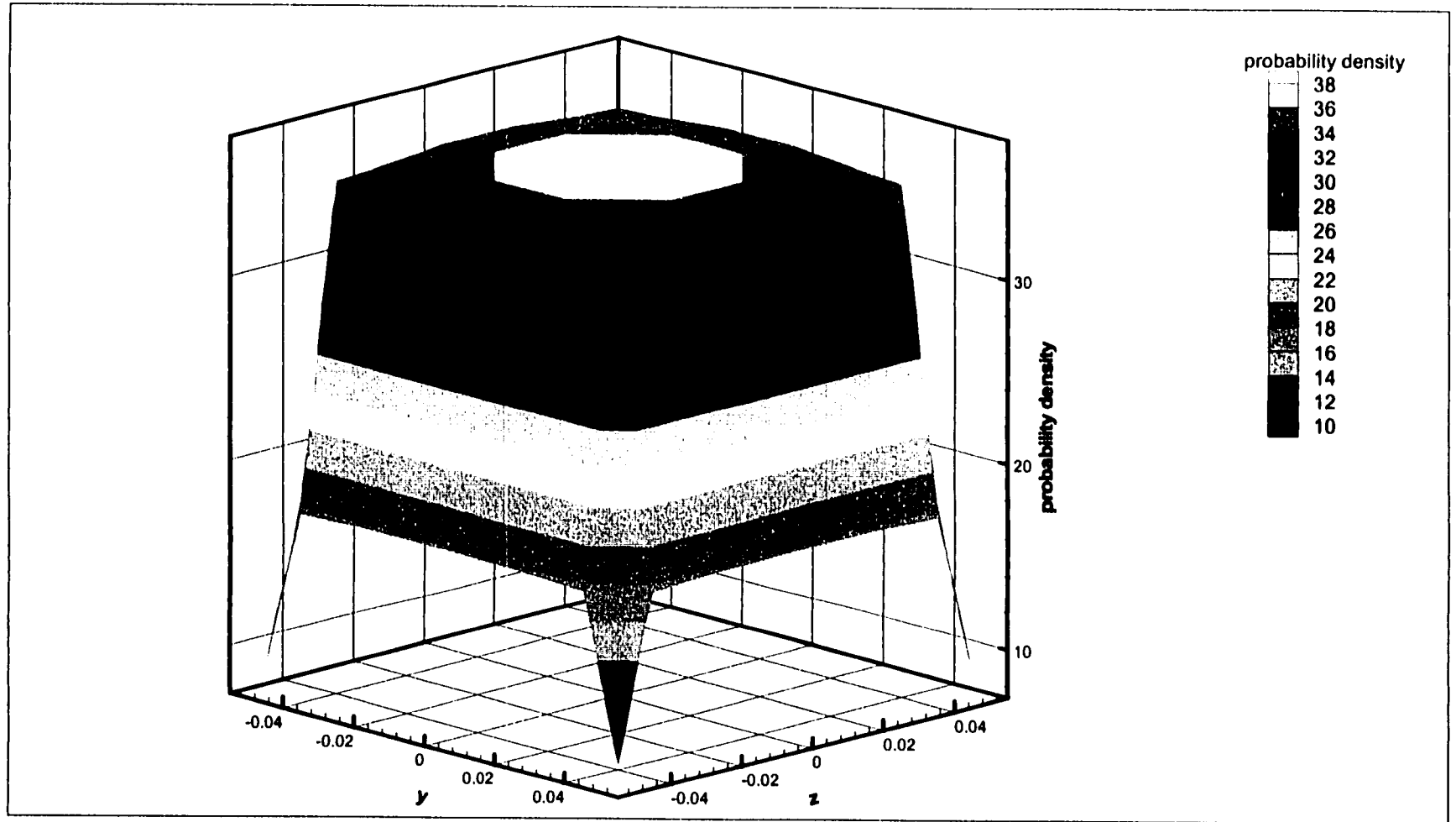


Figure 5.33. Probability distribution at cross-section  $x=9.99$ ,  $\mu=200$ ,  $t=0.09s$

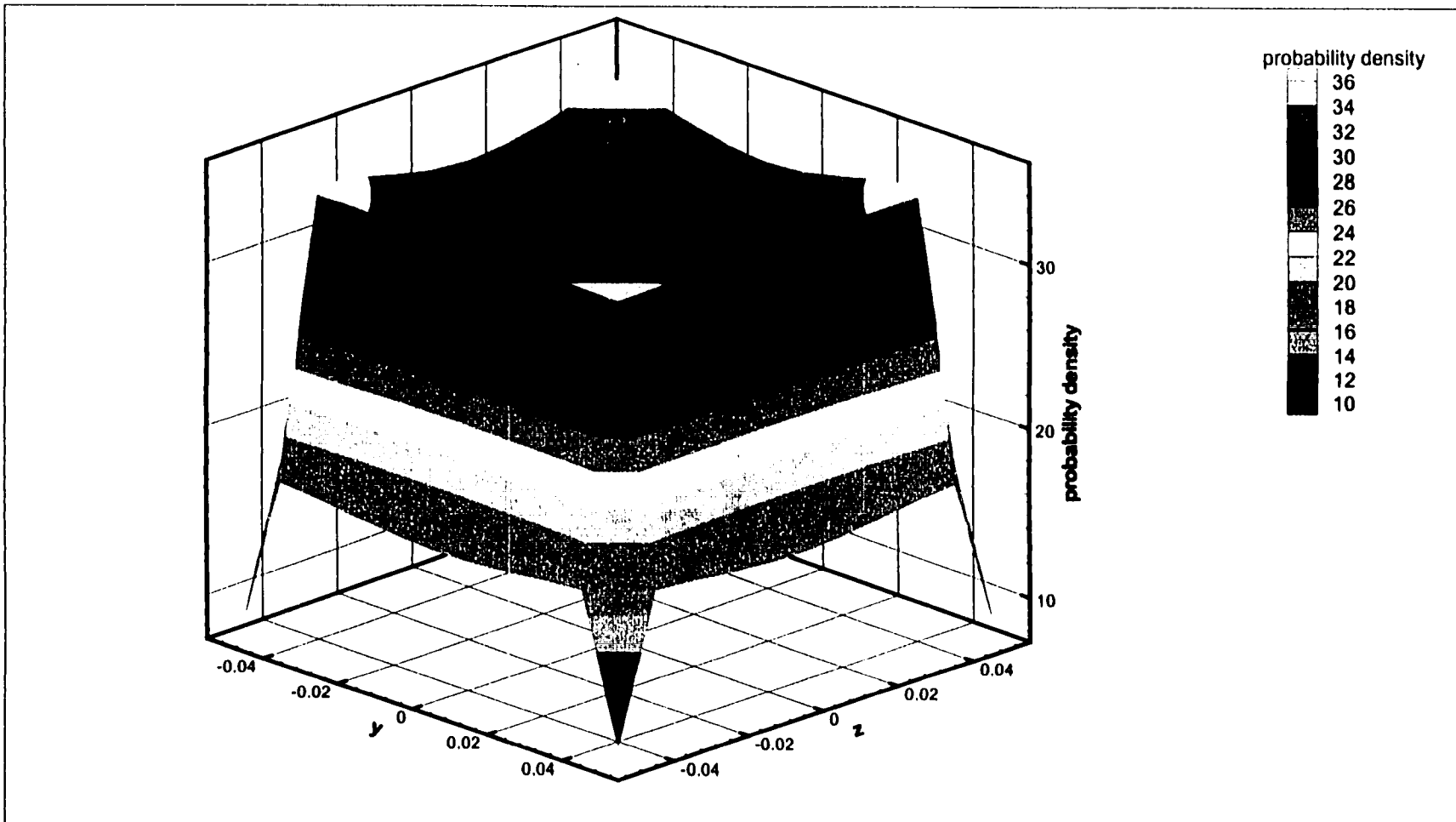


Figure 5.34. Probability distribution at cross-section  $x=9.99$ ,  $\mu=200$ ,  $t=0.1s$

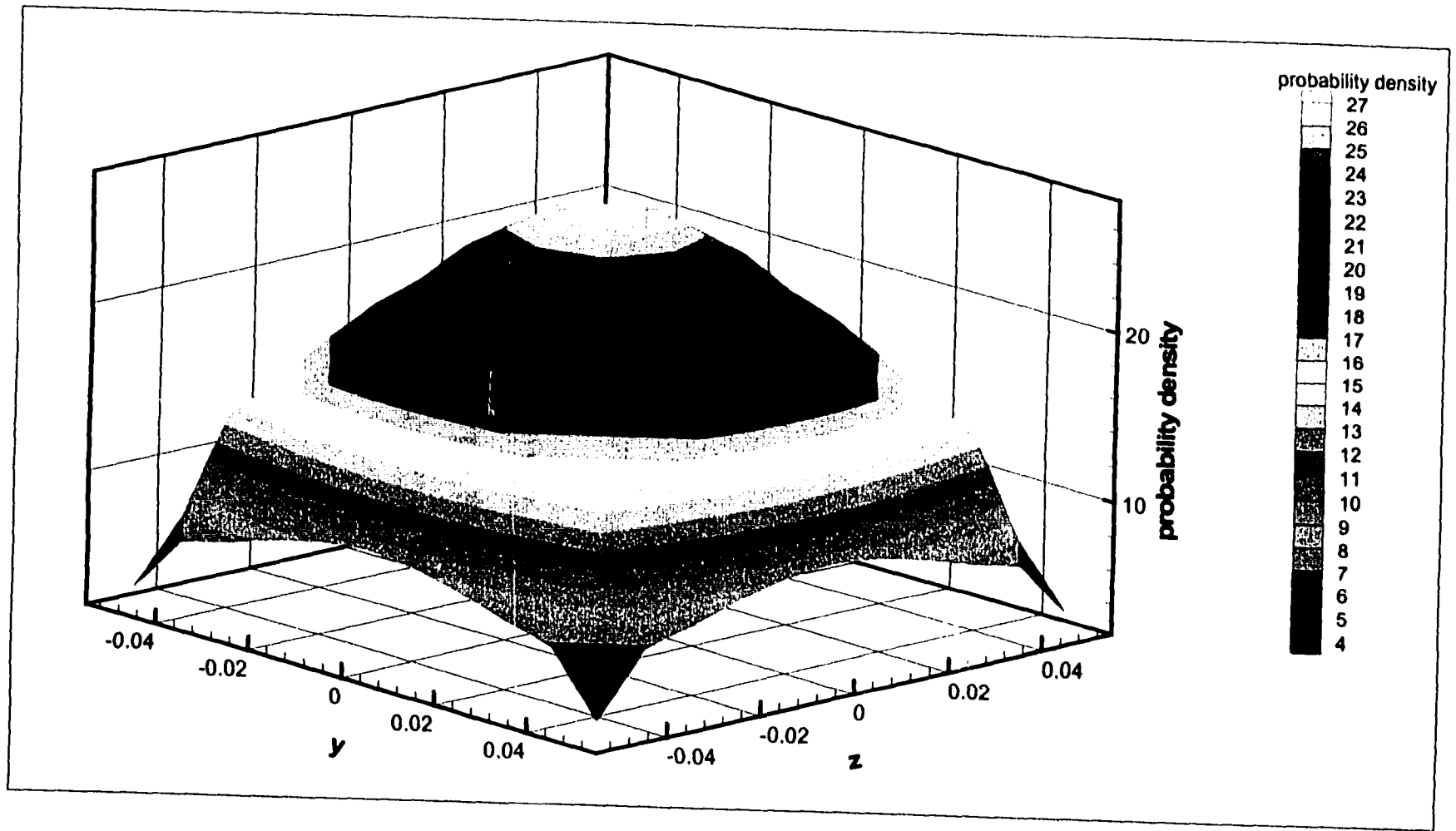


Figure 5.35. Probability distribution at cross-section  $x=3.0$ ,  $\mu=500$ ,  $t=0.004s$

Reproduced with permission of the copyright owner. Further reproduction prohibited without permission.

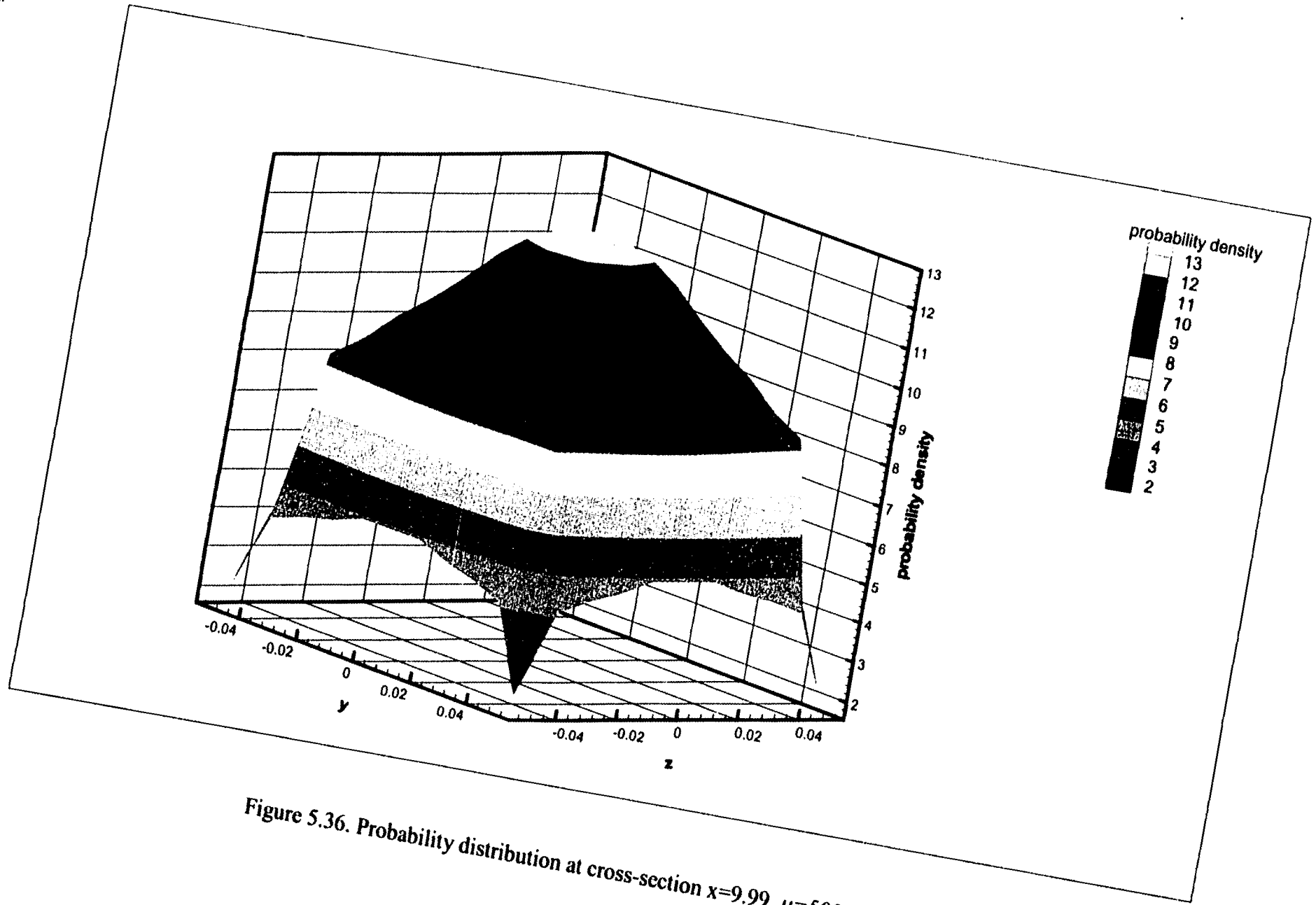


Figure 5.36. Probability distribution at cross-section  $x=9.99$ ,  $\mu=500$ ,  $t=0.028s$

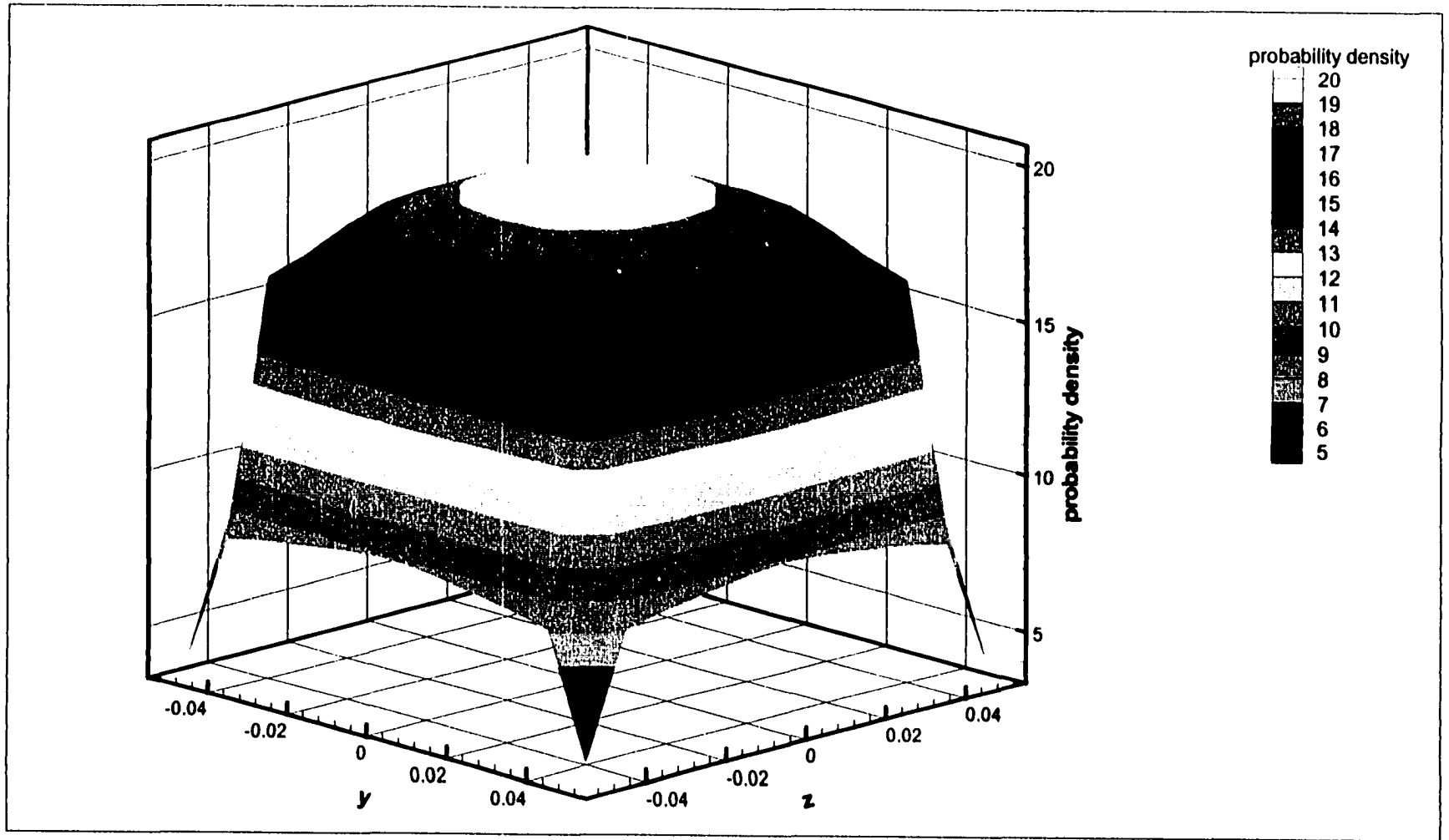


Figure 5.37. Probability distribution at cross-section  $x=9.99$ ,  $\mu=500$ ,  $t=0.032s$

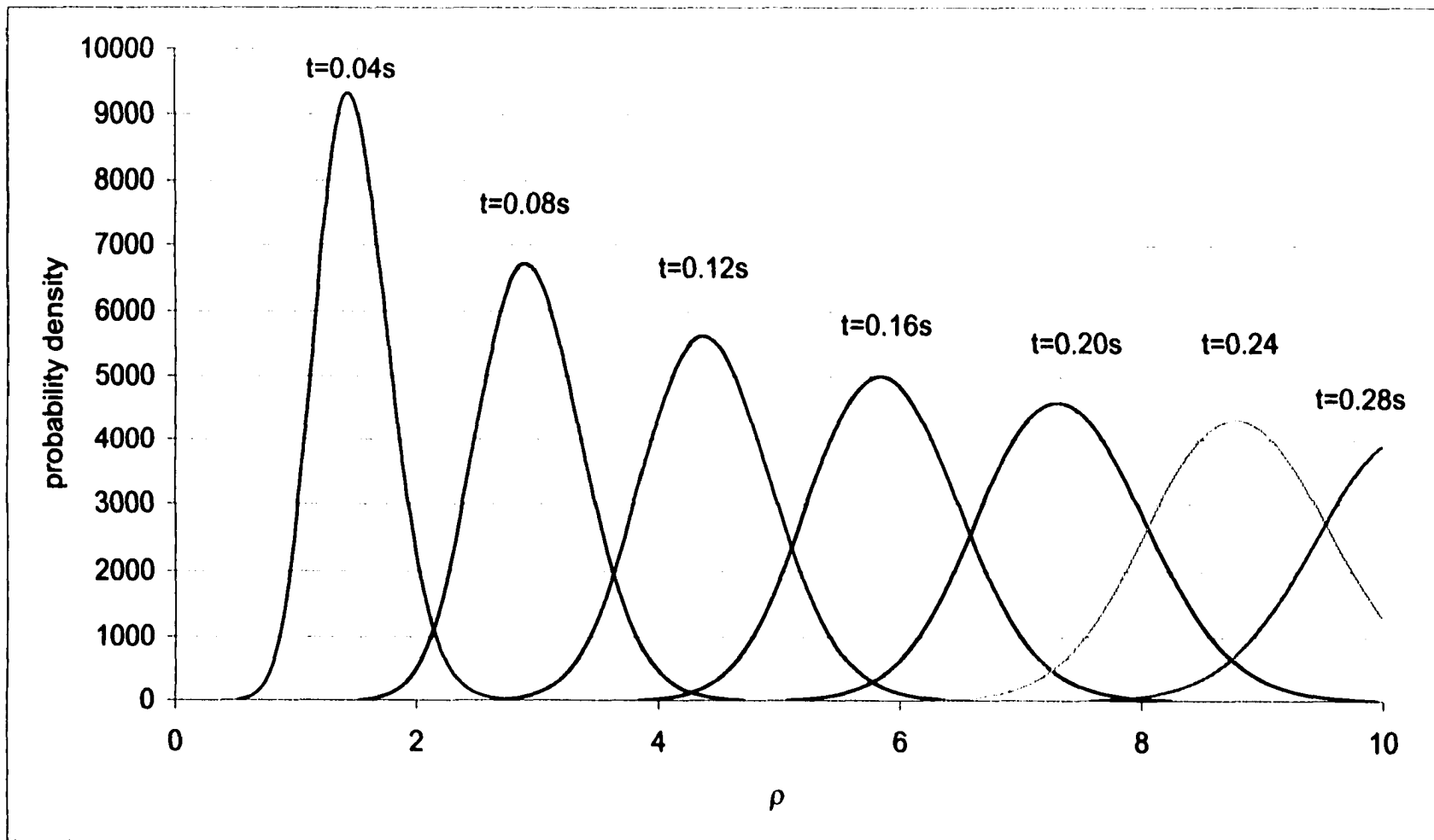


Figure 5.38. Probability distribution of  $\rho$  between 0.04 and 0.4 seconds  
2-D case,  $\mu = 50$

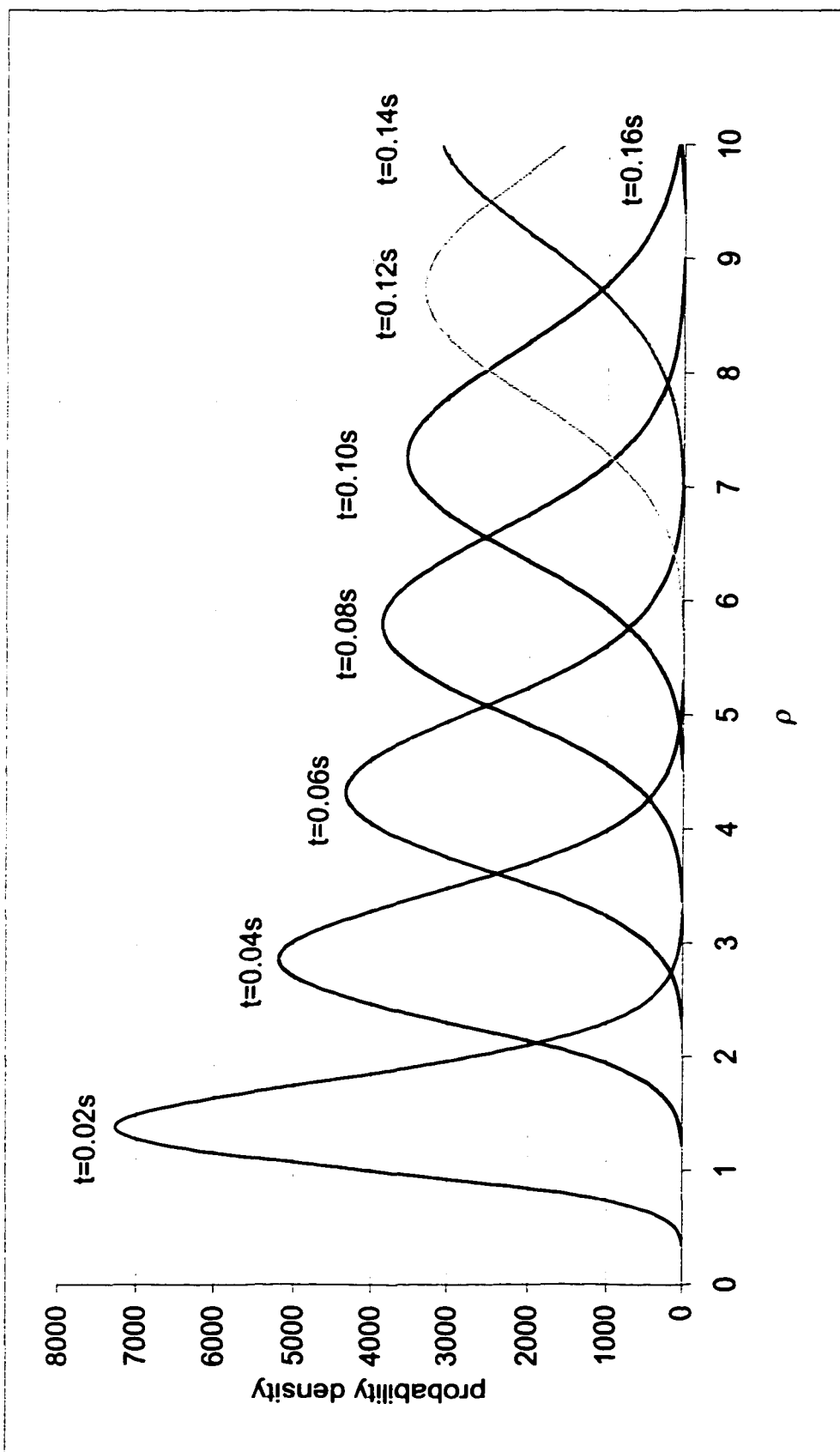


Figure 5.39. Probability distribution of  $\rho$  between 0.02 and 0.2 seconds  
2-D case,  $\mu=100$



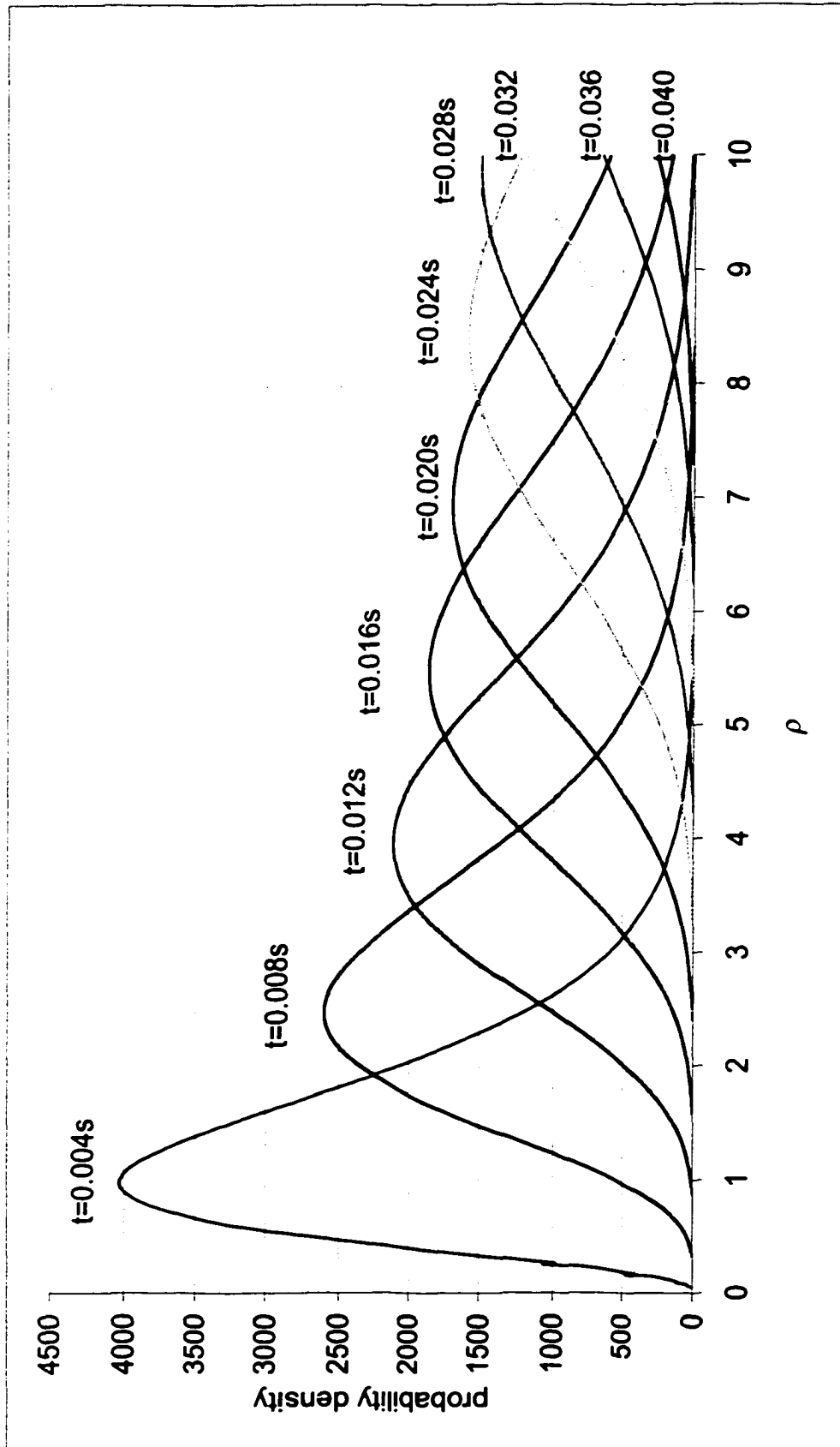


Figure 5.40. Probability distribution of  $\rho$  between 0.004 and 0.04 seconds  
2-D case,  $\mu = 500$

## **CHAPTER 6**

### **CONCLUSION AND FUTURE WORK**

Micro-channel flows have been modeled stochastically to investigate the characteristics of free molecular flow.

Results of the model by Taylor (1953) showed that when a solute in low concentration is injected into a liquid flowing through an infinite straight circular tube of uniform cross-section with a steady convective velocity, the concentration along the capillary (averaged over the cross-section) was asymptotically Gaussian.

The present work utilizes a stochastic approach based on particle motion to model flow in a micro-channel with finite boundaries. The parameters  $\mu_x$ ,  $\mu_y$ , and  $\mu_z$  in our model represent the velocities of the flow in the  $x$ ,  $y$ , and  $z$  directions. These parameters can be measured in future micro-flow experiments at the Louisiana Tech University Institute for Micro-manufacturing (IFM). In this study, hypothetical values for the velocities were made to investigate the various characteristics of the micro-flow. It is hoped this research can accurately predict the distribution of distance traveled by a particle in a three-dimensional channel. The experiments being performed at the IFM have been designed so that particles are tracked through the channel. Images of the particles are photographed at  $t=t_0$ ,  $t=t_0+\Delta t$ ,  $t=t_0+2\Delta t$ , etc. From these images one may calculate  $\mu_x$ ,  $\mu_y$ ,  $\mu_z$  and  $\phi$ . This information can then be applied to the model to predict the distribution of distance traveled by the particle and to determine the adequacy of the

model by comparing predicted and observed results. The model also predicts the residence time distribution in a flow channel or reactor. Knowledge of the Residence Time Distribution, or the distribution of the time a particle stays in a reactor, will be useful information in studies involving chemical reactions. Residence time determines the reaction yield of the product. From the transition probability density obtained in our model and the initial particle density (or number concentration), one can calculate also the distribution of particle or solute concentration in the micro-channel.

In terms of future work, it would be of interest to run computations for complex geometric configurations, and for straight channels with an orifice. Experimental work is also strongly suggested to verify the current model and improve model parameters. In fact Dr. Hegab (personal communication) has been performing some related flow measurements which will help to achieve this goal. Another interesting branch from this work is the extension to circular micro-channels. Circular micro-channels are comparable to numerous biological systems. Experimentation and modeling in this area using stochastic processes could be quite beneficial. For example, knowledge of the probability distribution of the distance drugs travel in the blood stream as a function of time could effect the quality of drug therapy and dosing systems.

## APPENDIX A

### FORTRAN CODE FOR THE STOCHASTIC MODEL

```
c Hilda Black          August 2000
c
c the purpose of the code is to numerically solve
c a partial differential equation related to fluid flow
c using the central and backward (i and i-1) difference methods.
c
c Parameters based on the physical parameters of Dr. Hegab's
c experiments at the Louisiana Tech Institute for Micromanufacturing
c
c prints Final Iteration only
c
c make sure nx*hx=10, ny*hy=.1, nz*hz=.1
c unit of measure is mm.
c the x length is approximately 10 mm.
c the y and z lengths are approximately 100 micrometer or 0.1 mm
c *****
  dimension uk(0:5001,0:11,0:11),
  *          ukp1(0:5001,0:11,0:11),
  *          ukp2(0:5001,0:11,0:11),
  *          f(0:11,0:11), b1(0:11), b2(0:11),
  *          a1(0:5001,0:11,0:11),dd(0:5001,0:11,0:11)
  double precision uk,ukp1,ukp2,f,b1,b2,a1,dd,
  *          hx,hy,hz,dt,dtxx,dtty,dtzz,dtx,dtz,
  *          a,aa,v,y,z,x,y,z,un,rho3D,rho2D,prob
c number of grid points
c from 0 to nx, 0 to ny, 0 to nz
  nx=1000
  ny=10
  nz=10
c grid size
  hx=0.01
  hy=0.01
  hz=0.01
c *****
c parameters see page 3 of proposal
c diffusivity coefficient of water, should = 1/re.
  phi = 0.125
c velocity
  uo = 500.0
c half of the length of y and/or z
  a = (ny*hy)/2.0
  aa=a*a
c *****
  dt=0.001
```

```

      dtxx=dt*phi/(2.0*hx*hx)
      dtyy=dt*phi/(2.0*hy*hy)
      dtzz=dt*phi/(2.0*hz*hz)
      dtx=dt*uo/(hx)
      dty=dt/(hy)
      dtz=dt/(hz)
c *****
c used to check convergence
      tol = 0.001
      maxsteps = 40
c *****
c initial conditions
c this group sets inner values to 1/v when i=0 so that only the first
c cross section has 1/v for the inner values. 1/v is the point volume
      do i=0,nx
        do j=0,ny
          do k=0,nz
            uk(i,j,k)=0
          enddo
        enddo
      enddo
c Original initial conditions
      do j=1,ny-1
        do k=1,nz-1
          v=hx*(ny-1)*hy*(nz-1)*hz
          uk(0,j,k)=1/v
        enddo
      enddo
c
1 format(1x,I4,1x,I2,1x,I2)
  Write(*,2)
2 format(1x,'NX',1x,'NY',1x,'NZ')
  Write(*,1) nx,ny,nz
  Write(*,3)
3 format(1x,'HX',1x,'HY',1x,'HZ')
  Write(*,9) hx,hy,hz
  Write(*,4)
4 format(1x,'V',1x,'1/V',1x,'PHI')
  Write(*,9) v,1/v,phi
  Write(*,5)
5 format(1x,'U0',1x,'a',1x,'tol')
  Write(*,9) uo,a,tol
  Write(*,6)
6 format(1x,'NX*HX',1x,'NY*HY',1x,'NZ*HZ')
  Write(*,9) nx*hx,ny*hy,nz*hz
  Write(*,7)
7 format(1x,'DT',1x,'MAXSTEPS')
  Write(*,8) dt,maxsteps
8 format(1x,f12.6,1x,I3)
9 format(1x,f12.6,1x,f12.6,1x,f12.6)
  print *, '*****'
c *****
c function for f see page 3 of proposal
      do j=0,ny
        do k=0,nz
          y=-a+j*hy
          z=-a+k*hz

```

```

        yy=y*y
        zz=z*z
        f(j,k)=(1.0-yy/aa)*(1.0-zz/aa)
    enddo
enddo
c
do j=0,ny
    y=-a+j*hy
    yy=y*y
    b1(j)=0.001*uo*(1.0-yy/aa)
enddo
c
do k=0,nz
    z=-a+k*hz
    zz=z*z
    b2(k)=0.001*uo*(1.0-zz/aa)
enddo
c iteration
12 do i=0,nx
    do j=0,ny
        do k=0,nz
            ukp1(i,j,k)=uk(i,j,k)
        enddo
    enddo
enddo
c *****
do i=1,nx-1
    do j=1,ny-1
        do k=1,nz-1
            dd(i,j,k)=uk(i,j,k)
            *          +dtxx*(uk(i+1,j,k)-2.0*uk(i,j,k)+uk(i-1,j,k))
            *          +dtyy*(uk(i,j+1,k)-2.0*uk(i,j,k)+uk(i,j-1,k))
            *          +dtzz*(uk(i,j,k+1)-2.0*uk(i,j,k)+uk(i,j,k-1))
        enddo
    enddo
enddo
c *****
do i=1,nx-1
    do j=1,ny-1
        do k=1,nz-1
            a1(i,j,k)=1.0 + 2.0*dtxx + 2.0*dtyy + 2.0*dtzz
            *          + dtx*f(j,k)
            *          + dty*b1(j)
            *          + dtz*b2(k)
        enddo
    enddo
enddo
c *****
count=0
c new calculation method
15 count =count+1
do i=1,nx-1
    do j=1,ny-1
        do k=1,nz-1
            if((j.le.((ny-1)/2)).and.(k.le.((nz-1)/2))) then
                un=dtxx*(ukp1(i+1,j,k)+ukp1(i-1,j,k))
                *      +dtyy*(ukp1(i,j+1,k)+ukp1(i,j-1,k))
            endif
        enddo
    enddo
enddo

```

```

*      +dtzz*(ukp1(i,j,k+1)+ukp1(i,j,k-1))
*      +dtx*f(j,k)*ukp1(i-1,j,k)
*      +b1(j+1)*ukp1(i,j+1,k)*dty
*      +b2(k+1)*ukp1(i,j,k+1)*dtz
*      +dd(i,j,k)
      else if (j.le.((ny-1)/2)) then
        un=dtxx*(ukp1(i+1,j,k)+ukp1(i-1,j,k))
*      +dtyy*(ukp1(i,j+1,k)+ukp1(i,j-1,k))
*      +dtzz*(ukp1(i,j,k+1)+ukp1(i,j,k-1))
*      +dtx*f(j,k)*ukp1(i-1,j,k)
*      +b1(j+1)*ukp1(i,j+1,k)*dty
*      +b2(k-1)*ukp1(i,j,k-1)*dtz
*      +dd(i,j,k)
      else if (k.le.((ny-1)/2)) then
        un=dtxx*(ukp1(i+1,j,k)+ukp1(i-1,j,k))
*      +dtyy*(ukp1(i,j+1,k)+ukp1(i,j-1,k))
*      +dtzz*(ukp1(i,j,k+1)+ukp1(i,j,k-1))
*      +dtx*f(j,k)*ukp1(i-1,j,k)
*      +b1(j-1)*ukp1(i,j-1,k)*dty
*      +b2(k+1)*ukp1(i,j,k+1)*dtz
*      +dd(i,j,k)
      else
        un=dtxx*(ukp1(i+1,j,k)+ukp1(i-1,j,k))
*      +dtyy*(ukp1(i,j+1,k)+ukp1(i,j-1,k))
*      +dtzz*(ukp1(i,j,k+1)+ukp1(i,j,k-1))
*      +dtx*f(j,k)*ukp1(i-1,j,k)
*      +b1(j-1)*ukp1(i,j-1,k)*dty
*      +b2(k-1)*ukp1(i,j,k-1)*dtz
*      +dd(i,j,k)
      end if
      ukp2(i,j,k)=un/a1(i,j,k)
    enddo
  enddo
enddo
c *****
c boundary conditions
c boundary points walls
  do i=1,nx-1
c y direction
  do k=1,nz-1
c y=-a
  j=0
  ukp2(i,j,k) = ukp2(i,j+1,k)
c y=a
  j=ny
  ukp2(i,j,k) = ukp2(i,j-1,k)
  enddo
c z direction
  do j=0,ny
c z=-a
  k=0
  ukp2(i,j,k) = ukp2(i,j,k+1)
c z=a
  k=nz
  ukp2(i,j,k) = ukp2(i,j,k-1)
  enddo
  enddo
enddo

```

```

c boundary points - enter - exit  c check these
  do j=0,ny
    do k=0,nz
c x=0
      i=0
      ukp2(i,j,k) = (phi*ukp2(i+1,j,k))/(phi+hx*uo*f(j,k))
c x=nx
      i=nx
      ukp2(i,j,k) = 0
    enddo
  enddo
c *****
c convergence test (global max)
  diffmax = 0.0
  do i=0,nx
    do j=0,ny
      do k=0,nz
        diff=abs(ukp1(i,j,k)-ukp2(i,j,k))
        if (diff.gt.diffmax) then
          diffmax=diff
        end if
      enddo
    enddo
  enddo
c
*****
*****
  if (diffmax.le.tol) goto 20
c grid computation(copy new values to old values)
  do i=0,nx
    do j=0,ny
      do k=0,nz
        ukp1(i,j,k)=ukp2(i,j,k)
      enddo
    enddo
  enddo
  goto 15
c
*****
*****
  20 nt=nt+1
  do i=0,nx
    do j=0,ny
      do k=0,nz
        uk(i,j,k)=ukp2(i,j,k)
      enddo
    enddo
  enddo
c
  if (nt.eq.maxsteps) goto 30
  goto 12
c printing
  30 sum=0.0
  print *, 'final iteration after', nt, ' steps:'
  ProbCount=0
  Write(*,110)
  110 format(1x,'X',1x,'Y',1x,'Z',2x,'rho2D',2x,'rho3D',2x,'PROB')

```



```

111 format (1x, f12.3, 1x, f12.3, 1x, f12.3, 1x, f14.2, 1x, f14.2, 1x, f14.7)
114 format (11f14.6)
c inner summation
  do i=1,nx-1
    do j=1,ny-1
      do k=1,nz-1
        x=i*hx
        y=-a+j*hy
        z=-a+k*hz
        rho2D=sqrt(x*x+y*y)
        rho3D=sqrt(x*x+y*y+z*z)
        prob=uk(i,j,k)*hx*hy*hz
        if(prob.gt. 0.000001) then
          sum=sum+prob
          write(*,111) x,y,z,rho2D,rho3D,prob
        end if
        if(uk(i,j,k)*hx*hy*hz.gt.1) then
          ProbCount=ProbCount+1
        end if
      enddo
    enddo
  enddo
c wall summation
  do j=1,ny-1
    do k=1,nz-1
      i=0
      x=i*hx
      y=-a+j*hy
      z=-a+k*hz
      rho2D=sqrt(x*x+y*y)
      rho3D=sqrt(x*x+y*y+z*z)
      prob=uk(i,j,k)*hx*hy*hz/2.0
      if(prob.gt. 0.000001) then
        sum=sum+prob
        write(*,111) x,y,z,rho2D,rho3D,prob
      end if
      if(uk(i,j,k)*hx*hy*hz.gt.1) then
        ProbCount=ProbCount+1
      end if
      i=nx
      x=i*hx
      rho2D=sqrt(x*x+y*y)
      rho3D=sqrt(x*x+y*y+z*z)
      prob=uk(i,j,k)*hx*hy*hz/2.0
      if(prob.gt. 0.000001) then
        sum=sum+prob
        write(*,111) x,y,z,rho2D,rho3D,prob
      end if
      if(uk(i,j,k)*hx*hy*hz.gt.1) then
        ProbCount=ProbCount+1
      end if
    enddo
  enddo
do i=1,nx-1
  do k=1,nz-1
    x=i*hx
    j=0

```

```

y=-a+j*hy
z=-a+k*hz
rho2D=sqrt(x*x+y*y)
rho3D=sqrt(x*x+y*y+z*z)
prob=uk(i,j,k)*hx*hy*hz/2.0
if(prob.gt. 0.000001) then
sum=sum+prob
write(*,111) x,y,z,rho2D,rho3D,prob
end if
if(uk(i,j,k)*hx*hy*hz.gt.1) then
ProbCount=ProbCount+1
end if
j=ny
y=-a+j*hy
rho2D=sqrt(x*x+y*y)
rho3D=sqrt(x*x+y*y+z*z)
prob=uk(i,j,k)*hx*hy*hz/2.0
if(prob.gt. 0.000001) then
sum=sum+prob
write(*,111) x,y,z,rho2D,rho3D,prob
end if
if(uk(i,j,k)*hx*hy*hz.gt.1) then
ProbCount=ProbCount+1
end if
enddo
enddo
do i=1,nx-1
do j=1,ny-1
x=i*hx
k=0
y=-a+j*hy
z=-a+k*hz
rho2D=sqrt(x*x+y*y)
rho3D=sqrt(x*x+y*y+z*z)
prob=uk(i,j,k)*hx*hy*hz/2.0
if(prob.gt. 0.000001) then
sum=sum+prob
write(*,111) x,y,z,rho2D,rho3D,prob
end if
if(uk(i,j,k)*hx*hy*hz.gt.1) then
ProbCount=ProbCount+1
end if
k=nz
y=-a+j*hy
z=-a+k*hz
rho2D=sqrt(x*x+y*y)
rho3D=sqrt(x*x+y*y+z*z)
prob=uk(i,j,k)*hx*hy*hz/2.0
if(prob.gt. 0.000001) then
sum=sum+prob
write(*,111) x,y,z,rho2D,rho3D,prob
end if
if(uk(i,j,k)*hx*hy*hz.gt.1) then
ProbCount=ProbCount+1
end if
enddo
enddo

```

```

c edge summation
  do i=1,nx-1
    j=0
    k=0
    x=i*hx
    y=-a+j*hy
    z=-a+k*hz
    rho2D=sqrt(x*x+y*y)
    rho3D=sqrt(x*x+y*y+z*z)
    prob=uk(i,j,k)*hx*hy*hz/4.0
    if(prob.gt. 0.000001) then
      sum=sum+prob
      write(*,111) x,y,z,rho2D,rho3D,prob
    end if
    if(uk(i,j,k)*hx*hy*hz.gt.1) then
      ProbCount=ProbCount+1
    end if
    j=0
    k=nz
    x=i*hx
    y=-a+j*hy
    z=-a+k*hz
    rho2D=sqrt(x*x+y*y)
    rho3D=sqrt(x*x+y*y+z*z)
    prob=uk(i,j,k)*hx*hy*hz/4.0
    if(prob.gt. 0.000001) then
      sum=sum+prob
      write(*,111) x,y,z,rho2D,rho3D,prob
    end if
    if(uk(i,j,k)*hx*hy*hz.gt.1) then
      ProbCount=ProbCount+1
    end if
    j=ny
    k=0
    x=i*hx
    y=-a+j*hy
    z=-a+k*hz
    rho2D=sqrt(x*x+y*y)
    rho3D=sqrt(x*x+y*y+z*z)
    prob=uk(i,j,k)*hx*hy*hz/4.0
    if(prob.gt. 0.000001) then
      sum=sum+prob
      write(*,111) x,y,z,rho2D,rho3D,prob
    end if
    if(uk(i,j,k)*hx*hy*hz.gt.1) then
      ProbCount=ProbCount+1
    end if
    j=ny
    k=nz
    x=i*hx
    y=-a+j*hy
    z=-a+k*hz
    rho2D=sqrt(x*x+y*y)
    rho3D=sqrt(x*x+y*y+z*z)
    prob=uk(i,j,k)*hx*hy*hz/4.0
    if(prob.gt. 0.000001) then
      sum=sum+prob

```

```

write(*,111) x,y,z,rho2D,rho3D,prob
end if
if(uk(i,j,k)*hx*hy*hz.gt.1) then
  ProbCount=ProbCount+1
end if
enddo
do j=1,ny-1
  i=0
  k=0
  x=i*hx
  y=-a+j*hy
  z=-a+k*hz
  rho2D=sqrt(x*x+y*y)
  rho3D=sqrt(x*x+y*y+z*z)
  prob=uk(i,j,k)*hx*hy*hz/4.0
  if(prob.gt. 0.000001) then
    sum=sum+prob
    write(*,111) x,y,z,rho2D,rho3D,prob
  end if
  if(uk(i,j,k)*hx*hy*hz.gt.1) then
    ProbCount=ProbCount+1
  end if
  i=nx
  k=0
  x=i*hx
  y=-a+j*hy
  z=-a+k*hz
  rho2D=sqrt(x*x+y*y)
  rho3D=sqrt(x*x+y*y+z*z)
  prob=uk(i,j,k)*hx*hy*hz/4.0
  if(prob.gt. 0.000001) then
    sum=sum+prob
    write(*,111) x,y,z,rho2D,rho3D,prob
  end if
  if(uk(i,j,k)*hx*hy*hz.gt.1) then
    ProbCount=ProbCount+1
  end if
  i=0
  k=nz
  x=i*hx
  y=-a+j*hy
  z=-a+k*hz
  rho2D=sqrt(x*x+y*y)
  rho3D=sqrt(x*x+y*y+z*z)
  prob=uk(i,j,k)*hx*hy*hz/4.0
  if(prob.gt. 0.000001) then
    sum=sum+prob
    write(*,111) x,y,z,rho2D,rho3D,prob
  end if
  if(uk(i,j,k)*hx*hy*hz.gt.1) then
    ProbCount=ProbCount+1
  end if
  i=nx
  k=nz
  x=i*hx
  y=-a+j*hy
  z=-a+k*hz

```

```

rho2D=sqrt(x*x+y*y)
rho3D=sqrt(x*x+y*y+z*z)
  prob=uk(i,j,k)*hx*hy*hz/4.0
  if(prob.gt. 0.000001) then
    sum=sum+prob
  write(*,111) x,y,z,rho2D,rho3D,prob
  end if
if(uk(i,j,k)*hx*hy*hz.gt.1) then
  ProbCount=ProbCount+1
end if
enddo
do k=1,nz-1
  i=0
  j=0
  x=i*hx
  y=-a+j*hy
  z=-a+k*hz
  rho2D=sqrt(x*x+y*y)
  rho3D=sqrt(x*x+y*y+z*z)
  prob=uk(i,j,k)*hx*hy*hz/4.0
  if(prob.gt. 0.000001) then
    sum=sum+prob
  write(*,111) x,y,z,rho2D,rho3D,prob
  end if
if(uk(i,j,k)*hx*hy*hz.gt.1) then
  ProbCount=ProbCount+1
end if
i=nx
  j=0
  x=i*hx
  y=-a+j*hy
  z=-a+k*hz
  rho2D=sqrt(x*x+y*y)
  rho3D=sqrt(x*x+y*y+z*z)
  prob=uk(i,j,k)*hx*hy*hz/4.0
  if(prob.gt. 0.000001) then
    sum=sum+prob
  write(*,111) x,y,z,rho2D,rho3D,prob
  end if
if(uk(i,j,k)*hx*hy*hz.gt.1) then
  ProbCount=ProbCount+1
end if
i=0
  j=ny
  x=i*hx
  y=-a+j*hy
  z=-a+k*hz
  rho2D=sqrt(x*x+y*y)
  rho3D=sqrt(x*x+y*y+z*z)
  prob=uk(i,j,k)*hx*hy*hz/4.0
  if(prob.gt. 0.000001) then
    sum=sum+prob
  write(*,111) x,y,z,rho2D,rho3D,prob
  end if
if(uk(i,j,k)*hx*hy*hz.gt.1) then
  ProbCount=ProbCount+1
end if

```

```

i=nx
  j=ny
  x=i*hx
  y=-a+j*hy
z=-a+k*hz
rho2D=sqrt(x*x+y*y)
rho3D=sqrt(x*x+y*y+z*z)
  prob=uk(i,j,k)*hx*hy*hz/4.0
  if(prob.gt. 0.000001) then
    sum=sum+prob
  write(*,111) x,y,z,rho2D,rho3D,prob
  end if
if(uk(i,j,k)*hx*hy*hz.gt.1) then
  ProbCount=ProbCount+1
end if
enddo
c corner summation
  i=0
  j=0
  k=0
  x=i*hx
  y=-a+j*hy
z=-a+k*hz
rho2D=sqrt(x*x+y*y)
rho3D=sqrt(x*x+y*y+z*z)
  prob=uk(i,j,k)*hx*hy*hz/8.0
  if(prob.gt. 0.000001) then
    sum=sum+prob
  write(*,111) x,y,z,rho2D,rho3D,prob
  end if
if(uk(i,j,k)*hx*hy*hz.gt.1) then
  ProbCount=ProbCount+1
end if
i=0
  j=0
  k=nz
  x=i*hx
  y=-a+j*hy
z=-a+k*hz
rho2D=sqrt(x*x+y*y)
rho3D=sqrt(x*x+y*y+z*z)
  prob=uk(i,j,k)*hx*hy*hz/8.0
  if(prob.gt. 0.000001) then
    sum=sum+prob
  write(*,111) x,y,z,rho2D,rho3D,prob
  end if
if(uk(i,j,k)*hx*hy*hz.gt.1) then
  ProbCount=ProbCount+1
end if
i=0
  j=ny
  k=0
  x=i*hx
  y=-a+j*hy
z=-a+k*hz
rho2D=sqrt(x*x+y*y)
rho3D=sqrt(x*x+y*y+z*z)

```

```

        prob=uk(i,j,k)*hx*hy*hz/8.0
        if(prob.gt. 0.000001) then
            sum=sum+prob
        write(*,111) x,y,z,rho2D,rho3D,prob
        end if
    if(uk(i,j,k)*hx*hy*hz.gt.1) then
        ProbCount=ProbCount+1
    end if
    i=0
    j=ny
    k=nz
    x=i*hx
    y=-a+j*hy
    z=-a+k*hz
    rho2D=sqrt(x*x+y*y)
    rho3D=sqrt(x*x+y*y+z*z)
    prob=uk(i,j,k)*hx*hy*hz/8.0
    if(prob.gt. 0.000001) then
        sum=sum+prob
    write(*,111) x,y,z,rho2D,rho3D,prob
    end if
    if(uk(i,j,k)*hx*hy*hz.gt.1) then
        ProbCount=ProbCount+1
    end if
    i=nx
    j=0
    k=0
    x=i*hx
    y=-a+j*hy
    z=-a+k*hz
    rho2D=sqrt(x*x+y*y)
    rho3D=sqrt(x*x+y*y+z*z)
    prob=uk(i,j,k)*hx*hy*hz/8.0
    if(prob.gt. 0.000001) then
        sum=sum+prob
    write(*,111) x,y,z,rho2D,rho3D,prob
    end if
    if(uk(i,j,k)*hx*hy*hz.gt.1) then
        ProbCount=ProbCount+1
    end if
    i=nx
    j=0
    k=nz
    x=i*hx
    y=-a+j*hy
    z=-a+k*hz
    rho2D=sqrt(x*x+y*y)
    rho3D=sqrt(x*x+y*y+z*z)
    prob=uk(i,j,k)*hx*hy*hz/8.0
    if(prob.gt. 0.000001) then
        sum=sum+prob
    write(*,111) x,y,z,rho2D,rho3D,prob
    end if
    if(uk(i,j,k)*hx*hy*hz.gt.1) then
        ProbCount=ProbCount+1
    end if
    i=nx

```

```

      j=ny
      k=0
      x=i*hx
      y=-a+j*hy
      z=-a+k*hz
      rho2D=sqrt(x*x+y*y)
      rho3D=sqrt(x*x+y*y+z*z)
      prob=uk(i,j,k)*hx*hy*hz/8.0
      if(prob.gt. 0.000001) then
        sum=sum+prob
      write(*,111) x,y,z,rho2D,rho3D,prob
      end if
    if(uk(i,j,k)*hx*hy*hz.gt.1) then
      ProbCount=ProbCount+1
    end if
    i=nx
    j=ny
    k=nz
    x=i*hx
    y=-a+j*hy
    z=-a+k*hz
    rho2D=sqrt(x*x+y*y)
    rho3D=sqrt(x*x+y*y+z*z)
    prob=uk(i,j,k)*hx*hy*hz/8.0
    if(prob.gt. 0.000001) then
      sum=sum+prob
    write(*,111) x,y,z,rho2D,rho3D,prob
    end if
  if(uk(i,j,k)*hx*hy*hz.gt.1) then
    ProbCount=ProbCount+1
  end if
  print *,'Over-all summation= ', sum
  print *,'ProbCount>1 is ', ProbCount
  print *,'*****'
end

```



## APPENDIX B

### C++ PROGRAM FOR PROCESSING X CROSS-SECTIONS

```
/******  
* HILDA BLACK      Spring 2000      *  
* code for data processing of research results      *  
* This program inputs the relevant data from a text file called*  
* "output.txt". Looks for the observations with cross-section *  
* x=val, where val is a value input by the user. Prints a      *  
* report listing the x, y, z, and Prob values for this      *  
* cross-section in a file called "out.out".      *  
*****/  
  
#include <iostream.h>  
#include <string.h>  
#include <iomanip.h>  
#include <fstream.h>  
#include <stdlib.h>  
#include <stdio.h>  
#include <math.h>  
  
FILE *fp;  
  
void main()  
{  
    // Variable and function declarations  
    int getInput();  
    int count =getInput();  
}  
  
int getInput()  
{  
    fp = fopen("out.out", "w");  
    if(fp != NULL)  
    {
```

```

ifstream inFile("output.txt", ios::in);
if(!inFile)
{
    cerr<<"Cannot open input file."<<endl;
    exit(0);
} //end of if
int count = 0;
double x,y,z,r2d,r3d,Prob,val;
cout <<"Enter a cross-section value."<<endl;
cin >> val;
inFile>>x>>y>>z>>r2d>>r3d>>Prob;
while (inFile.good())
{
    inFile>>x>>y>>z>>r2d>>r3d>>Prob;
    if(x==val)
    {
        fprintf(fp,"% .2f  % .2f  % .2f
%.7f\n",x,y,z,Prob);
    }
    count++;
};
return count;
} //end of if(fp != NULL)
else
{
    cout<<"File error."<<endl;
    return -1;
}
fclose(fp);
}

```

## APPENDIX C

### C++ PROGRAM FOR PROCESSING DATA ACCORDING TO RHO VALUES

```
/******  
* HILDA BLACK      August 2000      *  
* code for data processing of  research results      *  
* This program inputs the relevant data from a text file      *  
* "lastd.txt", sorts data by Rho in increasing order, and then *  
* prints out a report listing the Data for which the field      *  
* Y is different from 0.      *  
*****/  
  
#include <iostream.h>  
#include <string.h>  
#include <iomanip.h>  
#include <fstream.h>  
#include <stdlib.h>  
#include <stdio.h>  
#include <math.h>  
  
void main()  
{  
    // Variable and function declarations  
    int getInput();  
    int count =getInput();  
}  
  
//int getInput(struct DataType *Dat)  
int getInput()  
{  
    ifstream inFile("lastd.txt", ios::in);  
    if(!inFile)  
    {  
        cerr<<"Cannot open input file."<<endl;  
        exit(0);  
    }  
}
```

```
    }//end of if
    int count = 0;
double Rho,TempR,TempP,Prob;
    inFile>>Rho>>Prob;
    TempR=Rho;
    TempP=Prob;
    double sum=TempP;

    while (inFile.good())
    {
        inFile >> Rho>>Prob;
        if (Rho!=TempR)
        {
            printf("%.3f %f\n",TempR,sum) ;
            sum=Prob;
        }
        else
        {
            sum=sum+Prob;
        }
        TempR=Rho;
        TempP=Prob;
        count++;
    };//end of while (inFile.good())
    return count;
}
```

## APPENDIX D

### C++ PROGRAM FOR ORDERING DATA IN A SINGLE CROSS-SECTION

```
/******  
* HILDA BLACK    August 2000  
* code for data processing of research results  
* Data is represented by a record of the form  
*   struct DataType  
*   {  
*       double X;  
*       double Y;  
*       double Z;  
*       double Prob;  
*   }  
* This program inputs the relevant data from a text file  
* "out.out", sorts data by Y value and then Z value in  
* increasing order, and then prints out * * a report listing  
* the newly ordered Data for the required cross-section.  
*****/  
  
#include <iostream.h>  
#include <string.h>  
#include <iomanip.h>  
#include <fstream.h>  
#include <stdlib.h>  
#include <stdio.h>  
#include <math.h>  
  
struct DataType  
{  
    double X;  
    double Y;  
    double Z;  
    double Prob;  
};
```

```

void main()
{
    // Variable and function declarations
    struct DataType Data[1000];
    int getInput(struct DataType *dat);
    void outputData(struct DataType *dat, int records);
    void sortData(struct DataType *dat, int records);
    void sortDataZ(struct DataType *dat, int records);
    void Swap(struct DataType& dat1, struct DataType& dat2);
    int count =getInput(Data);
    int records = count;

    sortData(Data, count);
    sortDataZ(Data, count);
    outputData(Data, count);
}

int getInput(struct DataType *Dat)
{
    int count = -1;
    ifstream inFile("out.out", ios::in);
    if(!inFile)
    {
        cerr<<"Cannot open input file."<<endl;
        exit(0);
    }//end of if
    else
    {
        count = 0;
        while (inFile.good())
        {   inFile >> Dat[count].X >> Dat [count].Y >>
Dat [count].Z >> Dat [count].Prob;

            count++;
        };//while (inFile.good()) ;

    }
    return count-1;
}

void Swap(struct DataType& Dat1, struct DataType& Dat2)
{
    // Can only refer to Dat1.X, etc. (no array [] things)

```

```

        // Swaps two out-of-order structure elements
        // makes use of text book algorithm
        // swap(x, y) ---> Temp = x, x = y, y = Temp
        //creates comparable variable Temp to be used as a
"holding" spot
        struct DataType Temp;
        Temp = Dat1;
        Dat1 = Dat2;
        Dat2 = Temp;
}

void sortData(struct DataType *Dat, int records)
{
    // This function allows the use of Dat[i].Y and such...
    // Sorts the data by Y value in increasing order
    for(int i = 0; i < records; i++)
    {
        for(int j = 0; j <= i; j++)
            if(Dat[i].Y < Dat[j].Y)
                Swap(Dat[i],Dat[j]);
    }
}

void sortDataZ(struct DataType *Dat, int records)
{
    // This function allows the use of Dat[i].Z and such...
    // Sorts the data by Z value in increasing order
    for(int i = 0; i < records; i++)
    {
        for(int j = 0; j <= i; j++)
        {
            if(Dat[i].Y==Dat[j].Y)
                if(Dat[i].Z < Dat[j].Z)
                    Swap(Dat[i],Dat[j]);
        }
    }
}

void outputData(struct DataType *Dat, int records)
{
    // Can refer to Dat[i].X in here, etc.
    // Accepts pointer to Data array as argument
    // so looping on the array index is possible.
    for(int i = 0; i < records; i++)

```

```
    {  
        printf("%.3f   %.3f %.3f  
%.7f\n", Dat[i].X, Dat[i].Y, Dat[i].Z, Dat[i].Prob);  
    }  
}
```



## APPENDIX E

### FORTRAN CODE FOR THE IMSL INTEGRATION ROUTINE

```
// EXEC VSF2CLG, PARM.GO='NOXUFLOW'
//FORT.SYSIN DD *
C HILDA MARINO BLACK
C PAGE 221, EQ(71) FROM THE THEORY OF STOCHASTIC PROCESSES
C BY COX AND MILLER
C
C INTEGRATE ON INTERVAL (-INF,A)
C
C MODIFY VALUES FOR A, MU, SIG, AND T
C A=10
C MU=2,4,6,8,10
C SIG=.5
C T=0.25,0.5,0.75,1.0,1.25,1.5,1.75,2.0
C BOUND=A
C
C EXACT VALUE FOR INTEGRAL IS UNKNOWN
C CODE MODIFIED FROM IMSL EXAMPLE FOR QDAGI
C MIGHT NEED TO USE DQDAGI FOR DOUBLE PRECISION

      INTEGER      INTERV, NOUT
      REAL         ABS, ALOG, ATAN, BOUND, ERRABS, ERREST, ERROR,
&                ERRREL, EXACT, EXP,F, PI, RESULT, CONST,MUVAL,MU
      INTRINSIC    ABS, ALOG,EXP
      EXTERNAL     F, QDAGI, UMACH, CONST
      COMMON /INDATA/ A,MU,SIG,T
      DIMENSION MUVAL(5),TVAL(8)
      DATA MUVAL/2,4,6,8,10/,
&          TVAL/.25,.50,.75,1.0,1.25,1.50,1.75,2.0/
      CALL ERSET(0,1,0)

C                                     GET OUTPUT UNIT NUMBER
      CALL UMACH (2, NOUT)

C                                     SET LIMITS OF INTEGRATION
      A=10
      SIG=0.5
      DO J=1,8
         T=TVAL(J)
      DO I=1,5
         MU = MUVAL(I)
         BOUND = A
         WRITE(NOUT,1000)A,MU,SIG,T,BOUND
         INTERV = -1

C                                     SET ERROR TOLERANCES
      ERRABS = 0.0
```

```

ERRREL = 0.001
C ERREST IS THE ERROR ESTIMATE WHICH IS USEFUL FOR COMPARISON
C IF A SOLUTION FOR THE INTEGRAL IS KNOWN
  CALL QDAGI (F, BOUND, INTERV, ERRABS, ERRREL, RESULT, ERREST)
C
  PRINT RESULTS
  PI = CONST('PI')
  WRITE (NOUT,999) RESULT, ERREST
  ENDDO
  ENDDO
  STOP
999  FORMAT (' COMPUTED =',1PE10.3, 13X,'ESTIMATE =', 1PE10.3)
1000 FORMAT (//,5X,'A=',F5.1,/,5X,'MU=',F5.1,/,5X,
  & 'SIG=',F5.1,/,5X,'T=',F5.3,/,5X,'BOUND=',F5.1,/)
C99999 FORMAT (' COMPUTED =', F8.3, 13X, ' EXACT =', F8.3// ' ERROR ',
C & 'ESTIMATE =', 1PE10.3, 6X, 'ERROR =', 1PE10.3)
  END
C
  REAL FUNCTION F (X)
  REAL X,PI,SIG,MU,T,A,FRAC,EXP1,EXP2
  REAL ALOG
  INTRINSIC ALOG
  COMMON /INDATA/ A,MU,SIG,T
  PI=CONST('PI')
  FRAC=1.0/(SIG*SQRT(2*PI*T))
  EXP1=EXP(-(X-MU*T)*(X-MU*T)/(2*SIG*SIG*T))
C EXP1=EXP(-((X-MU*T)**2)/(2*(SIG**2)*T))
C
  EXP2=EXP(2*MU*A/(SIG*SIG)
  & -(X-2*A-MU*T)*(X-2*A-MU*T)/(2*SIG*SIG*T))
C EXP2=EXP((2*MU*A/(SIG**2))
C & -((X-2*A-MU*T)**2)/(2*(SIG**2)*T))
  F = FRAC*(EXP1-EXP2)
  RETURN
  END
//LKED.SYSLIB DD DSN=DA.IMSL.LIBRARY.IMSL20,DISP=SHR
//

```

## REFERENCES

- Ahmad, G. (1976). "Self-Similar Solution of Incompressible Micropolar Boundary Layer Flow over a Semi-Infinite Plate." *Int. J. Engng. Sci.*, Vol. 14, 639-646.
- Ariman, T., and Cakmak, A. S. (1967). "Couple Stresses in Fluids." *Phys. Fluids*, Vol. 10, 2497-2499.
- Ariman, T., Cakmak, A. S., and Hill, L. R. (1967). "Flow of Micropolar Fluids between Two Concentric Cylinders." *Phys. Fluids*, Vol. 10, 2545-2550.
- Ariman, T., Turk, M. A., and Sylvester, N. D. (1973). "Microcontinuum Fluid Mechanics – A Review." *Int. J. Engng. Sci.*, Vol. 11, 905-930.
- Ariman, T., Turk, M. A., and Sylvester, N. D. (1974). "Applications of Microcontinuum Fluid Mechanics." *Int. J. Engng. Sci.*, Vol. 12, 273-293.
- Arkilic, E. B., Breuer, K. S., and Schmidt, M. A. (1994). "Gaseous Flow in Microchannels." *Int. Mechanical Engineering Congress and Exposition*, Chicago, ASME, FED, Vol. 197, 57-66.
- Bailey, D. K., Ameel, T. A., Warrington, R. O. Jr., and Savoie, T. I. (1995) "Single Phase Forced Convection Heat Transfer in Microgeometries – A Review." *30<sup>th</sup> Intersociety Energy Conversion Engineering Conference*, Orlando, Florida.
- Beskok, A., and Karniadakis, G. E. (1992). "Simulation of Slip-Flows in Complex Micro-Geometries." ASME, DSC, Vol. 40, 355-370. Book No. G00743.
- Beskok, A. (1996). "Simulations and Models for Gas Flows in Microgeometries." Ph.D. Dissertation, Princeton.
- Beskok, A., Karniadakis, G. E., and Trimmer, W. (1996). "Rarefaction and Compressibility Effects in Gas Microflows." *J. Fluids Engng.*, Vol. 118, 448-456.
- Beskok, A., and Karniadakis, G. E. (1997). "Modeling Separation in Rarefied Gas Flows." *AIAA 97-1883*, Snowmass Village, CO.
- Bhattacharya, R. N. and Gupta, Vijay K., (1984) "On the Taylor-Aris Theory of Solute Transport in a Capillary", *Siam Journal of Applied Mathematics*, Vol. 44, 33-39

- Bhattacharya, R. N. and M.K. Majumdar, (1980) "On Global Stability of Some Stochastic Economic Processes: A Synthesis", *Quantitative Economics and Development*, L.R.Klein, M. Nerlove and S.C. Tsiang, eds., Academic Press, New York, 19-42.
- Bird, G. (1994). "Molecular Gas Dynamics and the Direct Simulation of Gas Flows." Oxford Engineering Science, Oxford University Press, New York.
- Can, N. H., Huy, N. X., and Cau, T. N. (1989). "On the Convective Motion in a Micropolar Viscous Fluid." *Int. J. Engng. Sci.*, Vol. 27, 1183-1202.
- Chen, C. S., Lee, S. M., and Sheu, J. D. (1998). "Numerical Analysis of Gas Flow in Microchannels." *Numerical Heat Transfer, Part A*, Vol. 33, 749-762.
- Choi, S. B., Barron, R. F., and Warrington, R. O. (1991). "Fluid Flow and Heat Transfer in Micro Tubes." *Micromechanical Sensors, Actuators, and Systems, DSC*, ASME, New York, Vol. 32, 123-134.
- Ciarletta, M. (1995). "On the Theory of Heat-Conducting Micropolar Fluids." *Int. J. Engng. Sci.*, Vol. 33, 1403-1417.
- Cox, D. R. and Miller, H. D. (1965). *The Theory of Stochastic Processes*, Chapman & Hall, London.
- Das, M. L., and Sanyal, D. C. (1990). "Unsteady Flow of a Micropolar Fluid Through a Rectangular Channel." *Int. J. Engng. Sci.*, Vol. 28, 863-870.
- Easwaran, C. V., and Majumdar, S. R. (1990). "Causal Fundamental Solutions for the Slow Flow of a MicroPolar Fluid." *Int. J. Engng. Sci.*, Vol. 28, 843-850.
- Epstein, A. H., et al. (1997). "Power MEMS and Microengines." *1997 International Conference on Solid-State Sensors and Actuators*, Chicago, June, 753-756.
- Eringen, A. C. (1969). "Micropolar Fluids with Stretch." *Int. J. Engng. Sci.*, Vol. 7, 115-127.
- Eringen, A. C. (1980). "Theory of Anisotropic Micropolar Fluids." *Int. J. Engng. Sci.*, Vol. 18, 5-17.
- Gass, V., van der Schoot, B. H., and de Rooij, N. F. (1993). "Nanofluid Handling by Micro-Flow-Sensor Based on Drag Force Measurements." *Proc 93 IEEE MicroElectroMechSys (MEMS)*, 167-172.
- Gravesen, P., Branebjerg, J., and Jensen, O. S. (1993). "Microfluidics – A Review." *J. Micromech. Microeng.*, Vol. 3, 168-182.

- Harley, J. C., Huang, Y., Bau, H. H., and Zemel, J. N. (1995). "Gas Flow in Micro-Channels." *J. Fluid Mech.*, Vol. 284, 257-274.
- Ho, C., and Tai, Y. (1996). "Review: MEMS and Its Applications for Flow Control." *J. Fluids Engng.*, Vol. 118, 437-447.
- Hung, C., Tsai, J., and Chen, C. (1996). "Nonlinear Stability of the Thin Micropolar Liquid Film Flowing Down on a Vertical Plate." *J. Fluids Engng.*, Vol. 118, 498-505.
- Kavehpour, H. P., Faghri, M., and Asako, Y. (1997). "Effects of Compressibility and Rarefaction on Gaseous Flows in Microchannels." *Numerical Heat Transfer, Part A*, Vol. 32, 677-696.
- Kline, K. A., and Allen, S. J. (1970). "Nonsteady Flows of Fluids with Microstructure." *Phys. Fluids*, Vol. 13, 263-270.
- Kolpashchikov, V. L., Migun, N. P., and Prokhorenko, P. P. (1983). "Experimental Determination of Material Micropolar Fluid Constants." *Int. J. Engng. Sci.*, Vol. 21, 405-411.
- Liu, Guohua, (1999). "The Micro-Channel Flow of a Micro-Polar Fluid", Doctor of Philosophy in Applied Computational Analysis and Modeling Dissertation, Louisiana Tech University.
- Nassar, R., Schmidt, J., and Luebbert, A., (1992). "A Stochastic Dispersion Model in Gas-Liquid Flow Systems", *Chemical Engineering Science*, Vol. 47, 3657-3664.
- Olmstead, W. E., and Majumdar, S. R. (1983). "Fundamental Oseen Solution for the 2-Dimensional Flow of a Micropolar Fluid." *Int. J. Engng. Sci.*, Vol. 21, 423-430.
- Papautsky, I., Brazzle, J., Ameal, T. A., and Frazier, A. B. (1998). "Microchannel Fluid Behavior Using Micropolar Fluid Theory." *Proceedings of the IEEE Micro Electro Mechanical Systems (MEMS)*, Heidelberg, Germany, 544-549.
- Peng, X. F., Peterson, G. P., and Wang, B. X. (1994a). "Heat Transfer Characteristics of Water Flowing Through Microchannels." *Exp. Heat Transfer*, Vol. 7, 249-264.
- Peng, X. F., Peterson, G. P., and Wang, B. X. (1994b). "Frictional Flow Characteristics of Water Flowing Through Microchannels." *Exp. Heat Transfer*, Vol. 7, 265-283.
- Peyret, R., and Taylor, T. (1990). "Computational Methods for Fluid Flow." Springer-Verlag.

- Pfahler, J. N. (1992). "Liquid Transport in Micron and Submicron Size Channels." Ph.D. Dissertation, University of Pennsylvania.
- Pong, K. C., and Ho., C. M. (1994). "Non-Linear Pressure Distribution in Microchannels." *Int. Mechanical Engineering Congress and Exposition*, Chicago, ASME, FED-Vol. 197, 51-56.
- Rees, D. A. S., and Bassom, A. P. (1996). "The Blasius Boundary-Layer Flow of a Microplar Fluid." *Int. J. Engng. Sci.*, Vol. 34, 113-124.
- Sabersky, R. H., Acosta, A. J., Hauptmann, E. G., and Gates, E. M., (1999). *Fluid Flow a First Course in Fluid Mechanics*, Prentice Hall, New Jersey.
- Stanley, Roger, (1997). "Two-Phase Flow in Microchannels", Doctor of Engineering Dissertation, Louisiana Tech University.
- Stokes, V. K. (1966). "Couple Stresses in Fluids." *Phys. Fluids*, Vol. 9, 1709-1715.
- Strickwerda, J. C., (1989). *Finite Difference Scheme and Partial Differential Equations*, Chapman & Hall, New York.
- Wegeng, R. S., and Drost, M. K. (1994). "Developing New Miniature Energy Systems." *Mechanical Engineering*, September, 82-85.
- Wegeng, R. S., Call, C. J., and Drost, M. K. (1996). "Chemical System Miniaturization." *PNNL-SA-27317*, Pacific Northwest National Laboratory.
- Yu, D., Warrington, R., Barron, R., and Ameel, T. (1994). "An Experimental and Theoretical Investigation of Fluid Flow and Heat Transfer in Microtubes." ASME/JSME International Thermal Engineering Conference, Maui, Hawaii.